REGULATION OF β-LACTAM RESISTANCE BY C-DI-AMP IN *LISTERIA MONOCYTOGENES*

By

Zepeng Tu

A dissertation submitted in partial fulfillment of

the requirements for the degree of

Doctor of Philosophy

(Food Science)

at the

UNIVERSITY OF WISCONSIN - MADISON

2024

Date of final oral examination: 07/26/2024

The dissertation is approved by the following members of the Final Oral Committee:

Tu-Anh Huynh, Assistant Professor, Food Science

Briana Burton, Associate Professor, Bacteriology

Jan-Peter van Pijkeren, Associate Professor, Food Science

Wilmara Salgado Pabón, Assistant Professor, Pathobiological Sciences

This thesis is dedicated to my family

who gave me everything I ever needed

and then a lot more

ACKNOWLEDGMENTS

I would like to extend my deepest gratitude to my graduate mentor, Dr. Tu-Anh Huynh. Your unwavering work ethic and rigorous approach to research have profoundly inspired me throughout my time in graduate school. The discussions we shared and the meetings we held consistently reminded me that science is not just a discipline, but a source of fun and discovery. I will sincerely miss our engaging conversations and the insightful guidance you provided. Thank you for being such a pivotal part of my academic journey.

I would like to extend my heartfelt thanks to my committee members, Dr. Jan-Peter van Pijkeren, Dr. Briana Burton, and Dr. Wilmara Salgado Pabón, for their invaluable support, insightful feedback, and expert guidance throughout my research journey. Thank you for consistently challenging me with tough questions, which pushed me to delve deeper and refine my thinking. At the same time, your constant encouragement and support have been a great source of motivation. I am truly grateful for your dedication and the role each of you has played in my academic and personal growth.

Special thanks to both past and present members of the Huynh lab, especially Dr. Aaron Gall, Dr. Cheta Siletti, Justin Chow, Steven Massa, Yuxing Chen, Xilin Li, Dr. Justin Dang, Shreya Sunil Kumar, Dr. Mallory Grace Spencer, and Dr. Mariana Paiva Rodrigues. Thank you, Aaron, for teaching me all the techniques and providing insightful comments and suggestions all the time. Thank you, Cheta, Justin Chow, Steven, and Yuxing, for being the best lab mates for the past couple of years. Thank you all for your kindness and support throughout my time in the lab.

Thank you to the Department of Food Science for providing an enriching academic environment and exceptional resources that have significantly contributed to my research and personal growth.

To my parents, thank you for your unconditional love, endless support, and the countless sacrifices you've made for me. Your unwavering belief in my abilities has been my constant source of strength and motivation. I am forever grateful for everything you have done to help me reach this point in my life. I hope to make you as proud of me as I am to be your child.

CONTENTS

LIST OF TABLES

LIST OF FIGURES

ABSTRACT

Listeria monocytogenes is a prominent foodborne pathogen that contaminates many food products. *L. monocytogenes* infection (listeriosis) can cause severe symptoms, resulting in high hospitalization and mortality rates. The Centers for Disease Control (CDC) estimates that *Listeria* causes 1,600 illnesses and 260 deaths per year in the United States alone. Currently, β-lactam antibiotics, such as ampicillin and penicillin, which specifically target the bacterial cell wall, are the primary choices for treating listeriosis. However, increasing numbers of *L. monocytogenes* isolated from food and environmental sources are antibiotic resistant, particularly for β-lactams. Therefore, studying the mechanisms of *L. monocytogenes* antibiotic resistance and developing new methods for treating *L. monocytogenes* infection are needed. C-di-AMP is a conserved second messenger in *L. monocytogenes* that are involved in many cellular processes. Either depletion or unregulated accumulation of this molecule in *L. monocytogenes* diminishes its growth and virulence and greatly sensitizes it to β-lactam antibiotics. Therefore, investigating how c-di-AMP regulates bacteria β-lactam resistance not only offers a promising avenue for developing targeted antimicrobial therapies but also contributes to our broader understanding of bacterial adaptation and resistance mechanisms.

As a second messenger, c-di-AMP binds and regulates many proteins of various functions. In particular, PstA is a highly conserved c-di-AMP-binding protein present in many pathogens. Here, we found that the apo form of PstA diminishes β-lactam resistance in the normal and c-di-AMP depleting strains, and that c-di-AMP-bound PstA promotes β-lactam resistance in the c-di-AMP accumulating mutant. Strikingly, PstA plays a negligible role in β-lactam resistance during hypoxic growth. In aerobic cultures, we found that the function of PstA requires the cytochrome bd oxidase (CydAB) of the respiratory electron transport chain, but independent from menaquinone regeneration. In addition, we also reported the attempts to identify PstA binding partners and their interaction with a potential target Ndh2. These findings offer crucial physiological insights that facilitate the identification of PstA molecular targets under conditions of cell wall stress. On the other hand, we previously found that the accumulation of c-di-AMP in *Listeria monocytogenes*

results in decreased peptidoglycan production and reduced cell wall thickness, indicating that c-di-AMP plays a regulatory role in β-lactam resistance by compromising bacterial cell wall integrity. We isolated and characterized suppressor mutants that exhibit resistance to β-lactams while maintaining elevated levels of c-di-AMP. We discovered that mutations in MreB, a cytoskeletal protein essential for shaping the cell by guiding peptidoglycan synthesis, reversed not only the β-lactam susceptibility of ΔPDE mutants but also their diminished virulence. Further investigations confirmed that these mutations reduce MreB activity. We observed that MreB mutations facilitate the restoration of cell wall synthesis and specifically reduce autolysis under conditions of cell wall stress in ΔPDE mutants. Collectively, our findings lay a solid foundation for a more detailed characterization of how c-di-AMP influences bacterial aerobic metabolism and cell wall integrity. This groundwork is crucial for unraveling the complex regulatory roles of c-di-AMP in bacterial β-lactam susceptibility, providing directions for potential therapeutic strategies. Future research will focus on further delineating the interaction networks of c-di-AMP with its proteins and exploring the broader implications of these interactions for bacterial physiology and pathogenicity.

Chapter 1

Introduction

Regulations of c-di-AMP on bacteria cell wall homeostasis and β-lactam resistance in *L. monocytogenes*

Contributions:

Tu Z. conceived the review topic, wrote and revised the manuscript.

Huynh TN. critically revised the manuscript.

1. REGULATIONS OF C-DI-AMP ON BACTERIA CELL WALL HOMEOSTASIS AND β-LACTAM RESISTANCE IN *L. MONOCYTOGENES*

1.1 Abstract

Listeria monocytogenes is one of the most prominent pathogens in public health, which causes severe systemic infections with high mortality rates. *Listeria monocytogenes* can survive in different environments with multiple stresses. Among mechanisms for *L. monocytogenes* adaptation, the small nucleotide c-di-AMP coordinates many important cellular processes and is essential for bacterial stress response. Notably, either depletion or accumulation of c-di-AMP results in increased susceptibility to β-lactams, a commonly used antibiotics that specifically target bacterial cell wall. However, the function of c-di-AMP in regulating bacteria cell walls targeting antibiotics remains elusive. Here, we summarized the currently known hypothesis of bacteria cell wall homeostasis and then discussed how β-lactam affects bacteria cell wall synthesis as well as its bactericidal effect. Finally, I summarized the signaling pathways of c-di-AMP, and discussed the potential mechanisms of how c-di-AMP regulates bacteria β-lactam susceptibility. Our review provides insights into the complex regulatory roles of c-di-AMP in *L. monocytogenes*, particularly in its response to β-lactam antibiotics. This work not only sheds light on the molecular mechanisms of bacterial resistance but also sets the stage for future studies that could lead to groundbreaking advances in combating bacterial infections.

1.2 *Listeria monocytogenes* is a serious food-borne pathogen

The survival and prosperity of any organism rely on its ability to utilize available resources optimally, respond to environmental stresses, outcompete rival organisms, and proliferate effectively. As a Gram-positive, facultative anaerobic bacterial pathogen, *L. monocytogenes* has evolved to well adapted to dramatically distinct habitats, including extracellular environments (as a saprophyte) and intracellular environments (as a cytosolic

pathogen)[1]. This dual lifestyle of *L. monocytogenes* exhibits a synergistic manner: thriving in the environment enables *L. monocytogenes* to grow to a sufficient amount to infect the host while succeeding as a pathogen, allowing it to be distributed across vast areas into new environmental niches. The combination of ecological resilience and severity of disease makes *L. monocytogenes* a formidable challenge in the realms of microbiology, public health, and food safety.

L. monocytogenes has historically been a concerning foodborne pathogen that contaminates many food products, especially raw milk, cheese, and ready-to-eat food. Following oral ingestion, *L. monocytogenes* can traverse the intestinal barrier, causing systemic infections[2]. The Centers for Disease Control and Prevention (CDC) estimates that *L. monocytogenes* causes 1,600 illnesses and 260 deaths per year in the United States alone. Notably, in 2017-2018, one of the world's most severe listeriosis outbreaks was in South Africa, caused by contaminated Polony, a ready-to-eat, processed meat product. 1,060 cases of listeriosis and about 216 deaths were confirmed during the outbreak[3], making *L. monocytogenes* the third leading cause of death due to foodborne pathogens[4].

As a saprophyte, *L. monocytogenes* displays motility within a temperature range of 22 - 28°C but becomes non-motile when temperatures rise above 30°C. This microorganism is capable of growing in temperatures ranging from -0.4°C to 45°C, with an optimal growth temperature of 37°C[5]. It can also thrive in environments with low water activity ($aW < 0.90$), a broad pH range of 4.6 to 9.5, and in salt conditions up to 20%[6]. These adaptive capabilities enable *L. monocytogenes* to endure and proliferate under the challenging conditions commonly found in food production facilities. In *L. monocytogenes*, the Sigma B factor (σ^B) is a prime example of how genetic regulation plays a critical role in the bacterium's ability to withstand environmental and physiological stresses. Since *L. monocytogenes* σ^B was first identified in 1998[7], over 300 genes, have been shown to be under transcriptional control of σ^B, and many of these genes are crucial for *L. monocytogenes* to adapt to various stress conditions, including osmotic, acidic, heat shock, and oxidative stresses[8,9]. For example, under osmotic stress, σ^B enhances the expression of transport systems (e.g., opuCA) to uptake external compatible solutes available in the environment to maintain the intracellular osmotic balance[10]. Therefore, the σ^B contributes

to *L. monocytogenes* infection by enhancing its survival in both cytosol and the host gastrointestinal tract. In addition, it also can directly control the expression of several virulence-associated genes, including *prfA*, which encodes the master virulence regulator. PrfA is another crucial protein that controls the expression of essential virulence genes including *hly*, *actA*, and *plcA/B*, enabling the bacterium to invade host cells, escape from intracellular compartments, and replicate within the host's cytoplasm[11,12].

The infection of *L. monocytogenes* usually begins in the small intestine, where macrophages easily engulf *L. monocytogenes*. Remarkably, *L. monocytogenes* also has the unique ability to induce its uptake into nonphagocytic cells through the internalin operon, which encodes the proteins InlA and InlB[13]. These proteins specifically bind to receptors on the host cell surface, thereby triggering the phagocytosis of the bacteria into cells typically not involved in engulfment processes. Once internalized into the host cell, *L. monocytogenes* must escape from the vacuole into the host cell cytoplasm, where it can grow and replicate. The key factor in this escape is the bacterium's secretion of the protein listeriolysin O (LLO)[14]. By disrupting the vacuolar membrane, LLO enables *L. monocytogenes* to break free into the cytoplasmic environment. Finally, after entry into the cytosol, *L. monocytogenes* hijacks the host cytoskeletal system to propel itself through the cytoplasm and into neighboring cells without ever exiting into the extracellular space, thus avoiding the detection by the host immune system. This intracellular movement is driven by ActA, a virulence factor that polymerizes actin at one pole of the bacterium, pushing it forward[15].

Besides its role as a primary foodborne pathogen, *L. monocytogenes* serves as an excellent model for research due to its genetic manipulability, well-established infection models, and comprehensively studied lifecycle. The genome of *L. monocytogenes* is relatively compact, comprising approximately 2.9 to 3.0 million base pairs (Mbp)[16]. This size is manageable compared to more complex bacteria, making *L. monocytogenes* an advantageous model for genetic manipulation. The genome encodes about 2,900 to 3,000 genes, which include a range of virulence factors crucial for its pathogenicity[17]. This genomic simplicity, combined with the bacterium's clinical importance, has facilitated the development of a wide array of molecular tools and techniques for dissecting its biology and interactions with the host. In addition, *L. monocytogenes* is genetically related to

another model organism, *Bacillus subtilis*, allowing many of the genetic tools designed for *B. subtilis* to be adapted for use with *L. monocytogenes*[18,19]. This compatibility enhances the toolkit available for studying *L. monocytogenes*, facilitating advanced molecular characterization of how *L. monocytogenes* responds to environmental stresses and infects susceptible cells, shedding light on the bacterium's survival strategies and pathogenic mechanisms.

Finally, given its status as a prevalent foodborne pathogen and its efficacy as a model organism, *L. monocytogenes* is extensively utilized in research to explore antibiotic resistance mechanisms[20]. This research has implications for treating listeriosis and enhances our understanding of resistance mechanisms in bacteria more generally. Currently, the β-lactam antibiotics (a bacteria cell wall targeting antibiotics), particularly ampicillin, are the first-line treatment for listeriosis[21]. The study of β-lactam resistance in *L. monocytogenes* has garnered the most attention. Although *L. monocytogenes* typically show great susceptibility to β-lactam antibiotics, the detection of β-lactam-resistant isolates in clinical [22] and food animals [23] raises important concerns. However, the exact mechanisms of how β-lactam kills *L. monocytogenes* and how it develops resistance are still elusive. The study of β-lactam resistance in *L. monocytogenes* can maintain the clinical effectiveness of treatments and ensure that these key antibiotics remain potent tools against infections. It also offers invaluable insights into the mechanism of how *L. monocytogenes* and other bacterial responses to cell wall stress enrich our broader knowledge of bacterial adaptability and resilience.

1.3 Bacteria cell wall synthesis and remodeling

The bacterial cell wall is an intricate, mesh-like structure that is crucial for maintaining the shape and structural integrity of most bacterial species. Due to its essential role in bacterial survival and its absence in eukaryotic organisms, the bacterial cell wall is a focus of extensive research, making this unique bacterial feature an ideal target for many potent antibiotics[24]. Moreover, fragments of the bacterial cell wall can induce immunostimulatory and cytotoxic effects, playing a critical role in bacterial pathogenesis and disease processes, further emphasizing the importance of bacterial cell wall in medical research and antibiotic development[25-27].

1.3.1 The structure of bacteria cell wall.

The bacterial cell wall is predominantly composed of peptidoglycan (PG), a complex mesh of linear glycan chains (composed of a poly-[N-acetylglucosamine (GlcNAc)-N-acetylmuramic acid (MurNAc)] backbone) that are cross-linked by short peptides attached to the MurNAc residues[28]. The standard peptide chain typically contains four to five amino acids, which can vary among bacterial species, providing different characteristics to the cell wall. The peptides are crucial for the integrity of the cell wall, as they cross-link adjacent glycan chains, forming a three-dimensional mesh-like structure[29].

In Gram-positive bacteria, the peptidoglycan layer is thick and multilayered, making up around 40-90% of the cell wall structure. This thickness not only provides substantial rigidity but also contains teichoic acids-phosphate-containing polymers that are either covalently bound to peptidoglycan (wall teichoic acids) or to the membrane lipids (lipoteichoic acids) [30]. Teichoic acids play roles in cell wall maintenance, ion regulation, and serve as receptors for certain viruses[31]. Contrarily, Gram-negative bacteria possess a much thinner peptidoglycan layer, which constitutes only about 5-10% of the cell wall[32]. This thin layer is located in the periplasmic space between the inner cytoplasmic membrane and the outer membrane. The outer membrane of Gram-negative bacteria is composed of lipopolysaccharides (LPS) and phospholipids, which confer additional protective functions and contribute to the pathogenicity of these bacteria. The presence of this outer membrane makes Gram-negative bacteria generally more resistant to antibiotics than their Gram-positive counterparts[33].

1.3.2 The process of bacterial cell wall synthesis.

The biosynthesis of bacteria cell wall is a dynamic and complex biochemical process involving multiple critical enzymes that orchestrate the assembly of the peptidoglycan layer. This process consists of over 20 reactions that are essential for cell growth, division, and maintenance of cellular integrity (**Fig 2.1**)[34].

1.3.2.1 Peptidoglycan precursors synthesis

The synthesis begins in the cytoplasm where the UDP-N-acetylmuramic acid (UDP-MurNAc) is produced from N-acetylglucosamine (NAG) by the action of the enzyme MurA, which adds an enolpyruvyl group, followed by reduction via MurB. Subsequently, a

pentapeptide chain is assembled on the UDP-MurNAc by the sequential action of MurC, MurD, MurE, and MurF. Each of these enzymes adds specific amino acids to construct a complete pentapeptide chain that is critical for later cross-linking steps[35]. The UDP-MurNAc-pentapeptide is then linked to a lipid carrier molecule, bactoprenol phosphate, on the cytoplasmic membrane, creating Lipid I. This reaction is catalyzed by the enzyme MraY. The enzyme MurG catalyzes the addition of an N-acetylglucosamine (NAG) molecule to Lipid I to form Lipid II, which now serves as the direct precursor for peptidoglycan synthesis[36]. Lipid II is essential as it comprises both glycan subunits and a peptide chain, ready for incorporation into the growing peptidoglycan layer.

1.3.2.2 Translocation and Assembly

Lipid II is translocated from the inner to the outer leaflet of the cytoplasmic membrane by dedicated flippases, MurJ[37]. This step is crucial as it positions the precursor on the outer side of the membrane, where peptidoglycan synthesis occurs[38]. Once outside the membrane, the glycosyltransferases (GTases) catalyze the polymerization of Lipid II into long glycan strands. This involves the sequential addition of disaccharide units to the growing end of the carbohydrate chain, effectively lengthening the peptidoglycan backbone (transglycosylation). The SEDS proteins (Shape, Elongation, Division, Sporulation) such as RodA and FtsW have also been implicated in this process[3940].

1.3.2.3 Cross-linking and Maturation

The final maturation of the peptidoglycan involves cross-linking peptide chains between adjacent glycan strands. This process is mediated by penicillin-binding proteins (PBPs), which are bifunctional enzymes possessing both transglycosylase and transpeptidase activities[41]. PBPs such as PBP1B and PBP3 catalyze the formation of peptide bonds between the amino acids in the pentapeptide chains of adjacent glycan strands, providing structural integrity to the cell wall[42]. Concurrently, autolysins such as lysozymes play a role in remodeling the peptidoglycan by selectively cleaving existing bonds within the peptidoglycan matrix to allow the integration of new material[43]. This controlled enzymatic degradation is critical for cell wall expansion during growth and division, which will be discussed later.

1.3.3 Bacteria cell elongation, shape determination, and cell division

The intricate processes of cell elongation, shape determination, and division are fundamental to the life cycle of bacteria, influencing almost everything from individual cell function to colony dynamics and pathogenicity. These processes are deeply intertwined with the synthesis and restructuring of peptidoglycan, maintaining a balance between structural integrity and flexibility. The proteins involved in these processes do not function in isolation but as part of a coordinated network that adjusts cell wall synthesis in real-time to meet the needs of the cell.

1.3.3.1 Cell elongation and shape determination

Cell elongation and shape determination in bacteria are governed by sophisticated networks of cytoskeletal components and cell wall synthesis enzymes. These networks ensure that growth is not only robust but also geometrically and temporally regulated. The Rod complex is a group of proteins, including MreB, MreC, MreD, RodA, RodZ, and PBP2, that play a crucial role in bacterial cell elongation and maintaining the rod-shaped morphology of certain bacteria, such as *B. subtilis* and *L. monocytogenes*[40]. The Rod complex is vital for the synthesis and remodeling of peptidoglycan, ensuring the cell maintains its cylindrical shape throughout growth and division. This system's functionality not only supports structural integrity but also adapts to environmental changes, supporting the bacterial ability to thrive in diverse conditions.

MreB - Architect of cellular morphology: MreB is pivotal in maintaining the rod shape of many bacteria, similar to how actin maintains cell shape in eukaryotes. It forms a helical structure underneath the cell membrane that dictates the sites of peptidoglycan insertion, crucial for longitudinal growth and cylindrical consistency. MreB dynamically interacts with key enzymes (discussed below) responsible for peptidoglycan synthesis. By guiding these enzymes, it ensures that cell wall materials are inserted in precise locations, which is critical for maintaining the cell's shape and preparing it for division[44,45].

Rod proteins - central to peptidoglycan assembly: As a key glycosyltransferase, RodA is responsible for polymerizing the glycan chains of peptidoglycan. It works in tandem with PBPs to catalyze the formation and extension of these chains. Its activity is crucial for extending the cell wall during growth phases, directly influencing the cell's ability

to elongate while maintaining its diameter and overall structural integrity[46]. RodZ plays a crucial role in stabilizing the interactions between RodA and MreB. By binding to MreB and possibly affecting its conformation, RodZ ensures that the Rod complex is correctly positioned and oriented relative to the MreB scaffold, optimizing the synthesis and integration of new peptidoglyca[47].

PBP2 - essential transpeptidase for cell wall stability: PBP2 is crucial for the transpeptidation step in peptidoglycan synthesis, where it cross-links the peptide side chains of adjacent glycan strands. This activity is essential for providing mechanical strength to the cell wall, enabling it to withstand turgor pressure and maintain its shap[48]. PBP2 often works in conjunction with the Rod complex, particularly with RodA, to ensure that newly formed glycan chains are immediately cross-linked, thereby stabilizing the cell wall as it grows. Its activity is finely tuned by the spatial cues provided by the MreB and the biochemical signals mediated by MreC and MreD[49].

MreC and MreD: structural mediators for peptidoglycan Integrity: MreC acts as a bridge between the cytoskeletal elements and the cell wall synthesis enzymes. It helps transmit structural and environmental signals to the synthetic system, potentially modulating enzyme activity according to growth demands or stress responses. While less is directly known about MreD's specific activities, it is believed to work closely with MreC to support the cell wall synthesis system, ensuring that the spatial patterning dictated by MreB is accurately followed[50].

1.3.3.2 Cell division

Cell division in bacteria is a meticulously coordinated process crucial for bacteria reproduction and survival. This process involves the precise duplication and segregation of genetic material, followed by the division of the cell into two daughter cells. The division must be accurately timed and positioned to ensure each daughter cell inherits the necessary components for survival and growth. The cell division is initiated by the formation of a division apparatus called the divisome at mid-cell[51]. The divisome assembles at the site where the bacteria cell will divide, organizing and orchestrating the processes needed to form a new cell wall between the dividing cells. This complex is critical for ensuring that division occurs correctly and that each daughter cell is properly formed with all necessary cellular components[52].

Formation of the Z-ring: Central to bacterial cell division is the protein FtsZ, a GTPase that polymerizes to form a ring at the future site of cytokinesis, known as the Z-ring[53]. The Z-ring serves as a scaffold for the assembly of the divisome and marks the cell center where division will occur. The dynamic nature of FtsZ, which can rapidly assemble and disassemble, allows the cell to adjust the timing and location of division in response to cellular and environmental cues[54]. The placement of the Z-ring is tightly regulated by systems such as the Min proteins and nucleoid occlusion. These systems prevent the Z-ring from forming over the nucleoid or at the poles of the cell, ensuring it only forms at the mid-cell position[55].

Assembly of the divisome: Once the Z-ring is established, it recruits a series of other proteins essential for cell division, including FtsA, ZipA, and a series of penicillin-binding proteins (PBPs) such as FtsI (PBP3). These proteins help connect the Z-ring to the cell membrane and begin the process of constructing the new cell wall that will eventually separate the two daughter cells[56]. FtsI is crucial for the synthesis of peptidoglycan at the division site, specifically involved in the transpeptidation process that cross-links the peptidoglycan strands. FtsW acts alongside FtsI, likely serving a role in transporting peptidoglycan precursors to the site of synthesis[57].

Peptidoglycan synthesis during division: The synthesis of peptidoglycan during cell division is highly coordinated with the overall process of cytokinesis. Enzymes involved in peptidoglycan synthesis are strategically positioned at the division site to integrate new material into the dividing cell wall. This ensures that the septum, the new cell wall forming between the dividing cells, is constructed robustly to maintain cell integrity[54]. Autolysins play a critical role during cell division by cleaving the old peptidoglycan, allowing for the insertion of new material at the division site[58]. This controlled degradation is essential for the expansion of the cell wall and the eventual separation of daughter cells.

Completion of cell division: As the divisome completes the synthesis of the septal peptidoglycan, constriction of the Z-ring facilitates the inward growth of the septum, ultimately leading to the physical separation of the daughter cells. This process is finely tuned to ensure that each daughter cell is a viable, complete entity capable of independent growth and replication.

1.3.4 Bacteria cell wall recycling

The peptidoglycan layer needs to be rigid enough to protect the protoplasts against intracellular pressures and extracellular stresses yet dynamic enough to allow bacteria to divide and elongate. In addition to peptidoglycan synthesis, the bacterial cell wall undergoes meticulous regulation to coordinate cell wall degradation, remodeling, turnover, and recycling[59-61]. These processes are essential not only for maintaining cellular integrity and morphology but also for ensuring effective responses to physiological challenges and external threats.

1.3.4.1 PG recycling in gram-negative organisms

The bacteria cell wall recycling in gram-negative organisms was the most well-studied. This process initiates with the cleavage and release of peptidoglycan fragments[62]. Enzymes responsible for cleaving the linkage existing in peptidoglycan are generally called PG hydrolases. These enzymes are also known as autolysins since they are potentially autolytic if their activity is uncontrolled[63]. Autolysins include peptide-cleaving carboxypeptidases, endopeptidases, and N-acetylmuramyl-L-alanine amidases, and glycan-cleaving lytic transglycosylases. The peptide stem of peptidoglycan is hydrolyzed by amidases and carboxypeptidases, and the glycan strand of the peptidoglycan is cleaved by lytic transglycosylases at the β-(1→4) glycosidic bond between the MurNAc and GlcNAc residues.

Subsequent to their release, PG fragments are transported into the cytoplasm. The AmpG membrane protein is identified as the main permease that transports muropeptides across the inner membrane into the cytoplasm in gram-negative bacteria. Previous studies confirmed that deletion of ampG in bacteria led to the release of over 40% of the PG per generation while a functional AmpG only resulted in <10% turnover [64]. Once getting inside the cytoplasm, the PG fragments are further degraded into their constituent sugar and amino acids. Enzymes like NagZ will initiate the breakdown of PG fragments. NagZ is an N-acetylglucosaminidase that hydrolytically cleaves the β-(1→4) glycosidic bond of anhydrodisaccharides to generate GlcNAc and anhydrosaccharides. Other enzymes such as L, D-carboxypeptidase LdcA, N-acetylmuramyl-l-alanine amidase AmpD, and anhydroMurNAc kinase AnmK are also playing important rolel in processing anhydromuropeptides in the cytoplasm, yielding MurNAc-6-phosphate and other side

products. Finally, the breakdown products are funneled back into the peptidoglycan biosynthesis pathway, reducing the need for de novo synthesis of these materials and conserving metabolic energy.

1.3.4.2 PG recycling in gram-positive organisms

In many fundamental aspects, the mechanisms and purpose of peptidoglycan recycling are less comprehensively understood in Gram-positive bacteria than in Gram-negative bacteria. The initial doubts regarding the significance of peptidoglycan recycling in Gram-positive bacteria stemmed from the distinct characteristics of their cell walls compared to those of Gram-negative bacteria. The cell wall of Gram-positive bacteria acts like an exoskeleton and is considerably thicker than that of Gram-negative bacteria. This structure is built through an inside-to-outside synthesis model, which likely necessitates the use of autolysins to "relax" the outermost layer of the cell wall, facilitating circumferential growth[65]. These features, combined with the presence of substantial amounts of cell-wall fragments found in the culture mediums of Gram-positive bacteria[66], led to the early belief that peptidoglycan recycling was not a significant process in these organisms.

However, this presumption is now called into question by a lot of direct experimental studies on cell wall recycling by gram-positives. One pivotal experiment highlighting the existence of peptidoglycan recycling pathways in gram-positive bacteria was conducted by Litzinger et al. on *B. subtilis*. They identified a cluster of six genes (initially annotated as *ybbIHFEDC*) where the first five gene products were found to be orthologous to the *E. coli* recycling proteins: MurQ (an etherase), MurR (a transcriptional repressor), MurP (a MurNAc phosphotransferase), AmiE (an N-acetylmuramyl-L-alanine-specific amidase), and NagZ (a glucosaminidase)[67]. This discovery provided strong molecular evidence for similar recycling mechanisms in gram-positive bacteria, analogous to those previously well-characterized in gram-negative bacteria. In addition, one study directly quantified and showed that three gram-positive model organisms, *S. aureus*, *B. subtilis*, and *S. coelicolor*, all recycle the sugar N-acetylmuramic acid (MurNAc) of their peptidoglycan during growth in rich medium[68]They also proved that the MurNAc-6P esterase (MurQ or MurQ ortholog) enzyme is critical in this process. Although PG recycling is not essential in gram-positive

bacteria, a huge set of recycling genes is maintained in almost all bacterial genomes, suggesting that the pathway must benefit bacterial cells.

1.3.5 Cell wall synthesis and hydrolysis enzymes of *Listeria*

The enzymes involved in cell wall synthesis are known as penicillin-binding proteins (PBPs). β-lactam antibiotics exert their bactericidal effects by covalently binding to and blocking the active site serine in the transpeptidase domain of PBPs, which are crucial for bacterial cell wall synthesis. This interaction can be exploited for the detection of PBPs using radioactively labeled penicillin. Early investigations revealed the presence of five PBPs in *L. monocytogenes* PBP1-5[69]. Subsequent genomic analyses of the genome of *L. monocytogenes* EGD-e[70] confirmed the existence of five high molecular weight (HMW) and five low molecular weight PBPs[71-73].

The HMW PBPs are categorized into two classes: Class A HMW PBPs, which are bifunctional with a cytoplasmic N-terminal, a single membrane-spanning region, followed by extracellular transglycosylase and transpeptidase domains. Class B HMW PBPs feature a noncatalytic domain replacing the transglycosylase domain. Specifically, in *L. monocytogenes*, two class A bifunctional HMW PBPs are encoded by *lmo1892* (PBP A1) and *lmo2229* (PBP A2), and three class B HMW PBPs are encoded by *lmo1438* (PBP B1), *lmo2039* (PBP B2), and *lmo0441* (PBP B3). Genetic studies have further delineated the roles of these PBPs in bacterial viability and pathogenicity. For instance, gene disruption studies have shown the essentiality of *lmo2039* (PBP B2)[71], while others like PBP B1 and PBP A1 are non-essential but critical for virulence as their inactivation results in severe virulence defects[71]. Moreover, inactivation of PBP A2 and PBP B3 has been associated with increased susceptibility to β-lactam antibiotics[74]. Interestingly, mutations leading to truncated PBPs have been identified in various *L. monocytogenes* strains. For instance, PBP A1 genes in some isolates have acquired premature stop codons resulting in truncated proteins, though these truncations do not affect the transpeptidase domains[75], suggesting limited functional impact. Conversely, more severe truncations in PBP B3 genes lead to significant loss of function due to the absence of most of the extracellular domain[76]. These findings illustrate the complexity and critical nature of PBPs in *L. monocytogenes*, affecting both the bacterium's structural integrity and its pathogenic potential. This underscores the importance of PBPs as targets for β-lactam antibiotics and

highlights the need for ongoing research to fully understand their roles and regulation in bacterial physiology and virulence.

On the other hand, *L. monocytogenes* also contains a group of seven peptidoglycan hydrolases. These enzymes are crucial for modifying and breaking down peptidoglycan. They are p60 (also known as CwhA or Iap)[77], p45[78], Ami[79], Auto[80], NamA (also referred to as MurA)[81], lmo0327[82], and IspC[83]. The p60 (CwhA/Iap), p45, and NamA (MurA) are primarily involved in the remodeling of the peptidoglycan layer that is essential for bacterial cell wall integrity. These enzymes facilitate crucial processes such as flagellar motility, cell division, and elongation, which are vital for the bacterium's mobility and multiplication. They also play roles in the secretion of bacterial proteins that may interact with the host environment[78,81,84]. Ami, Auto, and IspC serve more specialized functions particularly linked to the pathogenic aspects of the bacterium. Auto is notably distinct because it is found in *L. monocytogenes* but absent in the non-pathogenic *Listeria innocua*. This hydrolase is implicated in enhancing the bacterium's capability to invade host cells by possibly regulating the cell wall permeability, thereby facilitating the secretion of other virulence factors[85]. Ami and IspC are key players in the bacterium’s ability to adhere to host cells, an initial step crucial for infection and subsequent colonization[86,87]. Most of these hydrolases possess domains that are characteristic of murein hydrolase activity and are associated with cell wall binding. This suggests a direct involvement in the dynamic restructuring of the cell wall in response to various environmental or cellular cues. Additionally, some of these enzymes exhibit unique features that regulate their catalytic activities or their anchoring to the cell wall, reflecting sophisticated mechanisms of action that allow precise control over their function[80]. While the specialized roles of Ami, Auto, and IspC in virulence highlight the adaptive strategies *L. monocytogenes* employs to thrive and persist within host organisms. The presence of Auto, with its unique contribution to invasion, underscores the pathogen's evolved mechanisms to breach host cellular barriers and establish infection.

In summary, the complex function of PBPs and peptidoglycan hydrolases underscores a sophisticated regulatory mechanism that *L. monocytogenes* utilizes for cell wall maintenance and virulence adaptation. While PBPs are instrumental in building and maintaining the structural integrity of the cell wall through peptidoglycan synthesis and

remodeling, the peptidoglycan hydrolases concurrently modulate this structure to facilitate bacterial growth, division, and pathogenic interactions with the host. This balance is crucial for its survival and virulence, highlighting the potential of targeting these molecular pathways for developing antibacterial strategies. Ongoing research into the roles and regulation of these enzymes will further illuminate their contributions to bacterial physiology and open new avenues for therapeutic intervention, particularly in combating antibiotic-resistant strains.

1.4. The mechanism of action for β-lactam antibiotics

β-lactam antibiotics represent a pivotal class of antimicrobial agents, which are among the most extensively utilized in medical practice, addressing infections from mild community-acquired conditions to severe, life-threatening hospital-acquired infections. The hallmark of beta-lactam antibiotics is the β-lactam ring, which is essential for their antimicrobial activity. This ring mimics the D-Ala-D-Ala dipeptide of peptidoglycan precursors, allowing beta-lactams to interfere effectively with cell wall synthesis. The integrity of this ring is crucial; alterations or breakage within the ring can deactivate the antibiotic's effect, which underscores the targeted nature of these compounds against bacterial cells.

The history of beta-lactam antibiotics began with the serendipitous discovery of penicillin by Alexander Fleming in 1928. This discovery is marked as a revolution in antimicrobial therapy and led to the development of a plethora of beta-lactam antibiotics. Over the decades, chemists and microbiologists have refined the beta-lactam structure to enhance its bacterial killing efficacy, broaden its spectrum of activity, and overcome resistance mechanisms developed by bacteria. These modifications have resulted in the creation of several subclasses of beta-lactam antibiotics, each tailored for specific types of bacterial infections and resistance profiles.

1.4.1 β-Lactam-mediated inhibition of PG transpeptidase

β-lactam antibiotics inhibit bacterial cell wall synthesis primarily through their action on penicillin-binding proteins (PBPs). The PBPs are a group of enzymes involved in the formation of peptidoglycan, an essential component of the bacterial cell wall. Among their

various roles, the transpeptidase (TP) domain of PBPs is critical for forming cross-links between peptidoglycan chains, which provide structural integrity to the cell wall. The mechanism by which β-lactams inhibit this process is both sophisticated and highly specific.

The TP domains of PBPs contain three highly conserved active site sequence motifs essential for their catalytic function: (i) SXXK Motif: includes a catalytic serine nucleophile (S70) and a general base lysine (K73). The serine performs a nucleophilic attack on the β-lactam ring, crucial for the next steps in the inhibition mechanism. (ii) SXN Triad: plays a role in stabilizing intermediates during the reaction. (iii) KTG(T/S) Motif: involved in the overall structural configuration of the active site and potentially in substrate recognition[41]. The mechanism of TP inhibition is initiated by deprotonation of the catalytic S70 by K73. This action facilitates the nucleophilic attack by S70 on the β-lactam amide carbonyl carbon of the antibiotic, leading to the formation of a tetrahedral intermediate. This intermediate is transient but critical, stabilized by hydrogen bonding to conserved residues located in the oxyanion hole, which consists of main chain hydrogens from motifs (i) SXXK and (iii) KTG(T/S). Subsequently, the tetrahedral intermediate collapses, expelling the negatively charged nitrogen leaving the group. This group is likely stabilized by protonation from a nearby serine (S120 from the SXN triad), resulting in the formation of an acyl-enzyme intermediate. The formed acyl-enzyme intermediate is highly stable and resistant to hydrolysis. This resistance is presumably due to steric hindrance that blocks a requisite deacylating water molecule, which would normally cleave the acyl-enzyme bond to release the enzyme for further catalytic cycles[41,88].

1.4.2 Major classes of β-Lactams

Since the initial discovery of benzylpenicillin, a variety of other β-lactam classes have been developed, significantly enhancing our arsenal of antibiotics to counteract resistance. β-lactams are categorized into four distinct structural classes, all of them have the four-membered lactam core moiety. These classes include penicillins, cephalosporins, carbapenems, and monobactams. Collectively, these β-lactams represent a comprehensive and structurally diverse group of compounds. Each class exhibits unique

pharmacological properties and is tailored for specific clinical indications, allowing for targeted therapeutic strategies against a broad spectrum of bacterial infections.

1.4.2.1 Penicillins

The penicillins, initially derived from Penicillium fungi, represent the earliest form of “pure” antibiotic used in medical treatment. The transformative clinical testing of Fleming's purified penicillin extract in the early 1940s encountered unparalleled success, marking a pivotal advancement in the annals of medical history [89]. Structurally, the penicillin molecule is characterized by a five-membered thiazolidine ring fused at the 2′ and 3′ positions to the β-lactam ring. Presently, penicillins are classified into four major subclasses: (i) natural penicillins, (ii) penicillinase-resistant penicillins, (iii) aminopenicillins, and (iv) extended-spectrum penicillins[90]

The rise of bacterial resistance to natural penicillins promoted a period of intense innovation, leading to the development of novel semisynthetic derivatives of penicillins. These derivatives are synthesized using the 6-aminopenicillanic acid (6-APA) precursor molecule, a strategy that has broadened the antibacterial efficacy of this drug class[91]. Despite their long-standing importance in modern medicine, the increasing prevalence of bacterial resistance has diminished the efficacy of penicillins, necessitating the development of alternative β-lactam antibiotics. This situation underscores the dynamic nature of antibiotic development and the constant need for newer, more effective antimicrobial therapies to stay ahead of pathogen evolution.

1.4.2.2 Cephalosporins

Cephalosporins, a vital class of β-lactam antibiotics, were first discovered from cultures of the fungus *Cephalosporium acremonium*, isolated from a sewage outlet on the Italian island of Sardinia in 1948 by Giuseppe Brotzu[92]. He discovered this compound during his studies on the sewage of the Sardinian coast, noting its efficacy against bacteria like *Salmonella typhi*, which is responsible for typhoid fever. The discovery of cephalosporin C marked a significant advancement, particularly because of its activity against penicillin-resistant strains and its unique chemical structure that includes a D-α-aminoadipic acid side chain.

The core structure of cephalosporins is a six-membered dihydrothiazine ring fused to the β-lactam ring, which differs from the five-membered thiazolidine ring in penicillins. This dihydrothiazine ring attachment to the lactam core not only provides cephalosporins with distinct hydrophilic characteristics but also introduces less ring tension, making the β-lactam ring of cephalosporins less susceptible to nucleophilic attacks or hydrolysis by β-lactamase enzymes. Furthermore, the cephalosporin core allows for additional chemical modifications at the C3 position, a feature not present in penicillins. This site of variation has been exploited extensively in the development of semisynthetic derivatives, incorporating various side chains that enhance antimicrobial activity and pharmacokinetic properties[93].

1.4.2.3 Carbapenems

Carbapenems, derived from thienamycin—a product of Streptomyces cattleya—were discovered in the mid-1980s and represent a vital class of β-lactam antibiotics[94]. These antibiotics are structurally characterized by a five-membered unsaturated ring with a C1 carbon instead of the usual sulfur found in the lactam core of penicillins and cephalosporins. A distinctive feature is their hydroxyethyl side chain at the R1 position, which significantly enhances their resistance to β-lactamase-mediated hydrolysis[95].

Carbapenems are known for their broad-spectrum antimicrobial activity, superior to that of penicillins, cephalosporins, and β-lactam/β-lactamase inhibitor combinations. They can bind to multiple PBPs and resist or inhibit many β-lactamases, making them highly effective against resistant bacterial strains[96-98]. Due to their low oral bioavailability, carbapenems are primarily administered intravenously, limiting their use in hospital settings, especially for treating severe infections resistant to other antibiotics. Today, they are considered a last-resort option against multidrug-resistant Gram-negative pathogens, underscoring their crucial role in contemporary antimicrobial therapy.

1.4.2.4 Monobactams

Monobactams are synthetic, monocyclic β-lactam antibiotics distinguished by their unique structure, featuring variable organic groups at positions C2 and C4, and a crucial sulfonic acid moiety at N1. This configuration helps activate the β-lactam ring, enhancing the acylation of transpeptidases crucial for antibacterial activity[99]. Aztreonam, the only

clinically approved monobactam, was first introduced in 1984 and has since played a significant role in treating bacterial infections. Its structure includes a β-lactam ring bonded to a sulfonic acid group, making it highly resistant to β-lactamases and effective specifically against aerobic Gram-negative bacteria. Aztreonam binds with high affinity to PBP3 of susceptible Gram-negative pathogens but shows very poor acylation of Gram-positive PBPs, rendering it ineffective against Gram-positive infections[100]. Due to its targeted spectrum of activity, aztreonam is often used in combination with other antibiotics, such as in aztreonam-vancomycin therapy, to cover a broader range of pathogens. However, its relative stability against the increasingly prevalent metallo- β-lactamase (MBL) enzymes makes it a valuable asset in the fight against resistant bacterial strains[101].

1.4.3 Molecular pathways to cell death induced by β-lactams

When β-lactams were initially discovered, the prevailing theory for their bactericidal action posited that cell death resulted primarily from the inhibition of critical and conserved functions of key enzymes like FtsI or HMW PBPs. These enzymes are vital for the cross-linking in bacterial cell wall synthesis[102-104]. The inhibition of these enzymes was believed to compromise the cell wall's mechanical stability, making it unable to withstand the internal turgor pressure, ultimately leading to the cell's violent rupture[105].

However, subsequent research conducted in various laboratories has revealed that the relationship between β-lactam exposure, the inhibition of cross-linking enzymes, and the resulting cell death is far more complex than initially understood. While inhibiting these cross-linking functions leads to a loss of mechanical stability in the cell wall, this alone does not fully explain the mechanisms leading to cell death. This suggests that additional cellular processes and responses to β-lactam antibiotics contribute to bacterial lethality, indicating a multifaceted interaction between the drug and the bacterial cell beyond mere mechanical destabilization[106].

1.4.3.1 Autolysis and induced autolysis

One of the early insights into the complex effects of β-lactams on bacterial viability came from observations made in *S. pneumoniae*. This bacterium possesses an autolytic system that triggers a significant loss of viability when it reaches the stationary phase[107].

A critical component of this system is LytA, a peptidoglycan amidase that functions as an autolysin during the stationary phase. Intriguingly, when ethanolamine substitutes for choline in the cell wall, there is an observed tolerance to penicillin due to the inhibition of LytA's activity[108]. This discovery hinted at the significant role of autolysins in β-lactam-mediated bacteriolysis and was further supported by similar findings in other bacteria: genetic inactivation of amidases in *E. coli*[109] and endopeptidases in *B. subtilis* [110] confirmed the necessity of these enzymes for β-lactam efficacy. Despite the inhibition of these autolysins, β-lactam tolerance in these bacteria is not complete. The antibiotics still exert bacteriostatic effects, and in some cases, there is a gradual decline in bacterial viability, indicating that other autolysins or alternative cell death pathways may be in play.

These observations have led to the development of the balanced growth model of killing by β-lactams[111]. According to this model, the maintenance of the peptidoglycan layer requires a delicate balance between synthetic activities, primarily carried out by HMW PBPs, and lytic activities from autolytic peptidoglycan hydrolases such as LytA. β-lactam antibiotics disrupt this balance by inhibiting the synthetic activities of PBPs, tipping the scale towards lytic degradation by autolysins. Over time, the peptidoglycan structure weakens to the point where it can no longer sustain the turgor pressure of the cell, leading to the release of cytoplasmic contents and resultant cell death[112].

The model of cell death by autolysis continues to be a significant explanation for the bactericidal action of β-lactams, though it has been refined considerably over time[113]. Autolysins, the enzymes responsible for this process, are tightly regulated and reliant on specific cellular signals to trigger β-lactam-mediated bacteriolysis, which have been shown in various bacteria, including *E. coli*, *B. subtilis*, *S. pneumoniae*, *S. aureus*, and *E. faecium*. The connection between PBP inhibition and cell lysis could be decoupled by manipulating culture conditions. For instance, incubating these bacteria with β-lactams at acidic pH does not induce lysis, but transferring them to a neutral pH environment without β-lactams can trigger cell lysis[114]. This indicates that neutral pH conditions either activate autolysins directly or stimulate a signaling mechanism that leads to their activation.

In firmicutes, a detailed model explains how the local acidity within cell wall regions can control hydrolase activity, which includes autolysins. This local acidity is influenced by several factors, such as the buffering capacity and pH of the external environment, the

proton motive force, and the D-alanylation of cell wall teichoic acids. These elements interact to produce finely tuned variations in acidity across the cell wall, affecting the activity of cell wall-modifying enzymes[115]. However, this model presents challenges when applied to proteobacteria like *E. coli*, which lack the teichoic acids and the thick peptidoglycan layer that are pivotal to the firmicute model. Further research is still needed to unravel the complex relationships between β-lactam-induced cell lysis, autolysins, and their external conditions.

1.4.3.2 Futile cycle of cell wall synthesis induced by β-lactams

β-lactam antibiotics are renowned for their mechanism of action that involves the inhibition of PBPs. Recent insights have elucidated a complex phenomenon known as the "futile cycle" of PG synthesis and degradation, which significantly contributes to the bactericidal efficacy of these antibiotics[116]. The initiation of this cycle begins when β-lactams, such as mecillinam, bind to and inhibit the transpeptidase active sites of PBPs. These enzymes are vital for forming the cross-links between peptidoglycan molecules that provide structural stability and rigidity to the bacterial cell wall. When TP activities are inhibited, it not only prevents the formation of new cross-links but also triggers malfunctions within the cell wall synthesis machinery. Instead of a stable and continuously expanding cell wall, the bacteria start producing incomplete and mechanically weak PG structures that are unable to support the cell's structural needs. Compounding the effect of TP inhibition, the cellular mechanisms responsible for PG synthesis, particularly the Rod system, become dysregulated. The Rod system, integral for inserting new PG material into the existing wall, enters a state of overdrive under the influence of β-lactam antibiotics. In the presence of active β-lactams like mecillinam, which targets PBP2, the system engages in both the synthesis of new PG and its immediate degradation. This response results in a high turnover rate of PG material, where substantial energy and resources are expended to synthesize peptidoglycan that is simultaneously broken down before it can be utilized effectively in the cell wall. This cycle of non-productive expenditure not only depletes the bacterial cell of vital precursors but also drains its energy reserves, leading to cell death.

1.4.3.3 Killing by oxidative damage

The concept of oxidative damage as a mechanism of bacterial cell death induced by β-lactam antibiotics has been significantly developed since Kohanski et al.'s (2007) research regarding the stimulation of NADH oxidation via the electron transport chain in *E. coli*[117]. This hyperactivation of the electron transport chain leads to increased production of reactive oxygen species (ROS), such as superoxide and hydrogen peroxide. These ROS can damage iron-sulfur clusters in proteins, destabilizing ferrous iron, which then reacts with hydrogen peroxide in the Fenton reaction to produce hydroxyl radicals. These radicals are capable of directly damaging DNA, lipids, and proteins, thereby leading to cell death.

Subsequent studies have expanded on this model, showing that different bactericidal antibiotics can induce the TCA cycle and further hyperactivate the electron transport chain, culminating in increased ROS production. For instance, L-serine was found to enhance the susceptibility of *E. coli* to gentamicin by increasing NADH production, thereby stimulating endogenous ROS production[118]. Similarly, studies involving *S. epidermidis* demonstrated that ROS generation induced by the TCA cycle contributed significantly to the susceptibility of the bacteria to β-lactam antibiotics[119]. Therefore, efforts to detoxify ROS have also been shown to reduce susceptibility to antibiotics. For example, Fravega et al. reported that in fluoroquinolone-resistant *S. enterica* serovar Typhimurium mutants, the accumulation of H2S stimulated the expression of catalase and superoxide dismutases, helping the bacteria counteract oxidative stress[120]. Additionally, in *E. coli*, the adverse effects of protein aggregation caused by streptomycin were mitigated by overexpressing a hydrogen peroxide scavenger[121].

However, the role of ROS in antibiotic-mediated killing remains controversial. Some studies have indicated that certain bacterial species, like *L. monocytogenes*, do not produce ROS in response to antibiotic treatment[122]. Moreover, *S. pneumoniae*, which lacks an electron transport chain, the proposed primary source of ROS, still exhibits high susceptibility to bactericidal antibiotics[123]. Additionally, experiments showed no difference in survival of *E. coli* treated with various antibiotics under aerobic versus anaerobic conditions, suggesting that metabolic shifts induced by the antibiotics, rather than ROS production, might play a more critical role in the observed bactericidal effects[123].

Taken together, these analyses underscore that while oxidative damage can contribute to the bactericidal effects of β-lactams and other antibiotics, its role is complex and varies significantly depending on the bacterial species and environmental conditions. Understanding these dynamics is crucial for optimizing antibiotic use and potentially enhancing their efficacy through the targeted manipulation of bacterial metabolism and oxidative stress responses.

1.5 C-di-AMP regulations in bacterial physiology

Cyclic di-AMP (c-di-AMP) is a nucleotide-derived second messenger that has emerged as a crucial signaling molecule in a wide variety of bacteria. Since its discovery in *B. subtilis* during studies on DNA integrity and cellular stress responses, c-di-AMP has been recognized for its broad roles in bacterial physiology and pathogenesis[124]. This dinucleotide regulates essential processes such as osmoregulation, central metabolism, cell wall integrity, and ion transport, emphasizing its significance in bacteria physiology.

The c-di-AMP consists of two adenosine molecules connected by two phosphodiester bonds, forming a cyclic structure. This unique structure allows it to interact with a diverse array of protein targets within bacterial cells. These interactions can modulate a variety of cellular functions, making c-di-AMP a pivotal component of the bacterial intracellular signaling network. C-di-AMP's role as a second messenger was first elucidated through its effects on cell wall stress and osmotic pressure regulation in *B. subtilis*[125]. Subsequent research has expanded our understanding of other bacterial species, including pathogens like *L. monocytogenes* and *Staphylococcus aureus*, where c-di-AMP influences not only basic physiological processes but also interactions with host organisms. The widespread presence of c-di-AMP across both Gram-positive and Gram-negative bacteria, as well as its involvement in crucial cellular processes, highlights its evolutionary significance and underscores its potential as a target for novel antimicrobial strategies.

1.5.1 Homeostasis of c-di-AMP in bacteria

Cyclic di-AMP (c-di-AMP) is a crucial signaling molecule that is essential for the normal growth of many bacteria and archaea. An insufficient level of c-di-AMP is detrimental to bacteria and can result in bacteria lysis[126]. Conversely, unregulated accumulation of c-di-

AMP is also toxic, which impairs bacteria growth, causing abnormal cell formation[127]. Therefore, maintaining the intracellular balance of c-di-AMP is crucial, and the homeostasis of c-di-AMP in bacteria is primarily managed through the precise coordination of its synthesis, degradation, and potentially, secretion[128].

1.5.1.1 c-di-AMP synthesis via DACs

C-di-AMP is synthesized from two molecules of ATP catalyzed by diadenylate cyclase (DAC). This is arguably the principal mechanism that maintains intracellular levels of c-di-AMP[129]. To date, five primary types of diadenylate cyclases have been identified: DisA, DacA (also known as CdaA), CdaS, CdaM, and CdaZ[126]. All these enzymes share a common DAC domain. DisA contains an N-terminal DAC domain, a domain linker, and a C-terminal DNA-binding helix-hairpin-helix (HhH1) domain, which primarily functions to detect DNA damage. DacA is the most widespread class of DACs. It contains a DAC domain and three N-terminal transmembrane helices. The DacA activity can be inhibited through protein-protein interactions with the regulatory protein CdaR, which is co-encoded in the *dacA-cdaR-glmM* operon, which is prevalent in *Firmicutes*. In addition to the DAC domain, the sporulation-specific CdaS includes a YojJ domain, which likely acts as an autoinhibitory domain to limit c-di-AMP synthesis, thereby controlling sporulation processes[130,131]. CdaM is composed of a DAC domain paired with a single N-terminal transmembrane helix, reflecting the specialized lifestyle of host-dependent *Mycoplasma* cells[132]. Lastly, CdaZ combines a DAC domain with an N-terminal α/β domain (PK_C, PF02887 in the Pfam database)[133]. This structure is involved in the allosteric regulation of pyruvate kinase, although its specific ligand-binding functions in archaea require further investigation.

Initially, to identify the active site of DAC, Witte et al. (2008) successfully obtained and analyzed the crystal structure of tmDisA/3-deoxy ATP (cordycepin triphosphate) complex from *Thermotoga maritima*[129]. He modified the native ATP ligand to its 3-deoxy form to inhibit the enzymatic reaction by removing the 3-OH group necessary for reaction progression. As a result, the 3-deoxy ATP molecules, though inert, are observed in the active site of DisA, aligned in a face-to-tail configuration, allowing the two 3-OH groups of the two ATPs to mutually attack the corresponding α-phosphoryl groups to form a cyclic 12-member ring product of c-di-AMP. Further interest is drawn from the structure of the

DisA/c-di-AMP complex (PDB: 3C21). The crystals of this complex were formed without adding external c-di-AMP during the crystallization process, suggesting that the DisA enzyme was biochemically active during overexpression and purification, and capable of synthesizing c-di-AMP that subsequently bound within its active site with high affinity.

1.5.1.2 C-di-AMP degradation via c-di-AMP-specific PDEs

C-di-AMP-specific phosphodiesterases (PDEs) are crucial in hydrolyzing c-di-AMP to maintain its appropriate intracellular levels. They belong to two main classes, characterized by either a DHH/DHHA1 or an HD domain. These domains facilitate the hydrolysis of a single phosphodiester bond in c-di-AMP, converting it into the linear dinucleotide 5-pApA. Many enzymes containing the DHH/DHHA1 domains possess additional capabilities, allowing them to further cleave the pApA intermediate into the final hydrolysis product, adenosine monophosphate (AMP). This multi-step degradation process is crucial for regulating the intracellular levels of c-di-AMP, ensuring cellular functions are not disrupted by its overaccumulation[134-136].

To date, researchers have identified three main families of c-di-AMP-specific PDEs, each utilizing either a DHH/DHHA1 or HD domain to hydrolyze c-di-AMP. The first described PDE was GdpP[137], which is composed of two N-terminal transmembrane helices, a Per-Arnt-Sim (PAS) domain, a degenerated GGDEF domain, and a DHH/DHHA1 domain combination[138]. The DHH/DHHA1 domains are crucial for cleaving c-di-AMP, while the PAS domain acts as a sensor, responding to environmental signals such as oxygen, carbon monoxide, or nitric oxide through its tightly bound heme molecule. Additionally, the stringent response factor (p)ppGpp has been identified as a competitive inhibitor of GdpP's PDE activity[139]. DhhP represents another PDE type, consisting solely of the DHH/DHHA1 domain combination. It can hydrolyze c-di-AMP to pApA, which can subsequently be broken down to AMP by other RNases. Through bioinformatic analysis, it has been discovered that NrnA, a homolog of DhhP, does not directly degrade c-di-AMP. Instead, it functions as a nano-RNase, hydrolyzing short RNA oligonucleotides, including pApA, into AMP. The third identified c-di-AMP-specific PDE is PgpH, which features a unique structure comprising a membrane-anchored extracellular 7TMR-HDED domain followed by an integral membrane domain consisting of seven transmembrane helices (7TM) and a cytosolic HD-type PDE domain. The N-terminal transmembrane helix and the

7TM domain support the stability of the extracellular 7TMR-HDED domain, which senses external signals. The 7TM domain helps transmit these signals across the membrane to regulate the HD domain's PDE activity, which hydrolyzes c-di-AMP to pApA. Intriguingly, like GdpP, PgpH's activity is also inhibited by (p)ppGpp, indicating a potential crosstalk between the pathways mediated by these two nucleotide second messengers. This interconnected regulation highlights the complex network of signaling pathways that influence bacterial responses and survival strategies[136]. It is worth noting that GdpP is found only in *Firmicutes* and *Mollicutes*, while the pgpH-type PDEs are present in most bacteria phyla except for *Acidobacteria*, *Actinobacteria*, and *Mollicutes*. Among the *Firmicutes*, PgpH often coexists with GdpP, while in other bacteria and archaea, PgpH is usually found alongside DhhP-type enzymes.

1.5.1.3 Regulation via c-di-AMP export channels and regulatory proteins

In addition to metabolic enzymes that regulate c-di-AMP synthesis and hydrolysis, certain transporter and regulatory proteins also appear to be crucial in managing the levels of this important signaling molecule within cells. These proteins contribute to a more dynamic and responsive system for controlling c-di-AMP, ensuring that its concentration remains within a range conducive to optimal cellular function and adaptation to environmental changes.

Multidrug efflux pumps (MDRs) are transport systems located on the membranes of bacterial cells. Although it is reported that certain drugs can induce higher expression of MDR genes, their functions are not necessarily involved in the active efflux of drugs and antibiotics. Interestingly, some MDRs are involved in transferring signaling molecules across the cellular membrane. For instance, in *L. monocytogenes*, MDRs like MdrM and MdrT are known to export c-di-AMP from bacterial cells into infected macrophages during intracellular growth, as discussed in studies by Woodward et al.[140] and Yamamoto et al.[141]. Previous research indicated that antibiotics such as lincomycin and rhodamine 6G could induce the expression of MDRs in *L. monocytogenes*[142]. Further investigations revealed that the presence of these two antibiotics leads to an increase in MDR expression, which in turn promotes the secretion of c-di-AMP, thereby reducing its intracellular concentration in *L. monocytogenes*[143]. However, studies on *S. aureus* involving mutations in all three homologs of MdrM and MdrT, showed only a negligible change in extracellular c-di-AMP

levels, suggesting that the secretion of c-di-AMP by MDRs may vary significantly among bacteria[144].

In addition, In Group B *Streptococcus*, the degradation of extracellular c-di-AMP is facilitated by ectonucleotidases such as CdnP and NudP[145]. Both of these enzymes share a similar domain architecture, which includes a signal peptide, a metallo-phosphodiesterase (PDE) domain, a 5-nucleotidase domain, and a canonical LPxTG cell surface-localization motif. These structures allow CdnP to hydrolyze extracellular c-di-AMP into AMP. Subsequently, NudP further degrades AMP into adenosine. This sequential breakdown of c-di-AMP by CdnP and NudP is crucial for modulating the levels of extracellular nucleotides, impacting various cellular functions and interactions within the microbial community.

1.5.2 C-di-AMP binding targets

As a small nucleotide second messenger, the function of c-di-AMP in bacteria is achieved through binding with specific targets. These receptors typically include riboswitches, specialized binding proteins, and regulatory proteins that can directly recognize and respond to changes in the levels of c-di-AMP, thereby regulating various physiological processes within the cell. (**Table 1.1-1.2**) shows the list of currently identified c-di-AMP binding targets.

1.5.2.1 Protein receptors

To date, numerous proteins have been identified as receptors c-di-AMP, most of which are already characterized in bacterial species. These include the potassium transport protein KtrA[146], the Histidine kinase protein KdpD[147], the tetR-Family transcription factor DarR[126], The PII-like signal transduction protein PstA/DarA[126,148], and several others. In addition, c-di-AMP receptors are also present in eukaryotic host cells, for example, the stimulator of interferon genes (STING)[145,149], the DEAD-box RNA helicase 41 (DDX41)[150], the short-chain oxidoreductase RECON[151], and the endoplasmic reticulum membrane adaptor (ERAdP)[152].

The protein receptors of c-di-AMP tend to have diverse structures, yet they are relatively easier to purify for binding analysis due to the availability of various fused-tag sequences. Most of these receptors have been identified through high-affinity pull-down

assays and the comprehensive whole-genome Differential Radial Capillary Action of Ligand Assay (DRaCALA) technique[153]. Corrigan et al. (2013) first utilized c-di-AMP-coupled magnetic beads in an affinity pull-down assay to isolate a potential c-di-AMP receptor, KtrA, from *S. aureus*[146]. Subsequently, an identical chemical proteomics approach was performed in *L. monocytogenes* and identified 12 proteins that were statistically significant among replicates [154]. Similarly, Kampf et al. (2017) used biotinylated c-di-AMP to capture receptor proteins from cell lysates, employing streptavidin-coated beads for binding. The receptors bound to the biotinylated c-di-AMP were then eluted and identified using mass spectrometry[155]. This approach led to the identification of KtrC as a new c-di-AMP receptor in *Mycoplasma pneumoniae*[132]. Other receptors such as ERAdP[152], STING[152], and DDX41[156] in host cells were identified through precipitation assays, which function similarly to pull-down assays.

Another key method is the whole-genome DRaCALA technique, which tests the binding affinity of each protein candidate using radioactively labeled c-di-AMP. This technique successfully identified KdpD, the oligopeptide transporter OpuCA, and KtrA in *S. aureus* as c-di-AMP receptors[146]. As for protein receptor verification, three methods are typically used: 1) The Surface Plasmon Resonance (SPR) was used to confirm DarR[157] in *Mycobacterium smegmatis* and PstA[158] in *S. aureus* as new c-di-AMP-binding protein receptors. 2) The Isothermal Titration Calorimetry (ITC) was performed to verify Dar[159] in *B. subtilis* and CpaA[160] in *S. aureus* as c-di-AMP receptors, providing a quantitative measure of the binding affinity and thermodynamics of the interaction. 3) The Electrophoretic Mobility Shift Assay (EMSA) was used to confirm CabP from *Streptococcus pneumoniae* as a c-di-AMP binding receptor by demonstrating a shift in the mobility of a c-di-AMP-protein complex during gel electrophoresis[161].

1.5.2.2 c-di-AMP riboswitch

Riboswitches are RNA structures that regulate gene expression by altering their conformation in response to binding specific ligands, and they are categorized into different classes based on their ligands[162]. One such example is the *ydaO*/*yuaA* RNA element of *B. subtilis*. Although initially identified in 2004 as a potential riboswitch candidate, its specific ligand remained unknown for several years[163]. Subsequent research revealed that this RNA element was involved in controlling numerous genes

within the genomes of *B. subtilis* and other Gram-positive bacteria, indicating its significance in bacterial regulatory networks[164]. It was not until 2013 that Nelson et al. definitively identified *ydaO* as a c-di-AMP-responsive riboswitch, demonstrating its high affinity for this dinucleotide with a dissociation constant (K_D) in the nanomolar range. This discovery highlighted the specificity and critical role of *ydaO* in responding to cellular levels of c-di-AMP, a key signaling molecule in bacteria[165].

A comprehensive analysis of the distribution of c-di-AMP-specific riboswitches across all sequenced bacterial genomes available in the Rfam database[166] showed that c-di-AMP riboswitches are particularly prevalent within the *Actinobacteria* phylum, with a notable presence also in *Firmicutes*. Interestingly, this study also uncovered the presence of c-di-AMP riboswitches in some Gram-negative bacteria, specifically within the phyla *Cyanobacteria*, *Chloroflexi*, and *Armatimonadetes*.

Previous research has shown that the genes downstream of c-di-AMP riboswitches are predominantly involved in cell wall metabolism and osmolyte transport[163,164]. To gain deeper insights into the c-di-AMP regulatory mechanism, an analysis was conducted on the gene sequences downstream of the c-di-AMP riboswitch. These sequences were annotated using the Clusters of Orthologous Groups of proteins (COGs) database[167]. The analysis revealed that 45.7% of the downstream genes linked to various c-di-AMP riboswitches are involved in cell wall, membrane, or envelope biogenesis. Additionally, 19.3% participate in amino acid transport and metabolism, and 12.7% in inorganic ion transport and metabolism. For instance, c-di-AMP riboswitches were identified in the 5'-UTR regions of genes encoding specific proteins, such as a peptidoglycan binding domain-containing protein (Franean1 2508) in *Frankia sp. EAN1pec*, an ectoine-binding protein GYMC10 5669 in *Paenibacillus sp. Y412MC10*, and a sulfate transporter (Rcas 2371) in *Roseiflexus castenholzii DSM 13941*. These genes respectively regulate cell wall, membrane, or envelope biogenesis, amino acid transport and metabolism, and inorganic ion transport and metabolism.

1.5.3 Physiology functions regulated by c-di-AMP

1.5.3.1 Osmotic stress

Due to the semi-permeable nature of the cytoplasmic membrane, bacteria require various osmolytes to maintain osmotic balance, which is crucial for their growth and survival[168]. Osmotic balance is fundamental for sustaining cellular integrity and function, and any disturbance in osmotic pressure can result in significant changes in bacterial phenotypes, such as cell lysis, cellular shrinking, and increased sensitivity to β-lactam antibiotics[169]. One of the key roles of c-di-AMP in bacterial physiology is to regulate this osmotic pressure. By influencing the transport and retention of ions and other molecules, c-di-AMP helps to stabilize the internal environment of bacterial cells against external osmotic challenges. This function is vital for enabling bacteria to adapt to varying environmental conditions and maintain cellular homeostasis.

1) Control of potassium homeostasis

Recent studies have extensively documented the critical role of c-di-AMP in bacterial response to osmotic stress by regulating the homeostasis of potassium (K^+) and other osmolytes[170]. C-di-AMP influences K^+ transport by inhibiting the import systems such as Ktr/Trk, KimA, Kup, and Kdp, while facilitating K^+ export through transporters like CpaA and KhtT. The Ktr system from the Trk/Ktr/HKT family contains both high-affinity transporters like KtrA-KtrB and low-affinity transporters like KtrC-KtrD[171]. C-di-AMP interacts with the RCK_C (regulator of conductance of K^+) domains of regulatory proteins such as KtrA and KtrC through hydrogen bonds and hydrophobic interactions[146,172]. In bacteria such as *B. subtilis*, *S. aureus*, and *S. pneumoniae*, KtrA functions as a peripheral protein that assists the KtrB transporter in facilitating K^+ uptake, a process that is hindered when c-di-AMP binds to KtrA[161]. Similarly, in *B. subtilis* and *L. monocytogenes*, c-di-AMP binding to KtrC also obstructs K^+ uptake via the KtrC-KtrD system[173,174]. Moreover, other bacteria like *Mycoplasma pneumoniae* and *S. agalactiae* also encode homologs of these Ktr systems that interact with c-di-AMP[175].

In the case of HAK/KUP/KT family proteins, which are prevalent in bacteria, fungi, and plants, K^+ uptake is also modulated by c-di-AMP[176]. For instance, in *Lactococcus lactis*, the KupA and KupB transporters from this family bind c-di-AMP, leading to the inhibition

of their high-affinity transport activities[177]. Furthermore, KimA (formerly YdaO), another HAK/KUP/KT family member recently recognized for c-di-AMP binding, is involved in K^+ transport[178]. The expression of KimA N-terminal extracellular and transmembrane domain facilitates K^+ uptake in an *E. coli* model, while its C-terminal domain is necessary for c-di-AMP-dependent inhibition. The regulation of these transport systems is further controlled by the c-di-AMP-responsive *ydaO* riboswitch, which influences the expression of genes like kimA and ktrAB. The riboswitch can refold upon binding to c-di-AMP, thereby obstructing the transcription of kimA[179]. This complex regulatory mechanism involving c-di-AMP stresses its pivotal role in managing cellular osmotic balance through modulation of potassium transport pathways.

The Kdp complex serves as a crucial backup system to scavenge K^+ from the environment when external K^+ concentrations are low. This system is well-studied in *E. coli*, where it comprises the proteins KdpA, KdpB, KdpC, and KdpF, all encoded by the single *kdpFABC* operon. The expression of this operon is regulated by the two-component system KdpDE, which includes a sensor kinase (KdpD) and a response regulator (KdpE)[180]. In *S. aureus*, the regulation of the *kdpFABC* operon is similar in *E. coli*, with its expression also being controlled by the two-component system KdpDE. However, the regulation is further complicated by the interaction of c-di-AMP with the sensor kinase KdpD. Specifically, c-di-AMP binds to the universal stress protein (USP) domain of KdpD, inhibiting the kinase's activity, which in turn affects the regulation of potassium uptake[147]. Interestingly, some strains of *S. aureus* possess a second form of KdpD, named KdpD2, which similarly binds c-di-AMP at its USP domain, though the functional role of KdpD2 in K^+ homeostasis remains unclear[147]. In contrast, in *B. thuringiensis*, the control of the *kdpFABC* operon diverges from the two-component system and instead involves a c-di-AMP-responsive riboswitch. This riboswitch negatively regulates the operon under normal conditions. However, during potassium limitation, bacterial production of c-di-AMP decreases, which lifts the repression by the riboswitch, thereby enhancing the transcription of the *kdpFABC* operon and facilitating increased potassium uptake[181].

In addition to influencing K^+ uptake systems, c-di-AMP also plays a significant role in regulating K^+ homeostasis by modulating K^+ export mechanisms. In *B. subtilis*, the KhtT subunit of the KhtTU K/H antiporter (also known as YhaTU) interacts with c-di-AMP, which

subsequently induces the export of K^+ from the cell[182,183]. Additionally, CpaA (cation/proton antiporter A) found in both *B. subtilis*, and *S. aureus* is activated by binding with c-di-AMP, enhancing its antiport activity. One thing worth noting is that mutations in the monovalent cation exporter, NhaK, were identified during a suppressor screen for the c-di-AMP null mutant of *B. subtilis* in a medium containing 5 mM K^+. Unlike KhtT and CpaA, which include RCK_C domains and can bind c-di-AMP, NhaK does not have this capability[160,184].

The regulation of K^+ homeostasis by c-di-AMP involves multiple transporters and is intricately linked to the availability of K^+ in the environment. In *B. subtilis* and *S. pneumoniae*, the expression of the DacA, which synthesizes c-di-AMP, is notably reduced in low extracellular K^+ conditions, leading to lower intracellular c-di-AMP levels. Conversely, in environments rich in K^+, c-di-AMP levels rise markedly[185]. In *S. pneumoniae*, alterations in CabP, a KtrA homolog, result in decreased c-di-AMP accumulation, though the precise mechanisms remain to be fully understood. This complex network of interactions highlights a sophisticated regulatory system where environmental K^+ concentrations, K^+ transport mechanisms, and c-di-AMP levels are tightly coordinated. This coordination ensures that bacterial cells maintain optimal ionic balance and cellular function under varying environmental conditions.

2) Control of the uptake of compatible solutes

In response to hyperosmotic stress, many bacteria, including *B. subtilis*, rapidly accumulate large amounts of potassium as an immediate protective measure[186]. This initial response helps to counteract the osmotic imbalance caused by high external solute concentrations. However, for more sustainable long-term adaptation under such stress conditions, bacteria also accumulate compatible solutes, which are crucial for maintaining cell integrity and function. Compatible solutes are water-soluble organic molecules that are osmotically active but do not disrupt cellular processes, even when present at high intracellular concentrations. These molecules can either be directly uptaken from the environment or synthesized by the bacteria themselves. Among the commonly used compatible solutes in bacteria are proline, glycine betaine, carnitine, proline betaine, and trehalose. These solutes help stabilize proteins and cellular structures, protect against dehydration, and contribute to the maintenance of enzyme activity and cell volume under osmotic stress[168].

Numerous studies involving bacterial strains that either lack or accumulate c-di-AMP have underscored its critical role in osmotic adaptation. Strains with elevated levels of c-di-AMP, such as those in *L. lactis* and *L. monocytogenes*, exhibit increased sensitivity to salt stress[187-189]. For instance, in *Listeria. monocytogenes*, mutant strains that accumulate c-di-AMP due to the inactivation of the gene encoding a c-di-AMP degrading phosphodiesterase showed significantly increased salt sensitivity. Therefore, suppressor mutants capable of coping with this increased salt stress have been isolated. These suppressor mutants typically exhibit mutations in the single diadenylate cyclase gene, effectively reducing c-di-AMP synthesis[188]. Additionally, gain-of-function mutations in the KupB potassium transporter were identified, which likely serve to bypass the inhibitory effects of c-di-AMP binding to KupB[177]. Furthermore, mutations that inactivate the BusR repressor protein were also discovered[170]. BusR, part of the GntR family, contains an N-terminal GntR-type DNA-binding domain and a C-terminal RCK_C domain, and it functions to repress the expression of the glycine betaine uptake system BusAB in *L. lactis* and other lactic acid bacteria[190]. C-di-AMP binds to BusR and acts as a corepressor, thereby preventing the expression of the *busAB* operon in *L. lactis* and *S. agalactiae*[170,191]. The accumulation of c-di-AMP leads to the constitutive repression of this operon, hindering the bacteria's ability to manage osmotic stress by impairing the uptake of vital osmoprotectants like glycine betaine. Therefore, the inactivation of the *busR* gene in mutants allows for the uptake of osmoprotectants, enabling growth under osmotically challenging conditions despite high concentrations of c-di-AMP.

Just like potassium, c-di-AMP plays a crucial role in maintaining the proper homeostasis of osmolytes in bacteria. For bacteria mutants that accumulate c-di-AMP, the uptake of osmolytes becomes a growth-limiting factor, whereas their uncontrolled uptake in the absence of c-di-AMP can be detrimental to cell viability. For example, in *S. agalactiae*, mutant strains lacking c-di-AMP cannot survive in complex media unless they acquire suppressor mutations that inactivate the *BusAB* transporter, responsible for the uptake of compatible solutes. Similar phenotypes have also been reported in *Listeria monocytogenes* and *Staphylococcus aureus*, where mutations that inactivate the glycine betaine transporters GbuABC and OpuD, respectively, allow c-di-AMP deficient mutants to survive in rich media[185,192,193].

The necessity to inactivate genes involved in osmolyte transport in c-di-AMP-free strains indicates that c-di-AMP is integral to controlling osmolyte uptake. C-di-AMP not only binds to and inhibits proteins involved in transporting compatible solutes such as BusR. Moreover, it directly interacts with the ATPase subunit of the OpuC osmoprotectant ABC transporter in *L. monocytogenes*, *S. aureus*, *S. agalactiae*, and *B. subtilis*[136,182,194]. This interaction inhibits the uptake of compatible solutes by binding to the CBS domains of the OpuCA subunit of the transporter. Interestingly, bacteria like *B. subtilis* often possess multiple paralogous ABC transporters for the uptake of osmoprotectants. Although all three paralogous transporters OpuA, OpuB, and OpuC have been tested for c-di-AMP binding, only the OpuCA subunit has shown the capability to interact with this second messenger[136]. OpuC has the broadest substrate spectrum among the osmolyte transporters in *B. subtilis*[195], indicating that its regulation by c-di-AMP, particularly under conditions without osmotic stress, is critical for cellular efficiency and survival. This regulation highlights the sophisticated mechanisms bacteria employ to adapt to varying environmental osmotic conditions, utilizing c-di-AMP as a key regulatory molecule.

1.5.3.2 Central metabolism

Previous studies regarding the characterization of suppressor mutations that allow *L. monocytogenes* to grow in rich media in the absence of c-di-AMP as well as the identification of c-di-AMP-binding proteins through chemical proteomics indicate that pyruvate carboxylase (PycA) is a crucial target of c-di-AMP[154,192]. These results suggest that c-di-AMP plays a significant role in regulating central carbon and nitrogen metabolism. In *L. monocytogenes*, where the tricarboxylic acid (TCA) cycle is incomplete, the PycA is the sole enzyme producing oxaloacetate, a precursor necessary for citrate synthesis[196]. When c-di-AMP binds to PycA, it allosterically inhibits its activity, disrupting the normal flow of carbon into the TCA cycle.

Within its incomplete TCA cycle, *L. monocytogenes* convert citrate to 2-oxoglutarate, which is then used as a precursor for synthesizing glutamate and the osmoprotectant proline. However, in the absence of c-di-AMP, unrestricted activity of pyruvate carboxylase can lead to excessive accumulation of citrate. This accumulation is problematic as citrate can chelate iron, inhibiting bacterial growth[197]. This phenomenon was observed in a *L. monocytogenes* strain lacking c-di-AMP, which accumulated citrate to detrimental levels.

Remarkably, inactivating citrate synthase in this strain mitigated the issue, indicating that the overaccumulation of citrate was the limiting factor for growth[192]. Similarly, in *L. lactis*, c-di-AMP's inhibition of pyruvate carboxylase is thought to regulate aspartate biosynthesis, further illustrating its broad regulatory role in bacterial metabolism[198].

Studies involving a strain of *S. aureus* that lacks c-di-AMP have shown that this bacterium develops mutations affecting AlsT, the primary glutamine transporter. Glutamine is a precursor that can be readily converted into glutamate and the compatible solute proline. Therefore, the uptake of glutamine in this context could lead to toxic accumulations of osmolytes. Additionally, c-di-AMP appears to be non-essential under anaerobic conditions or when *S. aureus* undergoes mutations that disrupt respiration[199]. This suggests a link between respiration and the necessity for c-di-AMP, possibly due to its role in facilitating efficient potassium transport. The major potassium transporter KimA, which has a high proton demand, may not function effectively without respiratory activity[178], leading to compromised potassium transport crucial in the absence of c-di-AMP.

1.5.3.3 Interaction in signal networks of c-di-AMP and (p)ppGpp

To cope with nutrient deprivation, bacteria produce the alarmone (p)ppGpp, which triggers stringent responses to manage starvation. These responses crucially regulate various cellular processes including growth, DNA replication, RNA polymerase activity, and protein synthesis[200]. The synthesis and degradation of (p)ppGpp are mediated by Rel Spo homolog (RSH) proteins. The synthase domain of these proteins transfers two phosphates from ATP to either GTP or GDP, thus generating pppGpp or ppGpp, respectively (collectively referred to as (p)ppGpp). Interestingly, numerous studies have shown that (p)ppGpp and c-di-AMP signaling networks converge to coordinate bacteria physiology and stress response.

The connection between c-di-AMP and the alarmone (p)ppGpp was first identified in a study showing that deleting the gene encoding phosphodiesterase GdpP in *L. lactis* led to enhanced resistance to glucose starvation in acidic conditions. This result suggested that c-di-AMP accumulation might influence bacterial levels of (p)ppGpp[201]. Subsequent in vitro studies provided further insight, confirming that ppGpp inhibits the hydrolysis of c-di-AMP by two specific c-di-AMP phosphodiesterases, GdpP and PgpH[137]. Notably, while GdpP does not directly hydrolyze (p)ppGpp[202], (p)ppGpp can regulate the activity of PgpH

at an allosteric site. Further exploration in bacterial cells revealed that a mutant deficient in (p)ppGpp synthesis exhibited reduced levels of c-di-AMP, supporting the hypothesis that (p)ppGpp inhibits c-di-AMP phosphodiesterase activity in *vivo*. This dynamic between (p)ppGpp and c-di-AMP underscores a complex regulatory interaction where (p)ppGpp can modulate c-di-AMP levels, thereby influencing bacterial stress responses and viability under nutrient-limited conditions.

C-di-AMP is crucial for many bacteria when cultivated in nutrient-rich media[203]. In *L. monocytogenes* mutants lacking c-di-AMP, extensive sequencing of nearly 300 suppressor strains that can survive in rich media revealed that approximately 1.76% had mutations in the synthase domain of the *relA* gene, which disrupts (p)ppGpp production[193]. In the *Firmicute*, (p)ppGpp is synthesized by three synthases: RelA, RelP, and RelQ. The RelA serves a dual function, acting both as a synthase and a hydrolase for (p)ppGpp, whereas RelP and RelQ function solely as synthases[193]. This research proved that c-di-AMP becomes non-essential when the genes encoding (p)ppGpp synthases are deleted in *L. monocytogenes*, suggesting that the essentiality of c-di-AMP under rich medium conditions is to prevent the toxic accumulation of (p)ppGpp. Consistently, the homeostasis of (p)ppGpp is influenced by c-di-AMP; for example, deletion of *gdpP* in *S. aureus* significantly raises (p)ppGpp levels. This increase can be abolished by mutating the synthesis domain of RelA, but not by deleting *relP* or *relQ*, pointing to a particular dependence on RelA for the activation of (p)ppGpp synthesis by c-di-AMP[204]. However, c-di-AMP does not directly bind to RelA in vitro, suggesting that its activation occurs via an indirect mechanism. In 2020, a study in *L. monocytogenes* identified that CbpB, a c-di-AMP binding protein, binds and activates RelA synthetase domain. *L. monocytogenes* strains lacking c-di-AMP cannot grow due to elevated levels of (p)ppGpp. Since both PgpH and PdeA/GdpP function are inhibited by (p)ppGpp[136], the c-di-AMP and (p)ppGpp formed a homeostatic signaling loop within the cell: As c-di-AMP levels drop and cbpB is expressed, CbpB becomes free to bind RelA and activate its (p)ppGpp synthetase domain. Increased (p)ppGpp results in the inhibition of phosphodiesterases PgpH and PdeA/GdpP, leading to a buildup in c-di-AMP. c-di-AMP binds to free CbpB and prevents stringent activation[124]. This interplay underscores the complex regulatory networks controlling stress responses and growth in bacterial cells under varying environmental conditions.

CodY is a global transcriptional regulator responsive to GTP and branched-chain amino acids, known to repress genes involved in nutrient uptake and amino acid biosynthesis. During nutrient starvation, the accumulation of (p)ppGpp leads to a decrease in GTP levels, which disrupts CodY's ability to bind to DNA[205]. Interestingly, the lack of necessity for DACs in the Δ*relAPQ* mutant grown in rich media could be reversed by deleting *codY* [193]. Additionally, in minimal media, where CodY activity is likely reduced, DACs is no longer essential. And one study on urinary tract infections (UTIs) caused by *E. faecalis* showed that the expression of *gdpP* was significantly increased in a CodY-dependent manner after the bacteria transferred from culture medium to urine[206]. This indicates a connection between the CodY regulon and the c-di-AMP network that is independent of (p)ppGpp. Together, these findings suggest that c-di-AMP is crucial for bacterial growth in nutrient-rich conditions due to its role in preventing the toxic accumulation of (p)ppGpp, which can lead to detrimental changes in the expression governed by the CodY regulon. Further investigation is needed to fully understand the interplay between these regulatory networks and their implications for bacterial physiology.

1.5.3.4 Host immune response

Many pathogenic bacteria, including *S. aureus*, *L. monocytogenes*, and Group B *Streptococcus*, possess active intracellular enzymes that metabolize c-di-AMP. When these pathogens are engulfed by host phagocytes, they can release c-di-AMP which can be detected by specific receptors in the host cells, triggering a robust immune response[207]. To date, four proteins in eukaryotic host cells have been firmly identified as c-di-AMP receptors: STING, DDX41, RECON, and ERAdP[150,152].

STING (Stimulator of Interferon Genes) is a membrane protein located in the endoplasmic reticulum of phagocytes and can be activated by various cyclic dinucleotides (c-di-NMPs) such as c-di-AMP, c-di-GMP, and 3,3’-cGAMP released by pathogens, as well as 2',3'-cGAMP synthesized by the host's cyclic GMP-AMP synthetase (cGAS) in response to foreign DNA[208]. When activated by any of these cyclic dinucleotides, STING initiates a signaling cascade that activates downstream immunity-associated kinases. This signaling ultimately leads to the production of type I interferons (INFs) and pro-inflammatory cytokines, which are crucial components of the host immune response[209]. In the case of *L. monocytogenes*, which synthesize c-di-AMP by DacA, studies have shown

that when a *dacA*-overexpressing strain of *L. monocytogenes* is introduced into host cells, there is an increased production of the cytokine INF-β[140]. This result suggests that elevated levels of c-di-AMP can effectively activate STING, triggering a strong immune response in the host.

The helicase DDX41 plays a crucial role in activating a type I interferon (INF) immune response during the infection process. Functioning as a pattern-recognition receptor, DDX41 is capable of detecting specific signaling molecules and forming a complex with STING. The binding of either c-di-AMP or c-di-GMP to DDX41 enhances the formation of the DDX41-STING complex, which leads to a stronger INF response, strengthening the host's immune defense against pathogens[156].

Additionally, the host oxidoreductase RECON serves as a c-di-AMP receptor and plays a significant role in modulating the immune response. RECON is a negative regulator of NF-κB, a central mediator of the inflammatory process and a crucial component of various innate and adaptive immune responses[210]. When c-di-AMP binds to RECON during bacterial infection, it inhibits RECON's enzymatic activity. This inhibition leads to increased activity of NF-κB, promoting a pro-inflammatory state which enhances pathogen clearance. This mechanism provides an alternative to the STING-dependent signaling pathway in bolstering host defenses.

ERAdP is the last receptor for c-di-AMP that influences immune responses. Upon binding c-di-AMP, ERAdP activates TAK1 kinase, which in turn activates NF-κB. This activation leads to the production of pro-inflammatory cytokines in innate immune cells, culminating in the death of pathogenic bacteria. Both ERAdP and RECON appear to play similar roles in activating NF-κB when bound to c-di-AMP, thus forming a significant part of the host's immune response to bacterial infections[152].

1.5.3.5 β-lactam antibiotics resistance

Infections caused by antibiotic-resistant organisms represent a growing threat due to the increasing number of pathogens developing resistance to last-line antibiotics. Coupled with a slowdown in the development of new antibiotics, this presents a significant challenge for healthcare systems worldwide.

The β-Lactam antibiotics, such as penicillin and cephalosporins, target and inhibit penicillin-binding proteins (PBPs) that are crucial for the synthesis and maintenance of bacterial cell wall. Numerous studies have reported that c-di-AMP plays a role in β-lactam antibiotic resistance in different bacteria such as *L. monocytogenes*, *B. subtilis*, and *S. aureus*[189,192,211]. In general, mutations that decrease diadenylate cyclase activity has increased sensitivity to β-lactams. Notably, unregulated accumulation of c-di-AMP will also result in susceptibility to β-lactams, highlighting the delicate balance required in c-di-AMP levels for optimal bacterial cell wall maintenance and antibiotic resistance. However, the specific interactions and pathways between c-di-AMP signaling and β-lactam antibiotics remain to be fully clarified.

To date, many studies have indicated that disruptions in the metabolism of c-di-AMP impact the structural integrity of bacterial cell wall. This could be due to the direct regulatory effects of c-di-AMP or because fluctuations of this second messenger can render bacteria more susceptible or resistant to agents that indirectly compromise cell wall integrity (**Table 1.3**). Indeed, the synthesis of a cell wall lytic enzyme, which likely influences the stability of the cell envelope, is regulated in *Streptomyces coelicolor* via a riboswitch-mediated transcription-attenuation mechanism, affected by levels of c-di-AMP[212]. Furthermore, one *S. aureus* mutant strain deficient in the GdpP phosphodiesterase, which consequently accumulates c-di-AMP, shows increased amounts of cross-linked peptidoglycan[211]. In this bacterium, the rate of peptidoglycan crosslinking is significantly impacted by autolysins, such as AtlA and LytM[213,214], which break down the crosslinked peptide stems during peptidoglycan turnover. Notably, autolysin secretion is even increased in the absence of the GdpP enzyme[211]. Therefore, it appears that the enzymes involved in peptidoglycan synthesis are more likely to be influenced by c-di-AMP levels in *S. aureus* than those involved in its turnover or cleavage of crosslinks. However, the exact relationship between intracellular c-di-AMP levels and the activity of penicillin-binding proteins (PBPs) or carboxypeptidases, which operate in cell wall homeostasis, remains unclear. In addition, although the connection between c-di-AMP and cell wall metabolism has been established in *Actinobacteria*, the scenario in *Firmicutes* is less defined. The cell-wall-related phenotypes linked to c-di-AMP metabolism perturbations in *Firmicutes* might be interpreted differently.

Currently, the most popular theory explaining the relationship between c-di-AMP signal and bacterial cell wall integrity is the turgor model. Since c-di-AMP regulates the influx of inorganic ions, such as potassium, as well as low-molecular-weight compatible solutes in many bacteria, it's logical to assume that significant alterations in the levels of this second messenger nucleotide can lead to drastic changes in cellular turgor. Such disruptions in cellular turgor can affect the mechanical properties of the cell wall, potentially compromising the cell's ability to maintain its shape and withstand external stresses, thereby influencing its overall homeostasis and survival. Actually, the absence of c-di-AMP in *B. subtilis* and *L. monocytogenes* likely increases the cellular turgor to levels where the cell wall is no longer capable of withstanding the internal pressure, leading to cell lysis[127,173,192,215,216]. This hypothesis is strongly supported by observations that lysis does not occur when osmoprotectants (such as sucrose) are present, or when the concentration of extracellular osmolytes, like potassium ions, is reduced. These conditions help to stabilize the cellular turgor, reinforcing the cell wall integrity and preventing the catastrophic outcome of lysis, thus aligning well with the proposed impact of c-di-AMP on cell stability.

Based on the turgor model, increasing c-di-AMP level will reduce the turgor effect and therefore be more resistant to cell wall-targeting antibiotics. However, studies in *L. monocytogenes* showed that ΔPDE mutants are still highly sensitive to a lot of stress conditions, including the cell wall targeting antibiotics, β-lactams, and greatly attenuated for virulence[136]. In addition, similar phenotypes affecting growth, stress response, or virulence have been reported in c-di-AMP-accumulating mutants across a diverse range of bacteria, including *Bacillus subtilis*, *Bacillus anthracis*, *Mycobacterium tuberculosis*, *Streptococcus pneumoniae*, and *Streptomyces venezuelae*[127,135,217]. Notably, mutations in osmolyte transporters such as OppB or GbuABC only restored the viability of c-di-AMP depleting mutants (Δ*dacA*)[192], but not its susceptibility to cefuroxime, a β-lactam antibiotics. These results suggest that the regulation of c-di-AMP on bacteria cell wall integrity is more complicated than just cell turgor. Interestingly, Whiteley et al. also found that mutations of PycA, which reduced its activity, or *citZ* in Δ*dacA* mutant, rescued its sensitivity to β-lactams, indicating that c-di-AMP may affect bacteria cell wall-targeting antibiotics by mediating the central metabolism. The deregulation of bacterial metabolism may either

directly impair cell-wall synthesis, or result in the production of ROS, which is detrimental to bacteria, and can also be induced by antibiotics treatment.

To conclude, the regulation of c-di-AMP in bacteria is systematic; more than one pathway contributes to cell wall integrity. This small nucleotide messenger plays a critical role in managing essential cellular functions such as ion transport, turgor pressure, central metabolism, and probably the synthesis of peptidoglycan. The relationship between c-di-AMP and bacteria cell wall homeostasis warrants further investigation.

1.5 Figures and tables

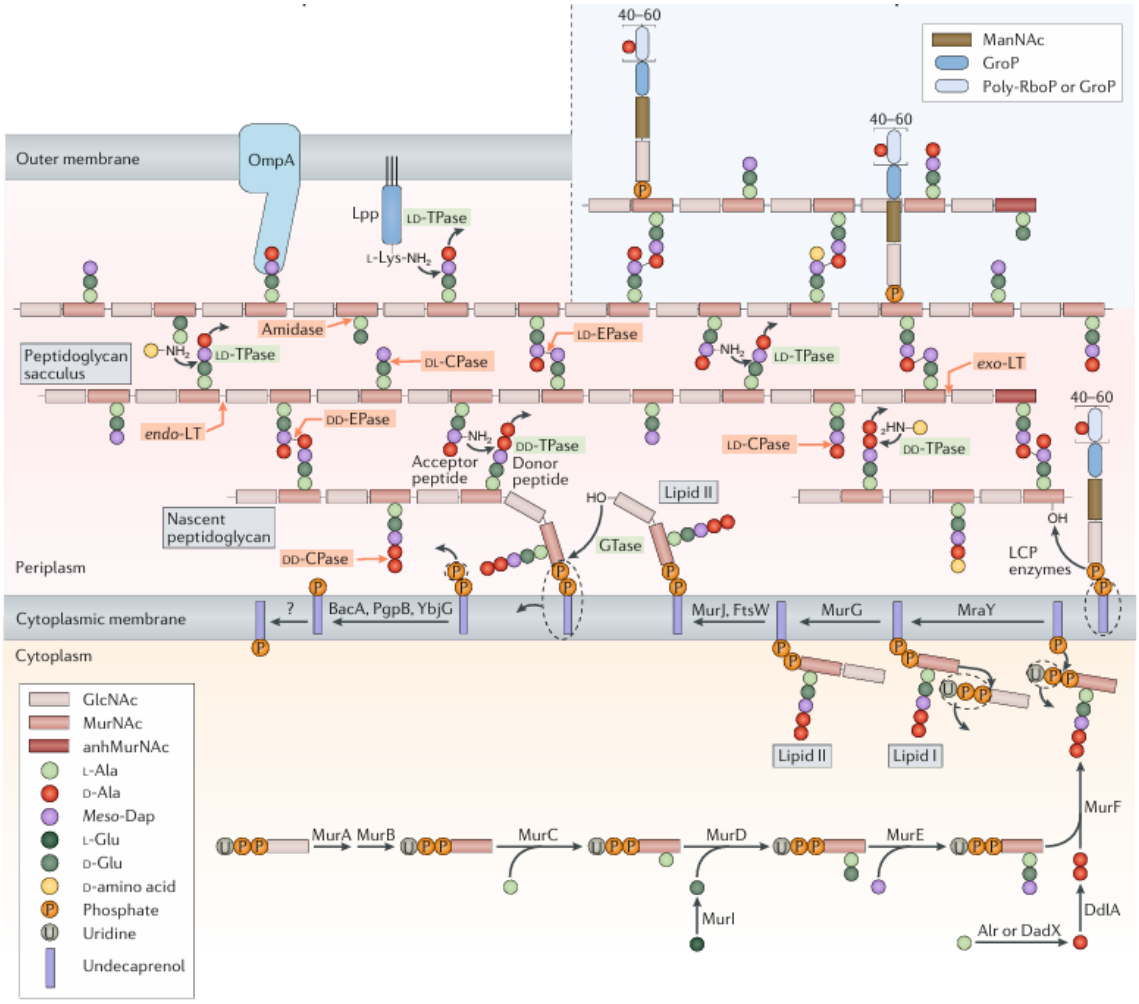

Fig 1.1 Peptidoglycan synthesis, cleavage and modification[218]. Shown are the necessary reactions and enzymes responsible for the synthesis and hydrolysis of peptidoglycan within the cell envelopes of Gram-negative (left) and Gram-positive (right) bacteria.

Table 1.1 Protein targets of c-di-AMP

Targets	Description	Species	Effect	Domain[a]	References
Transport proteins					
KimA	High-affinity potassium tranporter	*B. subtilis, L. monocytogenes, S. aureus, L. lactis*	Inhibition		(179,182)
KupA	Potassium transporter	*L. lactis*	Inhibition		(177)
KupB	Potassium transporter	*L. lactis*	Inhibition		(177)
KtrA	Gating subunit of potassium transporter	*B. subtilis, S. agalactiae*	Inhibition	RCK_C	(172,174,182,191)
KtrC	Gating subunit of potassium transporter	*B. subtilis, L. monocytogenes, S. aureus, M. pneumoniae*	Inhibition	RCK_C	(146,174,179,182,219)
CabP (TrKH)	Gating subunit of potassium transporter	*S. pneumoniae, S. agalactiae*	Inhibition	RCK_C	(161,191)
CpaA	Potassium exporter	*B. subtilis, S. aureus*	Activation	RCK_C	(146,160)
KhtT	Gating subunit of potassium exporter	*B. subtilis, S. aureus*	n.d.	RCK_C	(182)
CpeA	Cation proton exchange component	*S. venezuelae*	n.d.	RCK_C	(220)
OpuCA	ATPase subunit of osmoprotectant ABC transporter	*B. subtilis, L. monocytogenes, S. aureus, S. agalactiae*	Inhibition	CBS	(182,191,194,221)
MgtE	Magnesium transporter	*B. subtilis, L. monocytogenes, S. aureus*	n.d.	CBS	(182)
Signal transduction proteins					
PstA (DarA)	PII-like signal transduction protein	*B. subtilis, L. monocytogenes, S. aureus*	n.d.		(146,148,154,158,159,222)
CbpB (DarB)	Signal transduction protein, binding with RelA synthetase domain	*B. subtilis, L. monocytogenes*	Inhibition	CBS	(124,182,223)

CbpA		*L. monocytogenes*	n.d.	CBS	(223)
Enzyme					
PycA	Pyruvate carboxylase	*B. subtilis, L. monocytogenes, S. aureus, L. lactis*	Inhibition		(198,223)
Regulatory proteins					
KdpD	Two-component sensor kinase, for high-affnity potassium transporter	*L. monocytogenes, S. aureus, S. elongatus*	Inhibition	USP	(146,147,179,224)
NrdR	Repressor of the ribonucleotide reductase operon	*B. subtilis, L. monocytogenes, S. aureus*	n.d.		(154)
BusR	Repressor of the *busAB* osmoprotectant transporter genes	*L. lactis, S. agalactiae*	Corepressor	RCK_C	(170,191)
DarR	Transcription repressor	*M. tuberculosis*	Corepressor		(157)
The c-di-AMP riboswitch					
kimA	Regulation of *kimA* expression	*B. subtilis, B. thuringiensis*	Negative effector		(147,225)
ktrAB	Regulation of *ktrAB* expression	*B. subtilis, B. thuringiensis*	Negative effector		(165,181,184)
kdpFABC	Regulation of *kdpFABC* expression	*B. thuringiensis*	Negative effector		(165,181)
rpfA	Regulation of *rpfA* expression	*S. coelicolor*	Negative effector		(212)
ydaO	Regulates ion channels, responds to osmotic stress, facilitates cell wall metabolism and sporulation	*B. subtilis*	Negative effector		(134)

[a]Cells are blank where proteins do not possess a conserved c-di-AMP binding domain.

Table 1.3 Phenotypes associated with perturbation of c-di-AMP metabolism

Organism	Genotype	Phenotypes	C-di-AMP level	Suppression physiologically	Suppression genetically	References
L. monocytogenes	*dacA* depletion	Cell lysis, b-lactams sensitive, elongated cells	Decreased	Osmoprotective conditions	*dacA* expression	(216,226)
	Δ*dacA*	Cell lysis	No c-di-AMP		Inactivaton of *opp* and *gbu* genes (and many other genes, e.g., *pstA*)	(193)
	Δ*pdeA* (Δ*gdpP*)	Acid resistant, β-lactam resistant	Increased			(226)
	Δ*pdeA* (Δ*gdpP*) Δ*pgpH*	Salt hypersensitive, β-lactam resistant	Increased			(189)
	Δ*cdaR*	Increased lysozyme resistance	Increased			(216)
B. subtilis	*dacA* depletion	Cell lysis	Decreased	Osmoprotective conditions	*dacA* expression	(215)
	Δ*dacA* Δ*disA* Δ*cdaS*	Cell lysis during growth with potassium	No c-di-AMP	Low amounts of extracellular potassium	Mutations in the *nhaK* gene that probably enhance potassium ion export	(184)
	gdpP over-expression	β-lactams sensitive	Decreased			(215)
	Δ*gdpP* Δ*pgpH*	β-lactams sensitive	Increased			(189)
	Δ*gdpP cdaS* over-expression	Growth defect, curli formation	Increased			(127)
E. faecalis	*gdpP* and other mutations	β-lactams resistant	Increased			(227,228)
L. lactis	*gdpP* inactivation	Salt hypersensitive, temperature	Increased	Normal salt concentration	Mutations in *dacA* or *glmM*	(187,188)

		resistant, β-lactams resistant				
S. aureus	*dacA* G206S	Fast growth, β-lactams sensitive, salt tolerant	Decreased			(229)
	Δ*ltaS*	Cell lysis, increased cell size	Unknown	Osmoprotective conditions		(211)
	gdpP inactivation	β-lactams resistant, salt sensitive	Increased	Addition of 250 mM KCl		(146,230)
	Δ*gdpP*	β-lactams resistant, salt sensitive	Increased			(231)
S. mutans	Δ*dacA*	β-lactams sensitive	Decreased		*dacA*^{WT}	(232)
S. pneumoniae	Δ*gdpP*	β-lactams resistant	Increased		*gdpP* inactivation (and other mutations)	(233)
	Δ*gdpP* (*pde1*) Δ*pde2*	Shorter cells	Increased			(135)
S. suis	*dacA* R215S and other mutations	Lysozyme resistant, cell shape diversity	Unknown			(234)

Chapter 2

Publication

The role of *Listeria monocytogenes* PstA in β-lactam resistance requires the cytochrome *bd* oxidase activity

Zepeng Tu[1], David M. Stevenson[2], Darrel McCaslin[3], Daniel Amador-Noguez[2], TuAnh N. Huynh[1]*

[1]Food Science Department, University of Wisconsin – Madison

[2]Department of Bacteriology, University of Wisconsin – Madison

[3]Biophysics Instrumentation Facility, University of Wisconsin - Madison

*Corresponding author: thuynh6@wisc.edu

Contributions:

Tu Z. designed and performed the experiments for figure 2.1-2.3, 2.4A&C, 2.5-2.13, 2.15-2.16, analyzed and interpreted the data for 2.4B, 2.14.

Amador-Noguez D. performed the experiment for figure 2.4B.

Stevenson D.M. performed the experiment for figure 2.14.

Huynh TN. secured funding, conceived, designed, and supervised the study, and wrote and critically revised the manuscript.

2. THE ROLE OF *LISTERIA MONOCYTOGENES* PSTA IN β-LACTAM RESISTANCE REQUIRES THE CYTOCHROME BD OXIDASE ACTIVITY

2.1 Abstract

C-di-AMP is an essential second messenger that binds and regulates several proteins of different functions within bacterial cells. Among those, PstA is a structurally conserved c-di-AMP-binding protein, but its function is largely unknown. PstA is structurally similar to PII signal transduction proteins, although it specifically binds c-di-AMP rather than other PII ligands such as ATP and α-ketoglutarate. In *Listeria monocytogenes*, we found that PstA increases β-lactam susceptibility at normal and low c-di-AMP levels, but increases β-lactam resistance upon c-di-AMP accumulation. Examining a PstA mutant defective for c-di-AMP binding, we found the apo- form of PstA to be toxic for β-lactam resistance, and the c-di-AMP-bound form to be beneficial. Intriguingly, a role for PstA in β-lactam resistance is only prominent in aerobic cultures, and largely diminished under hypoxic conditions, suggesting that PstA function is linked to aerobic metabolism. However, PstA does not control aerobic growth rate, and has a modest influence on the tricarboxylic acid cycle and membrane potential – an indicator of cellular respiration. The regulatory role of PstA in β-lactam resistance is unrelated to reactive oxygen species or oxidative stress. Interestingly, during aerobic growth, PstA function requires the cytochrome *bd* oxidase (CydAB), a component of the respiratory electron transport chain. The requirement for CydAB might be related to its function in maintaining a membrane potential, or redox stress response activities. Altogether, we propose a model in which apo-PstA diminishes β-lactam resistance by interacting with an effector protein, and this activity can be countered by c-di-AMP binding or a by-product of redox stress.

2.2 Introduction

The small nucleotide c-di-AMP is an essential second messenger produced by thousands of bacterial species representative of most phyla[235,236]. Many bacteria, especially those in the Firmicutes phylum, require c-di-AMP for growth in rich laboratory media, although c-di-AMP levels must be regulated to avoid toxic accumulation[138,237]. Phenotypic characterization of bacterial mutants locked at low and high c-di-AMP revealed the multiple roles of c-di-AMP in many cellular processes, such as potassium homeostasis, central metabolism, stringent response, DNA integrity scanning, and cell wall metabolism[235]. Understanding of how c-di-AMP regulates these processes requires knowledge of its molecular targets and the function of those targets in bacterial cells. PstA, also called DarA (COG3870), is a conserved c-di-AMP-binding protein widespread among *Firmicutes*, and also present in several species of *Chloroflexota*, *Deinococcota*, and other minor phyla[235,238]. Of note, the nomenclature PstA also refers to a phosphate transport permease protein that is distinct from c-di-AMP-binding PstA. PstA binds c-di-AMP with a high affinity in the low micro-molar range, well within the physiological levels of c-di-AMP[146,148]. Furthermore, c-di-AMP binding is specific, as ATP, c-di-GMP and other related nucleotides do not bind to PstA[146,148]. However, the function of PstA remains obscure. Early predictions of PstA function were made based on its structural similarity to PII signal transduction proteins, such as GlnB and GlnK, which interact with and regulate effector proteins[148,158,159,222]. However, PstA structure is distinct from PII proteins in two loop regions, termed the T- and B- loops. Whereas PII proteins often harbor a large T loop that mediates protein-protein interactions, the PstA T loop is much shorter. Conversely, the B loop, which mediates ATP binding in PII proteins, is much enlarged in PstA and does not have signature residues for ATP binding[148,158,159,222]. Therefore, PstA likely engages in distinct cellular processes than PII proteins, although it is still predicted to interact with effector proteins. However, no interaction partners for PstA have been identified.

The Gram-positive bacterial pathogen *Listeria monocytogenes* requires c-di-AMP for growth in rich laboratory media and during infection. *L. monocytogenes* synthesizes c-di-AMP by a single diadenylate cyclase, DacA, and hydrolyzes it by the phosphodiesterases PdeA and PgpH[136,226]. In rich media, the Δ*dacA* mutant accumulates a toxic level of ppGpp that inhibits its growth, and also confers bacterial cell lysis and β-lactam susceptibility[193,226].

A deletion of *pstA* modestly rescues bacterial lysis in a *dacA*-depleted strain[148], as well as the growth of Δ*dacA* strain in rich media[192]. Interestingly, in minimal media that are permissive to Δ*dacA* growth with minimal lysis, Δ*dacA* is still highly sensitive to β-lactams, and this phenotype is largely suppressed by *pstA* deletion[192]. Together, these observations suggest that PstA is involved in cell wall homeostasis in *L. monocytogenes*, but the mechanisms for this regulation are unclear.

In this work, we explored the function of PstA in β-lactam resistance at normal, low, and high c-di-AMP levels in *L. monocytogenes*. We found that the apo form of PstA diminishes β-lactam resistance in the WT and Δ*dacA* strains, and that c-di-AMP-bound PstA promotes β-lactam resistance in the ΔPDE mutant that lacks both c-di-AMP phosphodiesterases. Strikingly, PstA plays a negligible role in β-lactam resistance during hypoxic growth. In hypoxic cultures, we found that the function of PstA requires the cytochrome *bd* oxidase (CydAB) of the respiratory electron transport chain, but independent from menaquinone regeneration. Our findings provide important physiological conditions for the identification of PstA molecular targets under cell wall stress.

2.3 Results

2.3.1 PstA diminishes β-lactam resistance at low and normal CDA levels, but promotes β-lactam resistance upon CDA accumulation

Both the depletion and accumulation of c-di-AMP sensitizes *L. monocytogenes* to β-lactams[189,192,226] (**Fig. 2.1A**) Since c-di-AMP binds PstA, we exploited a *dacA* mutant and a phosphodiesterase-deficient mutant (hereafter called ΔPDE), locked at low and high c-di-AMP levels respectively, to examine PstA function at different c-di-AMP availabilities in bacterial cells. Deletion of *dacA* is lethal for *L. monocytogenes* in the rich medium BHI, but *dacA* can be genetically depleted upon ectopic expression of an IPTG-inducible allele[226]. The conditionally depleted *dacA* (c-*dacA*) strain can still grow, albeit poorly, in BHI[226]. Because the WT, ΔPDE, and c-*dacA* strains exhibit different growth rates in BHI, we examined β-lactam susceptibility by normalizing the growth of each strain in the presence of antibiotics to that of the same strain in media only. The c-*dacA* Δ*pstA* strain was moderately improved for growth in BHI, consistent with previous studies[148,193] However, in the WT, c-*dacA*, and ΔPDE genetic backgrounds, neither *pstA* deletion nor over-expression exhibited appreciable effects on cefuroxime resistance (**Fig. 2.2**).

Because the lysis phenotype of c-*dacA* mutant in BHI can confound data interpretation on β-lactam resistance, we alternatively examined *L. monocytogenes* mutants in Listeria Synthetic Medium (LSM), a defined minimal medium that is permissive for the growth of a *dacA* null strain (*dacA::kan*, hereafter denoted as Δ*dacA*)[193]. In LSM, we found an apparent role for PstA in cefuroxime resistance at all c-di-AMP levels in bacterial cells. Deletion of *pstA* significantly rescued cefuroxime susceptibility in the Δ*dacA* strain, consistent with a previous study[192]; and we also found *pstA* over-expression to exacerbate Δ*dacA* susceptibility (**Fig. 2.1**). The effects of *pstA* deletion and over-expression in WT were similar, but less pronounced than in Δ*dacA* (**Fig. 2.1 and Fig. 2.3**). Interestingly, *pstA* mutations conferred the opposite effects in the ΔPDE strain, in which *pstA* deletion exacerbated the susceptibility of ΔPDE and *pstA* over-expression increased resistance (**Fig. 2.1**). Therefore, PstA promotes cefuroxime resistance in ΔPDE, and increases susceptibility in the WT and Δ*dacA* strains. Altogether, these data indicate that PstA is

important for cell wall integrity in LSM, but its function depends on c-di-AMP levels in bacterial cells.

2.3.2 C-di-AMP binding switches PstA function in β-lactam resistance

To determine if the differential effects of *pstA* mutations in the WT, Δ*dacA*, and ΔPDE strains is due to c-di-AMP binding, we sought to create a PstA variant that is defective for c-di-AMP binding. C-di-AMP binds PstA by interacting with multiple amino acid residues, for example the R/G-V/A-T tripeptide that coordinates the adenine bases[238]. Among those residues, single F36A and N41A mutations have been experimentally found to largely reduce c-di-AMP binding affinity, although neither mutation abolishes binding[148]. Therefore, we generated an F36A N41A double mutant variant ($PstA^{FN}$) to further diminish c-di-AMP binding. Western blot confirmed that $PstA^{FN}$ was expressed at a similar level to $PstA^{WT}$ in *L. monocytogenes* (**Fig. 2.4A**). The purified $PstA^{WT}$ and $PstA^{FN}$ proteins from *E. coli* exhibited similar circular dichroism spectra, indicating similar secondary structures (**Fig. 2.4B**). We next employed a thermal shift assay to interrogate c-di-AMP binding affinity by $PstA^{WT}$ and $PstA^{FN}$. As controls, we found that $PstA^{WT}$ binds c-di-AMP, but not ATP or NAD^+ (**Fig. 2.4C**). By varying c-di-AMP concentrations, we found that $PstA^{FN}$ is largely abolished for c-di-AMP binding (**Fig. 2.5**).

We introduced $PstA^{FN}$ to *L. monocytogenes* either by over-expressing $PstA^{FN}$ in the presence of the $pstA^{WT}$ allele, or by ectopically expressing $PstA^{FN}$ in the Δ*pstA* strains (**Fig. 2.5B-D**). In WT and Δ*dacA*, $PstA^{FN}$ appeared functionally equivalent to $PstA^{WT}$ in both ways of expression (**Fig. 2.5B-C**). By contrast, in the ΔPDE strain, $PstA^{FN}$ did not promote β-lactam resistance like $PstA^{WT}$ (**Fig. 2.5D**). Together, these data suggest that PstA largely functions in the apo form in WT and Δ*dacA*, and in the c-di-AMP-bound form in ΔPDE. The results also suggest that apo-PstA increases β-lactam susceptibility, and the c-di-AMP-bound form promotes β-lactam resistance.

2.3.3 A role for PstA in cefuroxime sensitivity is most prominent during aerobic growth and largely diminished in hypoxic cultures

We found PstA to be important for β-lactam resistance only in the defined medium LSM, but not in BHI. C-di-AMP is dispensable for *Staphylococcus aureus* growth in

anaerobic conditions, even in rich media[199]. Furthermore, some aerobic respiratory mutants of *L. monocytogenes* can grow in BHI but not in LSM[239]. These observations prompted us to examine if PstA phenotypic differences in these media were due to aerobic respiration. To test this, we re-examined *pstA* mutant strains in LSM under hypoxic conditions (**Fig. 2.6**). Strikingly, the phenotypes conferred by *pstA* deletion and over-expression were largely diminished in hypoxic cultures, regardless of c-di-AMP levels in bacterial cells. We noticed that PstA was still detrimental in hypoxic Δ*dacA* cultures at a low cefuroxime concentration, but its role was much reduced compared to aerobic cultures (compare **Fig. 2.1** and **Fig. 2.6**). These data suggest that the function of PstA in β-lactam resistance is related to aerobic metabolism.

Because the Δ*dacA* and ΔPDE strains both have multiple cellular defects that can confound PstA function, we chose to focus on understanding PstA function in the WT background for the following analyses. We found that the Δ*pstA* and WT + P_{spac}-*pstA* strains grew at similar rates to WT in aerobic LSM (**Fig. 2.3A**), so the role of PstA in β-lactam resistance is unrelated to growth rates but likely linked to other aerobic respiratory outputs.

2.3.4 The role of PstA in β-lactam resistance requires the cytochrome *bd* oxidase activity

The rates of bacterial respiration can affect antibiotic efficacy[240]. Both under normal growth and cefuroxime stress, *pstA* deletion and over-expression conferred negligible or modest effects on *L. monocytogenes* membrane potential, an output of the respiratory electron transport chain (ETC) (**Fig. 2.7**). Therefore, PstA does not appear to regulate aerobic respiration in *L. monocytogenes.*

Conversely, we examined whether respiratory ETC activity is required for PstA function in β-lactam resistance. The respiratory ETC in *L. monocytogenes* is comprised of a type II NADH dehydrogenase (Ndh1), terminal cytochrome oxidases (QoxABCD and CydAB), and an ATP synthetase[241,242]. To determine if ETC components are required for PstA function, we systematically disrupted each component and queried the resulting strains for cefuroxime susceptibilities. In almost all genetic backgrounds, *pstA* mutations did not significantly impact growth (**Fig. 2.8**). However, we noticed that PstA over-expression

reduced bacterial growth in the absence of the ATP synthase. In the WT strain, Δ*pstA* increased cefuroxime resistance and *pstA* over-expression increased susceptibility, as found above. We observed these phenotypes also in the absence of Ndh1, Qox, and the ATP synthase. Strikingly, PstA played no role in cefuroxime resistance in the Δ*cydA* or Δ*cydA* Δ*qoxA* strains (**Fig. 2.9B-C**).

2.3.5 PstA function is unrelated to potassium transport

As a component of the respiratory ETC, a function of CydAB is to maintain a proton motive force (PMF). Indeed, compared to WT *L. monocytogenes*, a *cydA*::Tn mutant has a severely reduced membrane potential, the main component of the PMF[243,244]. To determine if membrane potential correlates with PstA function, we compared the membrane potential of Δ*cydA* and Δ*cydA* Δ*qoxA* mutants with that of the Δ*ndh1*, *qoxA*::Tn, and *atpH*::Tn strains (**Fig. 2.10**). As expected, membrane potential was modestly reduced in *atpH*::Tn and significantly diminished in other mutants compared to WT. Interestingly, *cydA*::Tn and Δ*qoxA cydA*::Tn were the most affected strains, both exhibiting just ~25% of the WT membrane potential. Combined with our observation that a role of PstA is diminished in hypoxic conditions, these data raises the possibility that PstA function is dependent on a membrane potential.

A well-established function of c-di-AMP is to regulate osmolyte transport. Indeed, β-lactam susceptibility upon c-di-AMP depletion is proposed to be due to unregulated osmolyte influx that increases cell turgor[169]. Based on this model, a role for PstA in β-lactam resistance might be due to a PMF-driven osmolyte transporter. We focused on potassium, because many potassium transporters require a PMF and are regulated by c-di-AMP[169,235]. If apo-PstA increases cefuroxime susceptibility because it promotes potassium uptake or inhibits potassium export, then this toxic effect should be suppressed by potassium limitation. However, in both WT and Δ*dacA*, we found *pstA* deletion and over-expression to confer similar phenotypes at normal (4.8mM in LSM recipe[193]) and low (1mM and 0.1mM) potassium levels (**Fig. 2.11**). Therefore, the function of PstA in cefuroxime resistance is independent of potassium uptake.

2.3.6 Reactive oxygen species are not associated with PstA function in β-lactam resistance

Aerobic metabolism generates reactive oxygen species (ROS), which contribute to antibiotic lethality in *E. coli*[245]. If the function of PstA in β-lactam resistance is related to ROS formation, we would expect the Δ*pstA* strain to be reduced in ROS, and the WT + P_{spac}-*pstA* strain to accumulate ROS. Using the fluorescent dye H2DCFDA as a ROS reporter, we found a modest increase of ROS in the Δ*pstA* strain, although ROS accumulation was more pronounced in this mutant during growth with 0.5XMIC cefuroxime (**Fig. 2.12**). It is unclear whether the increased ROS levels in Δ*pstA* are physiologically impactful. The WT + P_{spac}-*pstA* strain exhibited similar ROS levels to WT under both normal growth and cell wall stress. Overall, ROS levels did not correlate with cefuroxime resistance conferred by *pstA* deletion and over-expression. Furthermore, the Δ*pstA* and WT + P_{spac}-*pstA* strains were similar to WT for H_2O_2 sensitivity, suggesting that PstA is not involved in oxidative stress response (**Fig. 2.13**). Together, these data indicate that the role of PstA in β-lactam resistance is unrelated to ROS or oxidative stress.

2.3.7 PstA has a modest role in the tricarboxylic acid activity of *L. monocytogenes*

The tricarboxylic acid (TCA) cycle is a major component of aerobic metabolism, and altered TCA activities have been shown to diminish β-lactam resistance in other bacteria[246]. *L. monocytogenes* has an incomplete TCA cycle that ends with the generation of α-ketoglutarate (**Fig. 2.14A**)[192]. Among TCA metabolites, we were able to detect pyruvate, citrate/isocitrate, and α-ketoglutarate at reliably quantifiable abundances in all strains (**Fig. 2.14B**). In the WT strain, cefuroxime treatment did not impact pyruvate and citrate levels, but modestly reduced α-ketoglutarate. Interestingly, the Δ*pstA* strain exhibited an approximately 2-fold increase in citrate/isocitrate levels compared to WT, although there was no change in α-ketoglutarate. Finally, over-expression of *pstA* resulted in a modest reduction in α-ketoglutarate, especially under cefuroxime stress (**Fig. 2.14B**). Neither *pstA* deletion nor over-expression altered NAD/NADH ratio, an indicator of redox balance and aerobic metabolism (**Fig. 2.15**). Overall, our analysis suggested a modest reduction of

TCA metabolites upon *pstA* over-expression, as well as increased citrate/isocitrate levels in the Δ*pstA* strain that do not globally impact TCA activity.

Given the interesting but rather inconsistent alterations in TCA metabolites, we independently queried the regulatory relationship between TCA activity and PstA by examining the effects of *pstA* mutations in the *citZ*::Tn strain, which does not synthesize citrate and is therefore disrupted for the TCA cycle. In the *citZ*::Tn genetic background, all strains exhibited significant growth defects that were most pronounced in the *citZ*::Tn Δ*pstA* strain, suggesting that PstA is important for another metabolic pathway in the absence of the TCA cycle (**Fig. 2.16**). The *citZ*::Tn strain was highly susceptible to cefuroxime, and this phenotype was exacerbated by either *pstA* deletion or over-expression (**Fig. 2.16**). However, the poor growth phenotypes of these mutants might be confounding factor in their cefuroxime susceptibility.

2.4 Discussion

Because PstA is widely present among Firmicutes, a major phylum of c-di-AMP-producing bacteria[235,236], understanding the function of PstA will provide significant knowledge on the function of c-di-AMP in bacterial cells. However, since its identification[146,154], the function of PstA in bacterial cells remain elusive despite extensive structural information in different bacteria[148,158,159,222]. Findings from our study point towards a functional relationship between PstA and aerobic metabolism under β-lactam stress in *L. monocytogenes*. Interestingly, despite a high affinity of c-di-AMP binding to PstA in vitro, apo-PstA appears to be a functional form and diminishes β-lactam resistance.

The structural resemblance between PstA and canonical PII proteins suggests that PstA functions in an analogous manner to other PII proteins, in that PstA likely interacts with and regulates effector proteins[247]. In the PstA structures that were previously solved for *L. monocytogenes*, *S. aureus*, and *B. subtilis*, apo-PstA exhibits flexible T- and B-loops that are stabilized upon c-di-AMP binding[148,158,159,222]. Because these loops mediate interactions between PII proteins with their partners, c-di-AMP binding is predicted to prevent the interactions of PstA with its effector proteins[222]. However, no effector proteins for PstA have been reported, and our own efforts at identifying PstA partners by co-immunoprecipitation have been unsuccessful, suggesting that interactions are transient. Our analysis of the $PstA^{FN}$ mutant, defective for c-di-AMP binding, indicates that apo-PstA is a functional form in β-lactam resistance. We propose that apo-PstA operates by binding partner proteins that are involved in cell wall stress response. C-di-AMP binding might abolish protein-protein interactions, or switch partners, as shown for PII proteins[247].

In the WT, Δ*dacA*, and ΔPDE genetic backgrounds, we observed interestingly differential roles of PstA in β-lactam resistance. If these opposite phenotypes are solely due to c-di-AMP availabilities, the $PstA^{FN}$ mutant should confer similar effects in these strains. Instead, we found $PstA^{FN}$ to be equivalent to $PstA^{WT}$ in the WT and Δ*dacA* strain, and play no role in cefuroxime resistance in ΔPDE. A simple interpretation is that PstA sequesters excess c-di-AMP in the ΔPDE cells, thereby alleviating the toxic effect of c-di-AMP accumulation in β-lactam resistance. It is also possible that c-di-AMP-bound PstA does not bind to partners that diminish cell wall integrity. This regulation would be

analogous to CbpB, another c-di-AMP-binding protein. Apo-CbpB interacts with RelA to activate ppGpp synthesis, and CbpB - RelA interaction is abolished by c-di-AMP[124,248,249]. We noticed also that PstA has the most pronounced role in β-lactam resistance in the Δ*dacA* strain. This is likely due to a physiological disturbance within Δ*dacA*, such as increased expression of a PstA interaction partner or osmolytes, as discussed below.

During aerobic growth, the function of PstA in β-lactam stress response appears to require the cytochrome *bd* oxidase CydAB. It is unlikely that PstA interacts with CydAB, since PstA is a cytoplasmic protein and CydAB is integrated in the membrane. Therefore, it is most likely that PstA requires an output of CydAB activity. Consistent with a previous study[243], we found CydAB to be the most important ETC component to maintain a membrane potential during aerobic growth. Therefore, PstA function might require a functional proton motive force (PMF). If correct, this raises the possibility that PstA regulates a PMF-driven transporter, analogous to the regulation of the ammonium transporter AmtB by the PII protein GlnK[250]. However, whether PstA indeed requires a PMF needs further validation, for instance by using different PMF inhibitors. Furthermore, our data exclude potassium transporters as targets of PstA regulation, but PstA might still regulate the uptake or biosynthesis of other osmotically active compounds.

In addition to its role in electron transport, the cytochrome *bd* oxidase in other bacteria, especially *E. coli*, also have other enzymatic activities in redox balancing, including catalase, peroxidase, sulfide oxidase, and reactive nitrogen species degradation[251]. If *L. monocytogenes* CydAB has a similar function in correcting redox imbalance, this will suggest that a PstA partner is inhibited by redox stress. However, those enzymatic activities have not been examined for *L. monocytogenes* CydAB, and should be considered in future investigations of PstA function.

Beyond cell wall homeostasis, our findings suggest that PstA contributes to specific components of *L. monocytogenes* aerobic metabolism, but not the overall metabolic output such as membrane potential or redox balance. Within the TCA cycle, over-expression of PstA modestly reduces pyruvate and α-ketoglutarate, and *pstA* deletion significantly elevates citrate/isocitrate. Together, these observations support a previous hypothesis that PstA might regulate pyruvate carboxylase or pyruvate dehydrogenase, although this model is yet to be biochemically validated[192]. Citrate accumulation was

previously proposed to be toxic to *L. monocytogenes* Δ*dacA* strain under cefuroxime stress[192]. Therefore, it was curious for us to observe increased citrate/isocitrate levels in the Δ*pstA* strain that is also increased in cefuroxime resistance. Our analyses of *pstA* mutations in the *citZ*::Tn strain revealed that a role for PstA in β-lactam resistance is likely independent of citrate/isocitrate, but suggest that PstA is important in maintaining another metabolic pathway in the absence of the TCA. In the presence of a fully functional respiratory ETC, we found PstA to have minimal impacts on the membrane potential or aerobic growth. However, *pstA* over-expression diminished *L. monocytogenes* growth in the absence of the ATP synthase, perhaps due to a combination of reduced TCA activity and energy output from the ETC.

Among different roles of c-di-AMP in bacterial cells, the regulation of osmolyte transport and turgor pressure is perhaps the mechanistically best-established function. C-di-AMP inhibits potassium and carnitine uptake, and activates potassium export, either through direct binding of osmolyte transporters or transcriptional regulation[169,235]. An unregulated osmolyte influx is proposed to be the underlying mechanism for β-lactam susceptibility at low c-di-AMP levels[169]. This model is supported by the observations that osmoprotectants suppress cell lysis conferred by c-di-AMP depletion. For *L. monocytogenes*, osmolyte transport is a likely contributor to the role of c-di-AMP in β-lactam resistance, but there is evidence for additional mechanisms by which c-di-AMP regulates cell wall homeostasis. First, the Δ*dacA* strain is still highly β-lactam sensitive in the chemically defined LSM medium that is permissive for its growth. Furthermore, we found negligible effects of potassium levels on cefuroxime susceptibility, both in the WT and Δ*dacA* strains. A previous genetic screen also revealed that the deletions of Opp or glycine betaine transporters can rescue Δ*dacA* growth but not cefuroxime susceptibility[192]. Finally, the ΔPDE strain is β-lactam sensitive and diminished for peptidoglycan precursors, despite a reduction in intracellular osmolytes[189,221]. Altogether, these observations highlight the intricate roles of c-di-AMP in cell wall metabolism that warrant further investigation.

Our study also revealed interesting observations about the relationship between aerobic metabolism and cefuroxime resistance in *L. monocytogenes*[246]. Whereas β-lactams markedly increases cellular respiration and TCA activity in *E. coli*[240,252], we found

that cefuroxime treatment of *L. monocytogenes* causes a modest increase in ETC and a modest decrease in TCA, which could lead to a redox imbalance in *L. monocytogenes* rather than a concerted metabolic upshift or downshift. Unlike *E. coli* in which β-lactams induces significant oxidative stress[245], *L. monocytogenes* exhibits modestly elevated ROS levels, and it is unclear whether they contribute to cefuroxime susceptibility. Interestingly, we found aerobic *L. monocytogenes* cultures to be more cefuroxime resistant than hypoxic cultures, contrasting with the contribution of cellular respiration to antibiotic susceptibility in *E. coli*[240]. More thorough investigations will be needed to dissect the contributions of central metabolism and respiration to cell wall-targeting antibiotic efficacy towards *L. monocytogenes*.

Our studies proved that the Apo-form of PstA increased *L. monocytogenes* β-lactam susceptibility while the c-di-AMP bound form of PstA increased *L. monocytogenes* β-lactam resistance. The PstA proteins are in Apo-form in WT and ΔdacA background but in c-di-AMP bound form in ΔPDE background. These results provide a perfect target point of inhibiting the binding between c-di-AMP and PstA to increase *L. monocytogenes* β-lactam sensitivity and improve antibiotics treatment efficiency. However, all of our experiments are done in the LSM a nutrient limited media and the cultures were grown at 37°C. a specific context that might not fully replicate the complex environments encountered by *Listeria* in natural settings or within the human body. In food products, *L. monocytogenes* may encounter varying levels of nutrients depending on the food type, processing, and storage conditions. In soil, the bacteria might face even more extreme nutrient variability and competition with other microorganisms. However, within the human body, *Listeria* encounters nutrient-rich environments like the bloodstream or nutrient-limited scenarios within certain cellular compartments. The body's immune responses also alter the availability of certain nutrients as a defense mechanism against pathogens. These conditions will change the intracellular c-di-AMP levels in *L. monocytogenes* and result in different binding pattern of c-di-AMP and PstA. Besides, in food and soil, temperatures can significantly vary, which affects bacterial metabolism, growth rates, and stress responses. These fluctuations can also influence how *L. monocytogenes* responds to environmental stresses as well as its survival strategies. These factors need to be considered when developing new treatments for *L. monocytogenes*.

2.5 Materials and methods

2.5.1 Bacterial strains and culture conditions

L. monocytogenes and *E. coli* strains in this study are listed in **Table 2.1**. *L. monocytogenes* cultures were grown in Brain Heart Infusion (BHI) broth at 37°C, improved *Listeria* synthetic medium (LSM, for WT, ΔPDE, and their derivatives), or LSM (for Δ*dacA* and its derivatives)[193]. The *dacA* conditional deletion mutant (c-*dacA*) mutant and its derivatives were maintained in BHI + 0.5mM IPTG agar, and IPTG was removed in BHI broth cultures, as previously described[226].

2.5.2 Antibiotic susceptibility assays

Antibiotic susceptibility in BHI was assessed by bacterial growth in 96-well plates containing 200 μL BHI only, or BHI plus two-fold dilutions of cefuroxime. Overnight cultures grown in BHI with shaking at 37°C was inoculated into each well, and bacterial growth was measured by OD_{600} at 37°C with intermittent shaking for 14 hours in a plate reader. For each strain, growth rates at each cefuroxime concentration were normalized to growth rate in BHI only of the same strain.

Antibiotic susceptibility in LSM was assessed by bacterial growth with shaking at 37°C for 16 hours. These cultures were inoculated to the same initial OD_{600} with overnight LSM cultures. For each strain, final OD_{600} in LSM + cefuroxime was normalized to OD_{600} in LSM only of the same strain.

2.5.3 Quantification of bacterial membrane potential

Bacterial cultures were grown in LSM to mid-log phase (OD_{600} ~ 0.4 – 0.6), washed, and diluted to $5x10^8$ cfu/mL in phosphate-buffered saline (PBS). Membrane potential was quantified using the fluorescent dye DiOC 2(3) (3,3'-diethyloxacarbocyanine iodide) based on published procedures with some modifications[239,253]. DiOC 2(3) (Thermo Fisher) was added to a final concentration of 4 μM and incubated for 30 minutes in the dark. As a control, the proton ionophore CCCP (carbonyl cyanide 3-chlorophenylhydrazone) (Sigma) was added at a final concentration of 5 μM and pre-incubated for 10 minutes prior to DiOC 2(3) addition[239,243]. Fluorescence by DiOC 2(3) was measured in a Biotek Synergy H1

plate reader by excitation at 488 nm and emission at 622 nm (green)/530 nm (red). Membrane potential was quantified by red/green fluorescence ratio.

2.5.4 Quantification of reactive oxygen species

Bacterial cultures were grown in LSM to mid-log phase (OD_{600} ~ 0.4 – 0.6), washed, and diluted to $5x10^8$ cfu/mL in PBS. 200 μL of diluted cultures were transferred into a black 96-well plate with 80 nM of H2DCFDA (2',7'-dichlorodihydrofluorescein diacetate) (Invitrogen). Fluorescence was measured in the Biotek Synergy H1 plate reader by excitation at 490 nm and emission at 530 nm over 30 minutes. Reactive oxygen species were quantified by the rates of increase in fluorescence intensity over 30 minutes.

2.5.5 Quantification of TCA metabolites by LC-MS

Bacterial cultures were grown in LSM or LSM + 0.5xMIC cefuroxime to mid-log phase (OD_{600} ~ 0.4 – 0.6), and rapidly filtered through a nitrocellulose membrane. Bacterial metabolite extraction and quantification were performed as previously described[254]. Total metabolites were extracted from bacterial cells using a cold extraction solvent (40% acetonitrile, 40% methanol, 20% water). Samples were analyzed on a Dionex UHPLC system coupled with a hybrid quadrupole–high-resolution mass spectrometer (Q Exactive Orbitrap; Thermo Scientific), using an Acquity UPLC BEH C18 column (Waters). Solvent A was composed of 97% water, 3% methanol, 10 mM tributylamine, pH 8.1-8.2. Solvent B was 100% methanol. Mobile phase was run on a gradient from 5 – 95% solvent B over 25 minutes. MS data in mzXML format was used for metabolite identification with the MAVEN software[255].

2.5.6 Protein purification

pstA and *pstA* F36A N41A were cloned from *L. monocytogenes* into pET20b with NdeI and XhoI restriction enzymes, and transformed into *E. coli Rosetta* for the expression of PstA-6xHis and PstA F36A N41A-6xHis proteins. For protein expression, *E. coli* cultures were grown at 37°C to OD_{600} ~ 0.7–0.9, and induced with 0.5 mM IPTG at 16°C overnight. Cultures were harvested by centrifugation. Cell pellets were lysed by sonication in lysis buffer (40 mM Tris-HCl, pH 8, 300 mM NaCl, 1 mM phenylmethylsulfonyl fluoride) and centrifuged. Proteins were purified using the His-Pur NiNTA resin (Thermo Scientific) as

previously described[189], and buffer exchanged into assay buffer (40 mM Tris-HCl pH 7.5, 100 mM NaCl, 20 mM $MgCl_2$). Protein concentrations were determined using the Bradford assay (Bio-Rad).

2.5.7 Thermal shift assay

Purified $PstA^{WT}$-6xHis and $PstA^{FN}$-6xHis proteins were tested for ligand binding using the thermal shift assay. Reactions were performed in PBS and included: 10 μM protein, 5xSYPRO Orange (Invitrogen), and ligand to a final volume of 25 μL. Fluorescence was monitored in a CFX96™ Real-Time System (Bio-Rad) with FRET detection, starting with an initial 2-minute incubation at 10°C, followed by a step-and-hold increase of 0.5°C for 10 seconds until 95°C. Melting temperatures were determined by the Biorad software.

2.5.8 Western blotting

FLAG-*pstA* was cloned into pPL2 for expression from the P_{hyper} constitutive promoter. pPL2-P_{spac}-FLAG-*pstA* (WT or F36A N41A mutant) was integrated into the Δ*pstA* strain, and the resulting cultures were tested for cefuroxime susceptibility to ensure that FLAG-*pstA* was functional. For immunoblotting, bacterial cultures were grown in LSM to OD_{600} ~0.5. Cell pellets were harvested by centrifugation and lysed by sonication. Cell lysates were loaded onto an SDS-PAGE gel with Precision Protein ladder (Bio-Rad). Proteins were transferred to a nitrocellulose membrane by the wet transfer method. The membrane was blocked with 5% nonfat milk, incubated with the anti-FLAG M2 antibody (Sigma) at 1:2,500 dilution. The secondary antibody was horseradish peroxidase-conjugated anti-mouse polyclonal antibody (Promega). The protein ladder was detected with StrepTactin-horseradish peroxidase conjugate (Bio-Rad). The membrane was visualized using a Clarity Western ECL substrate kit (Bio-Rad).

2.5.9 Circular Dichroism

CD spectra were recorded using an Aviv Model 420 Circular Dichroism Spectrophotometer (Aviv Biomedical, Inc, Lakewood, NJ) at 4 °C using 0.1 cm path length cuvettes. Data were corrected by subtraction of a buffer blank recorded in the same cuvette. Protein concentrations of stock solutions were based on results from a microplate based Bradford assay using BSA as a standard. Stock solutions were volumetrically

diluted as needed for the CD measurements. The $PstA^{WT}$ concentration was 0.40 mg/mL and the $PstA^{FN}$ was 0.33 mg/mL. The CD signal was converted to molar ellipticity using the above concentrations, 0.1 cm path length and a mean residue weight of 111 for both proteins.

2.5.10 NAD/NADH assay

Listeria cultures were grown in LSM at 37 °C with shaking to mid-log phase (OD600 ~ 0.4 – 0.6), washed, and diluted to $5x10^8$ cfu/mL in PBS. Resuspended bacteria were then lysed by a 1:1 addition of 1% dodecyl trimethylammonium bromide (Fisher Scientific) for 5 minutes with agitation. *Listeria* lysates were then processed to measure NAD/NADH levels using the NAD/NADH-Glo™ assay (Promega) according to the manufacturer's protocol.

2.6 Figures and tables

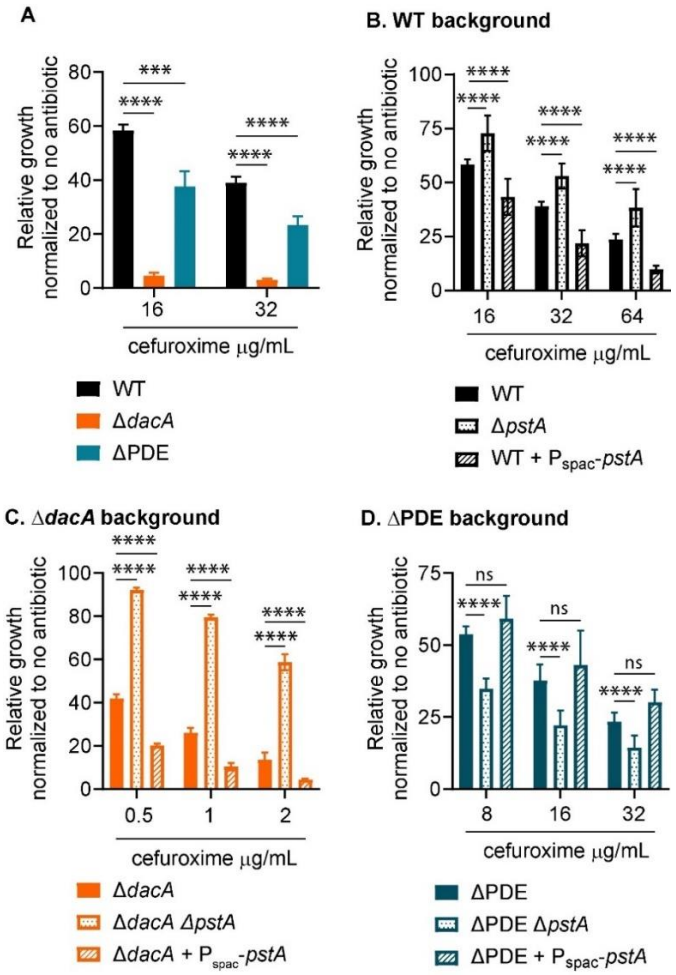

Figure 2.1 PstA diminishes β-lactam resistance at normal and low c-di-AMP levels in bacterial cells, and increases resistance at high c-di-AMP levels. *L. monocytogenes* cultures were grown with shaking in LSM with varying cefuroxime concentrations for 16 hours. For each strain, OD_{600} of cultures grown in cefuroxime were normalized to OD_{600} of the same strain grown in LSM only. (**A**) Both the Δ*dacA* and ΔPDE strains are sensitive to cefuroxime compared to the WT strain. (**B-D**) The effects of *pstA* deletion and over-expression on cefuroxime resistance were examined in the WT, Δ*dacA*, and ΔPDE genetic backgrounds. Data are average of three independent experiments. Error bars represent standard deviations. Statistics: two-way ANOVA; ***, P<0.001; ****, P<0.0001.

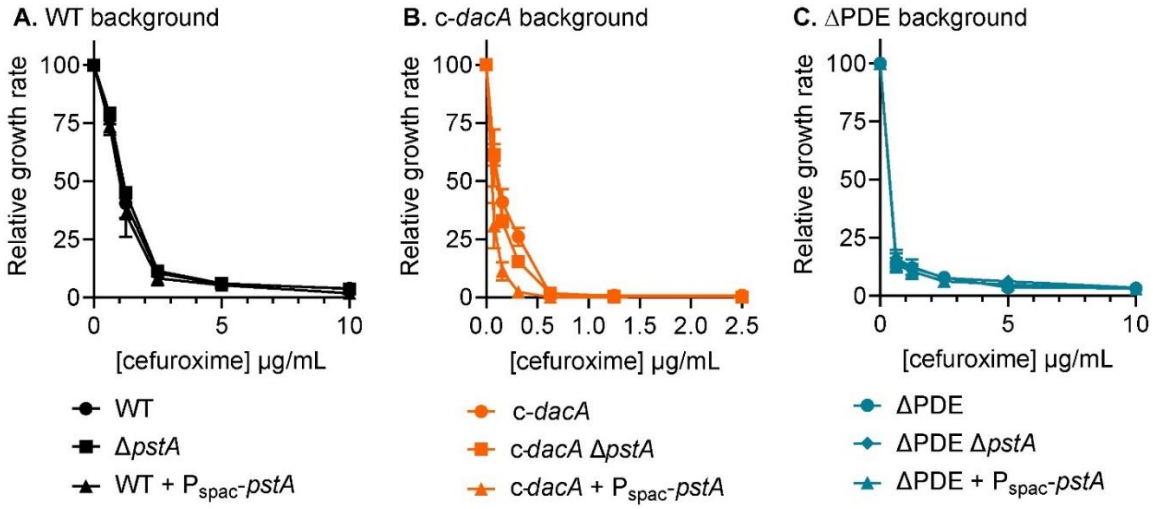

Figure 2.2 PstA has a negligible role in β-lactam resistance in rich media. *L. monocytogenes* cultures were grown in BHI broth, in the absence or presence of varying cefuroxime concentrations. For each strain, growth rates in cefuroxime were normalized to growth rate in BHI only. *C-dacA* indicates conditional deletion of the *dacA* gene, accomplished by ectopic expression of an IPTG-inducible *dacA* allele and deletion of the native *dacA* gene.

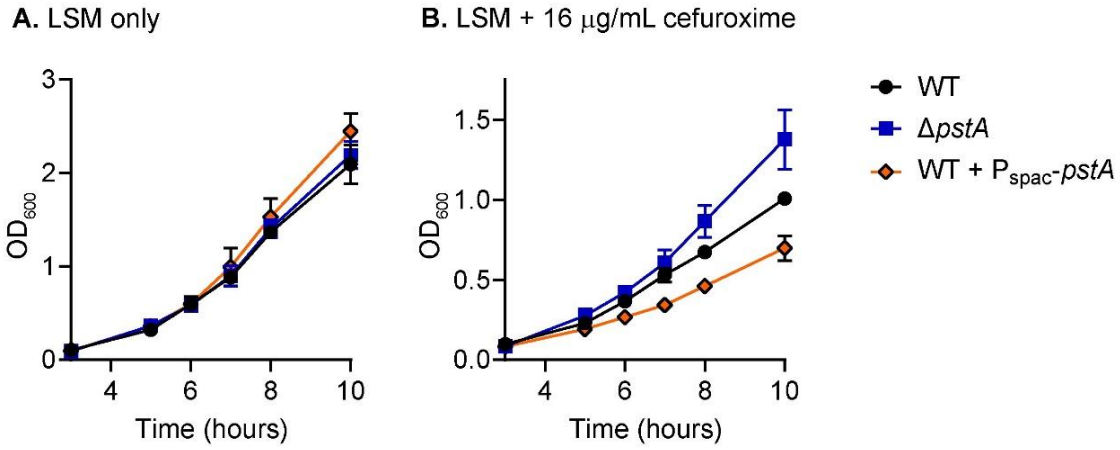

Figure 2.3 PstA does not regulate growth rates but diminishes cefuroxime resistance in aerobic cultures. *L. monocytogenes* cultures were grown in LSM (**A**) or LSM + 16 μg/mL cefuroxime (**B**), with shaking at 37°C. Data are average of three experiments.

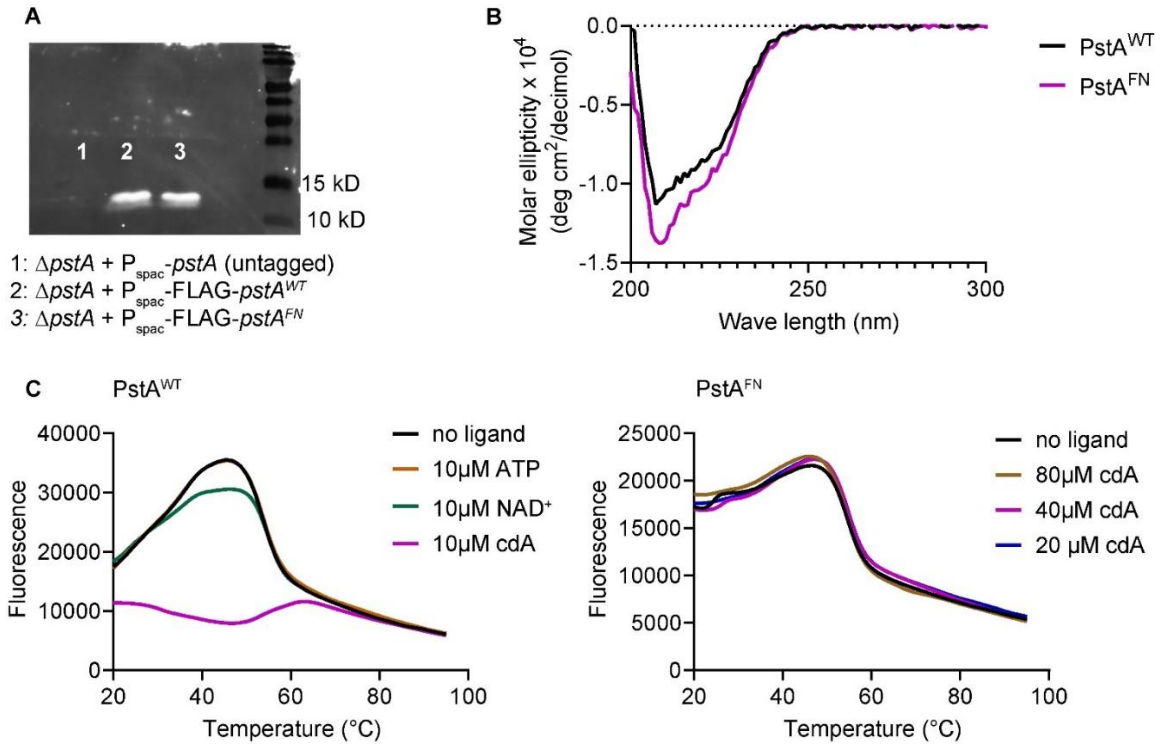

Figure 2.4 The PstA F36A N41A (PstA^{FN}) mutant is defective for c-di-AMP binding. (**A**) Western blot showing the detection of FLAG-PstA^{WT} and FLAG-PstA^{FN} using an anti-FLAG antibody. An isogenic strain expressing untagged *pstA* was examined as a control. (**B**) Circular dichroism spectra of PstA^{WT}-6xHis and PstA^{FN}-6xHis proteins. (**C**) Thermal shift assay for PstA^{WT}-6xHis and PstA^{FN}-6xHis, using 10μM protein and indicated ligands.

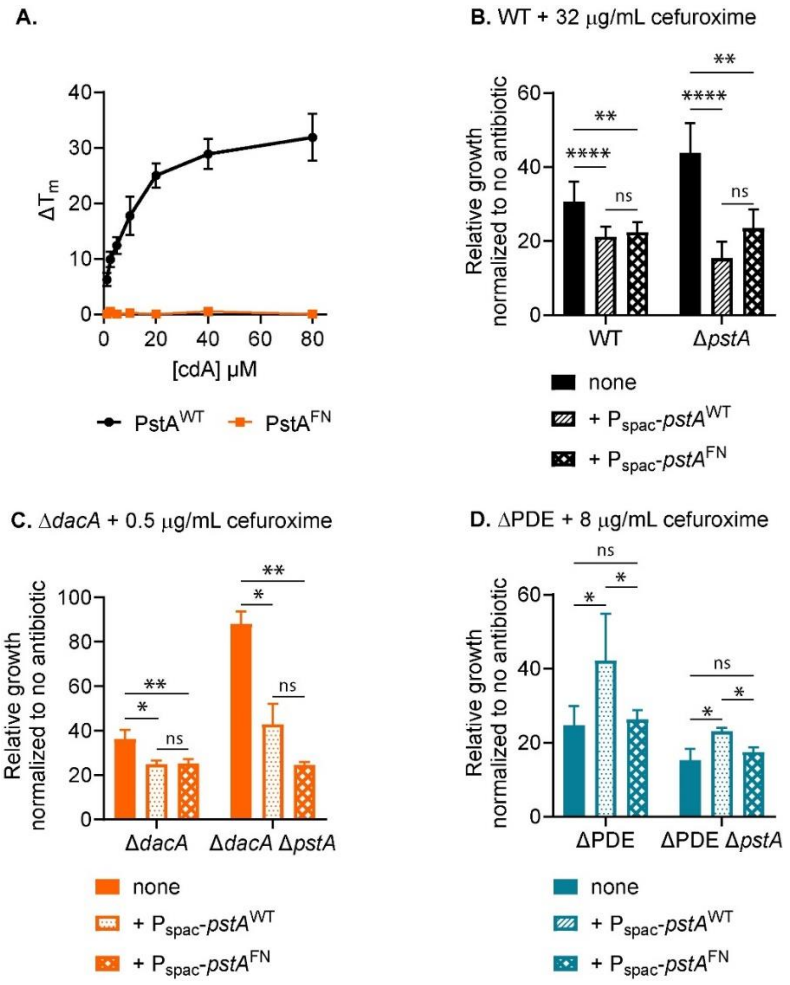

Figure 2.5 The PstA F36A N41A (PstA^{FN}) mutant, defective for c-di-AMP binding, is functionally equivalent to PstA^{WT} in the WT and Δ*dacA* strain, but not in the ΔPDE strain. (**A**) Binding of c-di-AMP to PstA^{WT} and PstA^{FN} proteins, determined by thermal shift assay. ΔT_m was calculated as melting temperatures at varying c-di-AMP concentrations compared to the absence of c-di-AMP in each experiment. (**B-D**) Cefuroxime susceptibility in LSM. *L. monocytogenes* cultures were grown with shaking in LSM with varying cefuroxime concentrations for 16 hours. For each strain, OD_{600} of cultures grown in cefuroxime were normalized to OD_{600} of the same strain grown in LSM only. In each genetic background, *pstA* was ectopically expressed from a constitutive promoter (P_{spac}) in the presence or absence of the native *pstA* allele. Data are average of three independent experiments. Error bars represent standard deviations. Statistics: two-way ANOVA. ns, non-significant; *, P<0.05; **, P<0.01; ****, P<0.0001.

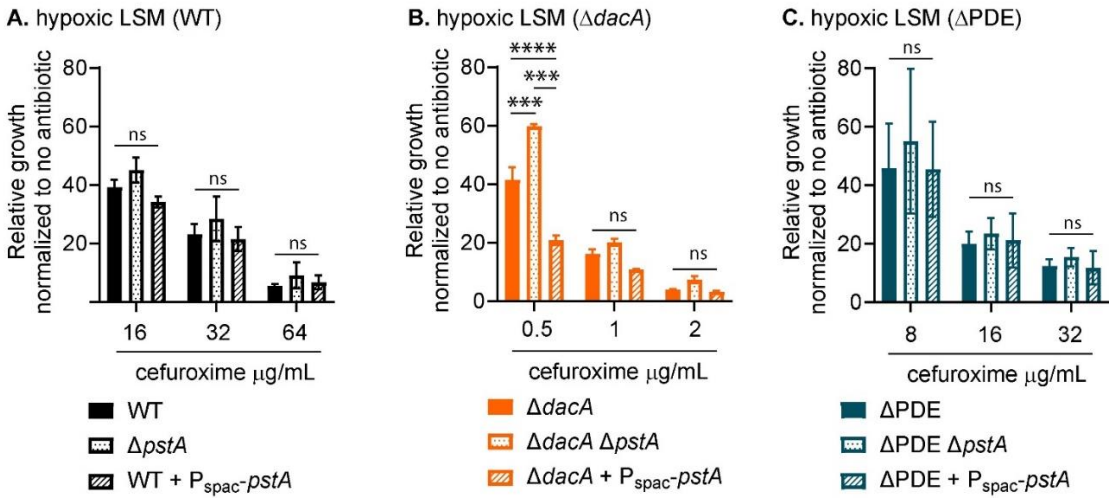

Figure 2.6 A role for PstA in β-lactam resistance is largely diminished under hypoxic conditions. *L. monocytogenes* cultures were grown static in LSM in a hypoxic chamber. For each strain, OD_{600} of cultures grown in cefuroxime were normalized to OD_{600} of the same strain grown in LSM only. The effects of *pstA* deletion and over-expression were examined in the WT (**A**), Δ*dacA* (**B**), and ΔPDE (**C**) genetic backgrounds. Data are average of three independent experiments. Error bars represent standard deviations. Statistics: one-way and two-way ANOVA. ns, non-significant; *, P<0.05; **, P<0.01; ****, P<0.0001.

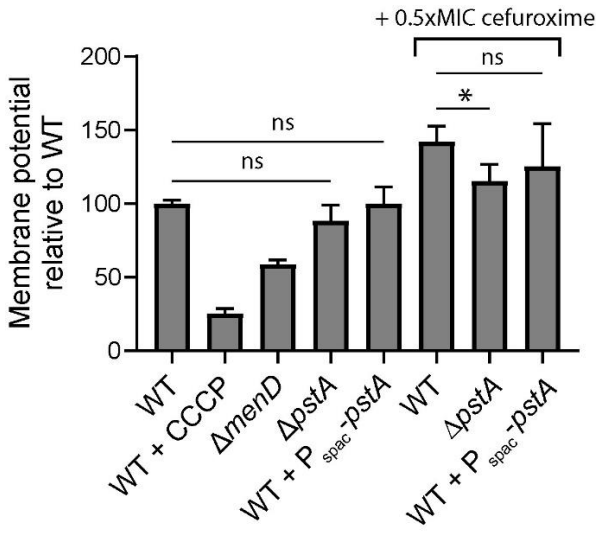

Figure 2.7 PstA has a negligible role in regulating aerobic respiration. Membrane potentials of *L. monocytogenes* cultures were quantified by staining with DiOC 2(3) and normalized to the value of the WT culture in each experiment. As a control, the WT strain was treated with 5 μM of the ionophore CCCP, which does not affect *Listeria* viability (17, 21). The Δ*menD* strain, deficient for menaquinone synthesis and diminished in membrane potential, was quantified as another control. Data are average of three independent experiments. Error bars represent standard deviations. Statistics: one-way ANOVA. *, $P < 0.05$.

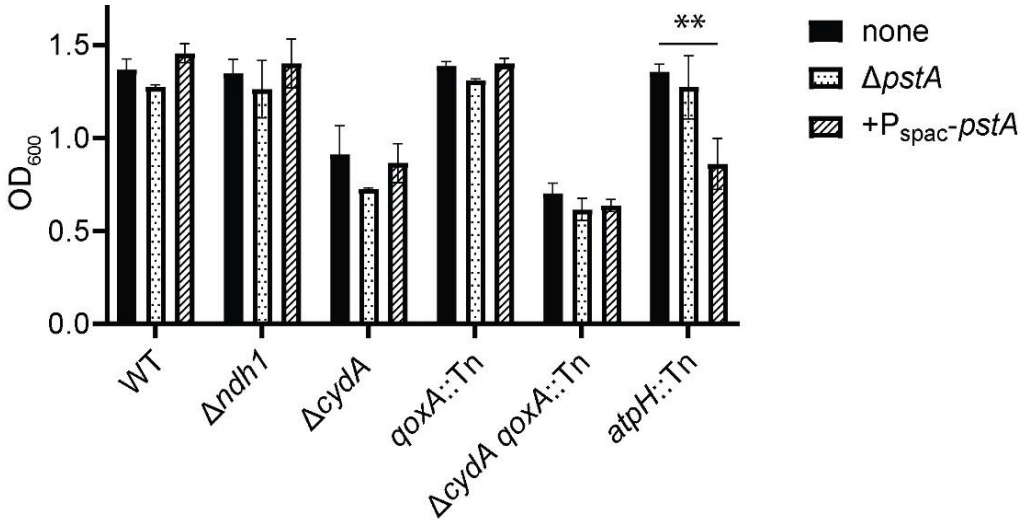

Figure 2.8 Growth of electron transport chain mutants upon *pstA* deletion and over-expression. Cultures were grown with shaking in LSM for 16 hours and OD_{600} values were recorded. Data are average of three independent experiments.

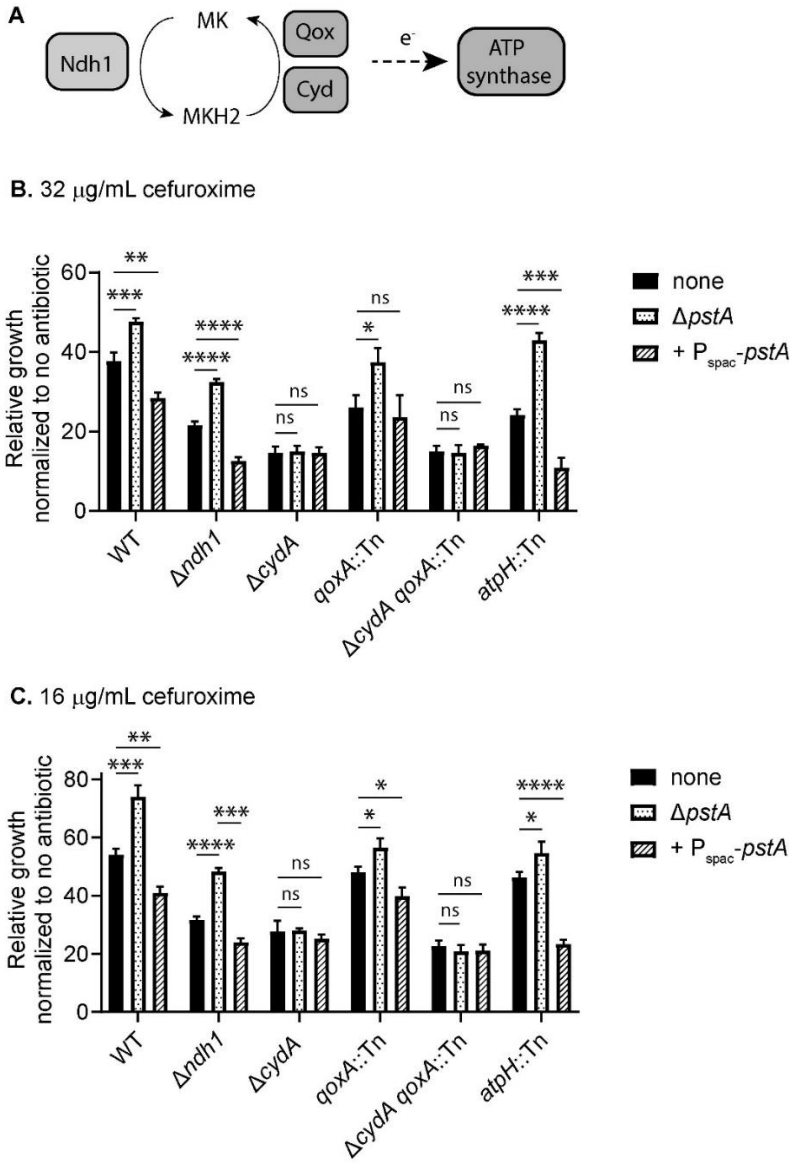

Figure 2.9 The function of PstA in β-lactam resistance requires the cytochrome *bd* oxidase. (**A**) Schematic of the respiratory electron transport chain (ETC) components in *L. monocytogenes*. (**B-C**) The effects of *pstA* deletion and over-expression were examined in the absence of each ETC component. Data are average of three independent experiments. Error bars represent standard deviations. Statistics: two-way ANOVA. *, P<0.05; **, P<0.01; ***, P<0.001; ****, P<0.0001.

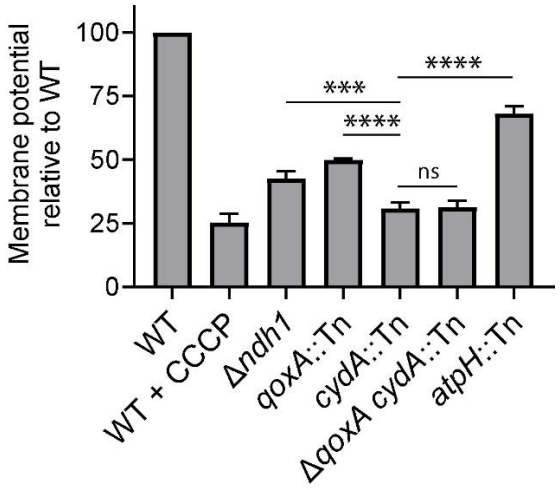

Figure 2.10 CydAB is important for maintaining a membrane potential. Membrane potentials of *L. monocytogenes* cultures were quantified by staining with DiOC2(3) and normalized to the value of the WT culture in each experiment. The WT strain treated with 5 μM of the ionophore CCCP was quantified as a control[199] Data are average of three independent experiments. Error bars represent standard deviations. Statistics: one-way ANOVA. ****, $P < 0.001$.

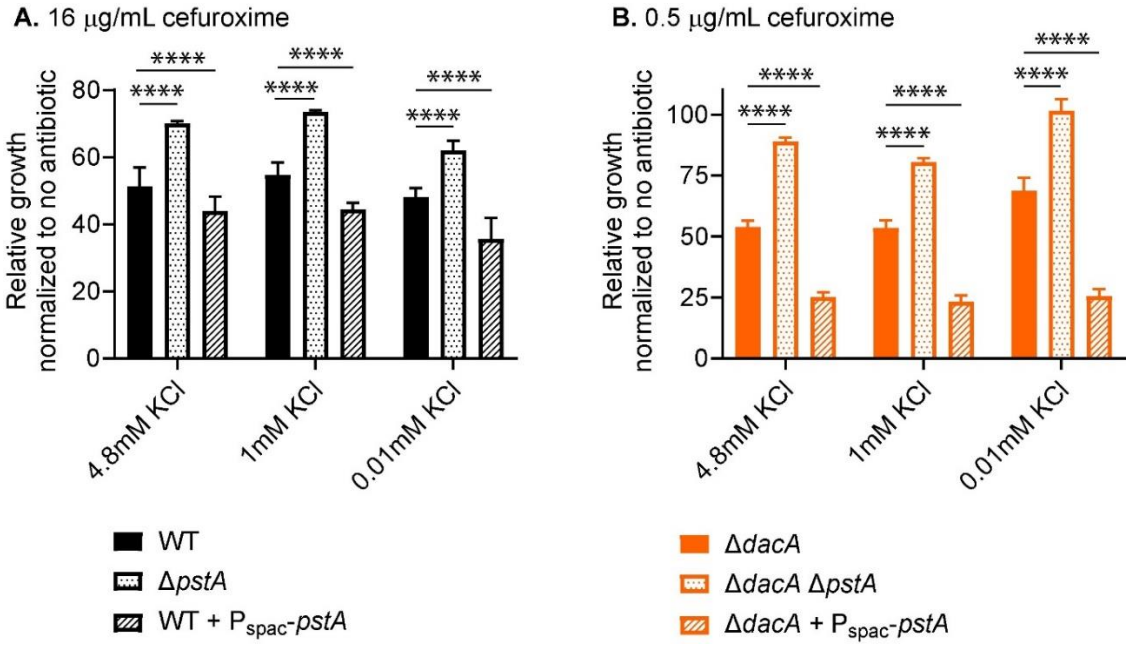

Figure 2.11 The function of PstA in β-lactam resistance is not affected by potassium availability. *L. monocytogenes* cultures were grown with shaking in LSM with 4.8mM (normal recipe), 1mM, or 0.01mM KCl for 16 hours. For each strain and at each potassium concentration, OD_{600} of cultures grown in cefuroxime were normalized to OD_{600} of the same strain grown in the absence of antibiotic. Data are average of three independent experiments. Error bars represent standard deviations. Statistics: two-way ANOVA; ****, P<0.0001.

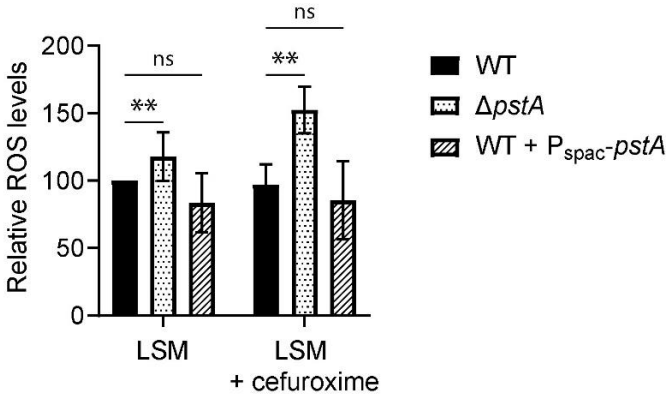

Figure 2.12 The function of PstA in β-lactam resistance is unrelated to reactive oxygen species formation. Reactive oxygen species were quantified with the fluorescent dye H2DFCDA, and fluorescence values were normalized to that of the WT strain grown in LSM only in each experiment. Cefuroxime treatment was achieved by growing *L. monocytogenes* in LSM + 0.5xMIC cefuroxime of each strain (32 μg/mL for WT and Δ*pstA*, 16 μg/mL for WT + P_{spac}-*pstA*). Data are average of four independent experiments. Error bars represent standard deviations. Statistics: two-way ANOVA. **, P<0.01.

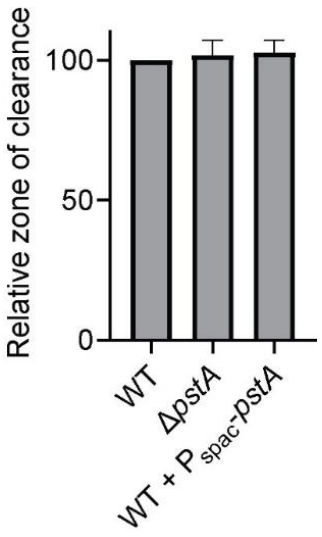

Figure 2.13 PstA is not involved in H_2O_2 sensitivity. Disk diffusion assay on LSM agar with sterile disks containing 2 μL of 35% H_2O_2.

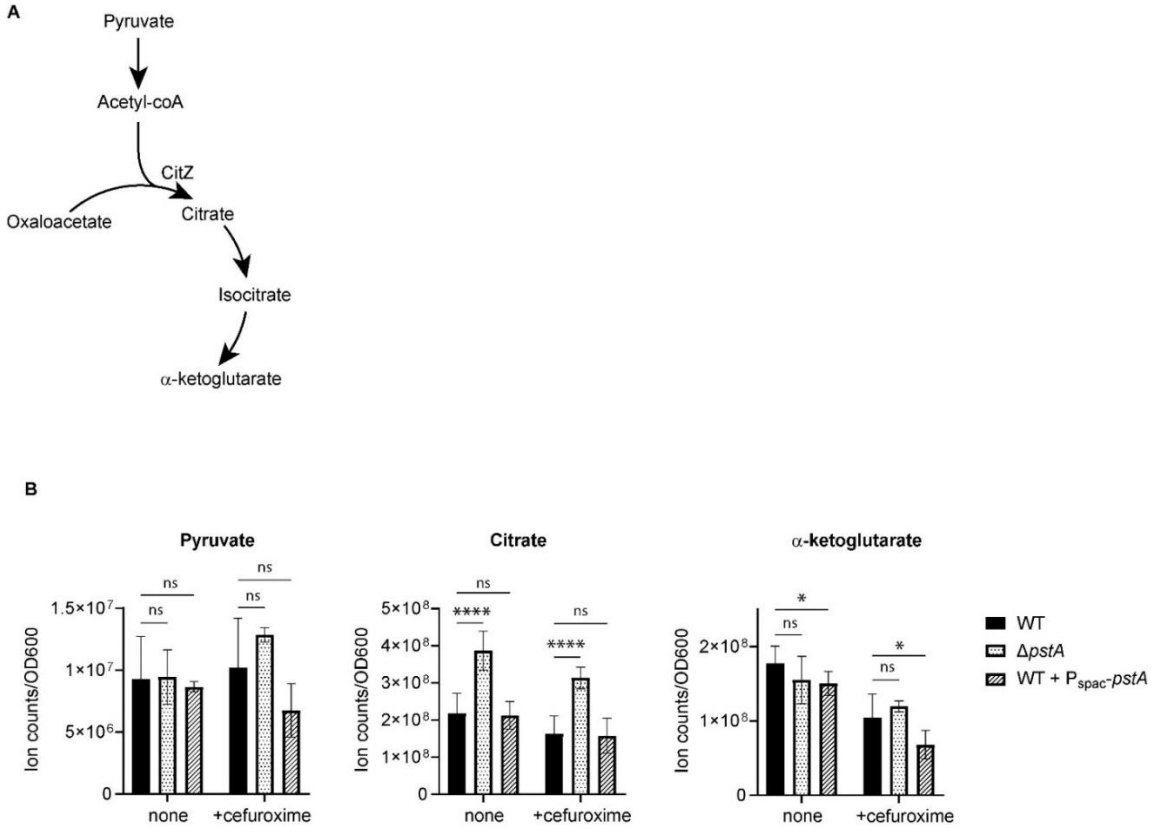

Figure 2.14 PstA has a modest role in the tricarboxylic acid cycle (TCA) activity of *L. monocytogenes*. (**A**) Schematic of the TCA cycle in *L. monocytogenes*. (**B**) LC-MS quantification of pyruvate, citrate/isocitrate, and α-ketoglutarate for cultures grown in LSM only or LSM + 0.5xMIC cefuroxime of each strain (32 μg/mL for WT and Δ*pstA*, 16 μg/mL for WT + P_{spac}-*pstA*). Statistics: two-way ANOVA; *, P<0.05; ****, P<0.0001.

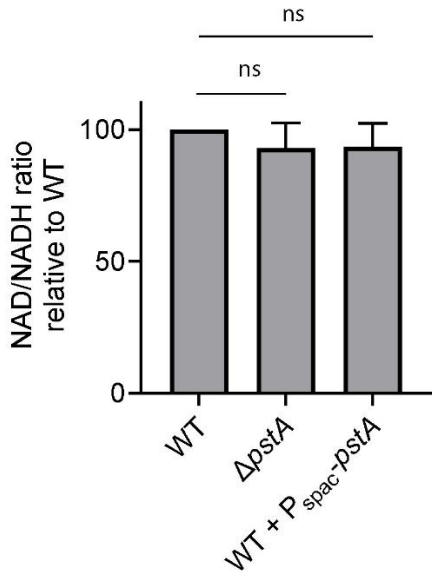

Figure 2.15 PstA does not regulate redox balance in *L. monocytogenes*. *L. monocytogenes* cultures were grown in LSM to OD_{600} ~0.5 and quantified for NAD/NADH ratio, which was normalized to that of WT in each experiment. Data are average of three experiments. Statistics: one-way ANOVA.

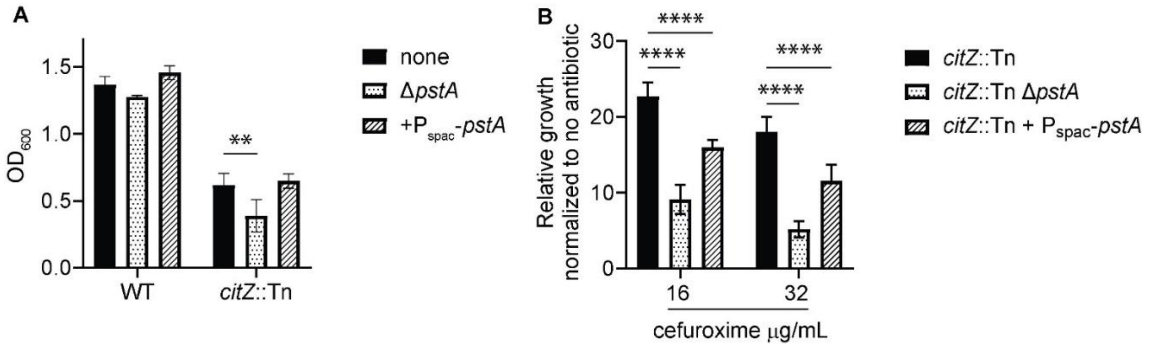

Figure 2.16 Disruption of the TCA cycle diminishes aerobic growth and β-lactam resistance. A. Growth of *pstA* mutants in LSM was recorded as OD_{600} of shaken cultures after 16 hours. **B.** Cefuroxime susceptibility was determined by normalizing growth in cefuroxime against growth of each strain in LSM only. Data are average of three independent experiments. Error bars represent standard deviations. Statistics: two-way ANOVA. ** P<0.01; ****, P<0.0001.

Table 2.1 Strains used in this study

Strain number	Genotype	Source
L. monocytogenes (derivatives of strain 10403S)		
TNHL262	*c-dacA*	(226)
TNHL951	*dacA*::kan (Δ*dacA*)	(193)
TNHL22	Δ*pdeA* Δ*pgpH* (ΔPDE)	(136)
TNHL349	Δ*pstA*	This study
TNHL387	P_{spac}-*pstA*	This study
TNHL345	*c-dacA* Δ*pstA*	This study
TNHL408	*c-dacA* P_{spac}-*pstA*	This study
TNHL354	ΔPDE Δ*pstA*	This study
TNHL388	ΔPDE P_{spac}-*pstA*	This study
TNHL952	Δ*dacA* Δ*pstA*	This study
TNHL953	Δ*dacA* P_{spac}-*pstA*	This study
TNHL848	P_{spac}-*pstA*^{FN}	This study
TNHL579	Δ*pstA* P_{spac}-*pstA*	This study
TNHL849	Δ*pstA* P_{spac}-*pstA*^{FN}	This study
TNHL503	Δ*ndh1*	(243)
TNHL499	Δ*cydA*	(243)
TNHL496	*qoxA*::Tn	(243)
TNHL882	Δ*cydA qoxA*::Tn	(243)
TNHL936	*atpH*::Tn	(243)
TNHL966	Δ*ndh1* Δ*pstA*	This study
TNHL967	Δ*ndh1* P_{spac}-*pstA*	This study
TNHL891	Δ*cydA* Δ*pstA*	This study
TNHL893	Δ*cydA* P_{spac}-*pstA*	This study
TNHL890	*qoxA*::Tn Δ*pstA*	This study
TNHL892	*qoxA*::Tn P_{spac}-*pstA*	This study
TNHL883	Δ*cydA qoxA*::Tn Δ*pstA*	This study
TNHL884	Δ*cydA qoxA*::Tn P_{spac}-*pstA*	This study
TNHL937	*atpH*::Tn Δ*pstA*	This study
TNHL938	*atpH*::Tn P_{spac}-*pstA*	This study
E. coli		
TNH457	pPL2-P_{spac}-*hly* 5'UTR-*pstA* in XL1B	This study
TNH498	pPL1-P_{spac}-*hly* 5'UTR-*pstA* in XL1B	This study
TNH528	pKSV7-Δ*pstA* in XL1B	This study
TNH431	pET20b-*pstA* in Rosetta	This study
TNHL910	pET20b-*pstA* F36A N41A in Rosetta	This study
TNHL870	pPL1-P_{spac}-hly 5'UTR-*pstA*^{FN} in XL1B	This study

Chapter 3

Appendix for PstA project

Investigation for the function of PstA in bacteria respiration and infection

Contributions:

Tu Z. designed and performed the experiments for figure 3.1-3.11, wrote the manuscript.

Huynh TN. secured funding, conceived, designed, and supervised the study, and critically revised the manuscript.

3. INVESTIGATION FOR THE FUNCTION OF PSTA IN BACTERIA RESPIRATION AND INFECTION

3.1 Abstract

PstA has been identified as a conserved c-di-AMP binding protein for decades in *Bacillus subtilis*, *Listeria. monocytogenes*, *Staphylococcus aureus,* and other Gram-positive bacteria. Despite numerous attempts to determine the role of PstA, its biological function remains elusive. Our previous studies have demonstrated that PstA plays a pivotal role in modulating β-lactam resistance in *L. monocytogenes*. This regulation of β-lactam susceptibility varies depending on c-di-AMP levels: the apo form of PstA under normal or c-di-AMP depleted background increases *L. monocytogenes* susceptibility; while c-di-AMP-bound form under c-di-AMP accumulated background enhances its resistance, particularly under the aerobic conditions. However, the specific molecular mechanisms underlying PstA's regulation of β-lactam susceptibility are still unclear. Here, several experimental findings we got have provided potential avenues for investigating PstA: There is a remarkable growth defect for Δ*pstA* mutant when glycerol is used as the sole carbon source under aerobic conditions, suggesting a role of PstA in aerobic respiration or glycerol metabolism, Further, PstA regulates bacteria intracellular growth and survival of *L. monocytogenes*, particularly in low c-di-AMP background. Deletion of pstA rescued c-di-AMP depletion mutant growth defect in macrophages and plaque formation in fibroblasts. Additionally, we also tried to identify specific PstA-binding proteins through various methods, and tested the interaction between PstA and Ndh2, but the results were unsatisfactory. These experimental findings provide valuable insights and direction for future research on the role of PstA in regulating β-lactam resistance.

3.2 Introduction

PstA (PII-like signal transduction protein A) is one of the c-di-AMP binding proteins that are present in many *Firmicutes*. It was first identified by a genome-wide DraCALA screen in *S. aureus*[146]. Subsequently, different studies further verified the bindings between PstA and c-di-AMP in various bacterium including *L. monocytogenes*[148] and *B. subtilis*[159]. In addition, the crystal structures, as well as binding patterns of PstA and c-di-AMP, have also been reported in these three organisms. The core domain of PstA shares the highly conserved architecture of the GlnB/K PII proteins, which is structurally representative of the larger PII family of proteins[148]. Two loops (B-loop and T-loop) in PstA that connect the various β-strands and α-helices have notable differences compared to canonical PII proteins, allowing it to specifically recognize c-di-AMP instead of other nucleotides that typically bind other PII proteins. In addition, the loops on PII proteins are essential for them to bind with other proteins, suggesting different binding targets for PstA and PII proteins[256]. Similar to PII proteins that bind their ligands, three c-di-AMP molecules are bound to symmetrically equivalent locations at the inter-monomer interfaces of the PstA homotrimer. However, unlike the roles of PII proteins in nitrogen regulation, very limited information is known about the biological function of PstA.

Previous studies identified that either clean deletion of *pstA* (Δ*pstA*) or mutations on PycA, which reduces its activity, concomitantly suppressed the essentiality of CDA and the sensitivity of the Δ*dacA* null mutant to β-lactam antibiotics[192]. These results suggest that PstA may play a role in bacteria metabolisms. Recently, our studies further proved that the regulation of PstA on L. monocytogenes β-lactam susceptibility varies depending on c-di-AMP levels: the apo form of PstA under normal or c-di-AMP depleted background increases *L. monocytogenes* susceptibility. In contrast, when c-di-AMP is accumulated due to the deletion of both c-di-AMP phosphodiesterases, PstA will bind with c-di-AMP and enhance its resistance[257]. Strikingly, we also found that PstA plays a negligible role in β-lactam resistance during hypoxic growth. In addition, during aerobic growth, PstA function requires the cytochrome bd oxidase (CydAB), a component of the respiratory electron transport chain. The requirement for CydAB might be related to its function in maintaining a membrane potential, or redox stress response activities. The exact molecular mechanisms of PstA regulating *L. monocytogenes* remain elusive.

Multiple attempts have been made to characterize the function of PstA. Aaron Whitely's previous research has employed three distinct methodologies, including pull-down assays, immunoprecipitation, and yeast two-hybrid assays to identify the binding partners of PstA. All his assays consistently reported a potential target that interacts with PstA: the NADH dehydrogenase Ndh2 (Lmo2638). On the other hand, one chemical proteomics technique has been utilized to delineate the c-di-AMP interactome within *Listeria monocytogenes*[146]. This investigation successfully isolated 12 proteins that exhibited statistically significant interactions when compared to the control group. Out of these, six proteins - PstA, CbpA, CbpB, PdeA, NrdR, and PycA - were definitively confirmed to be directly associated with c-di-AMP. Interestingly, Ndh2 also emerged as one of the top hits, although the direct interaction between c-di-AMP and Ndh2 was not substantiated. We suspect that Ndh2 could be affinity-purified by another c-di-AMP binding protein, with PstA emerging as a plausible candidate given its intrinsic characteristics as a regulatory protein. Additionally, considering the previously proposed role of PstA in facilitating aerobic metabolism in *Listeria monocytogenes*, it is reasonable to hypothesize that PstA interacts with Ndh2 and modulates its enzymatic activity during cell wall stress.

Here, we reported our attempts and findings for investigating the function of PstA and its binding proteins: There is a remarkable growth defect for Δ*pstA* mutant when glycerol is used as the sole carbon source under aerobic conditions, suggesting a role of PstA in aerobic respiration or glycerol metabolism, Further, PstA regulates bacteria intracellular growth and survival of *L. monocytogenes*, particularly in low c-di-AMP background. Deletion of pstA rescued c-di-AMP depletion mutant growth defect in macrophages and plaque formation in fibroblasts. Additionally, we also tried to identify specific PstA-binding proteins through various methods, and tested the interaction between PstA and Ndh2, although the results were unsatisfactory. These experimental findings offer valuable insights into PstA's role in regulating β-lactam resistance, providing a clear direction for future research. Subsequent studies could delve deeper into the biochemical pathways involving PstA, exploring its interactions with proteins, to better understand their impact on bacterial antibiotic resistance. This research could unveil new therapeutic targets to combat resistant bacterial strains, enhancing the effectiveness of β-lactam antibiotics.

3.3 Results

3.3.1 PstA exhibits a growth defect in LSM when glycerol is used as the sole carbon source.

Differences in the regulation of *L. monocytogenes* susceptibility to cefuroxime by PstA under aerobic and hypoxic conditions suggest that PstA may play a role in regulating *L. monocytogenes* aerobic respiration. In order to characterize the function of PstA in *L. monocytogenes* aerobic metabolism, we first tested the aerobic growth of *pstA* mutants in a wild-type (WT) background. An aerobic respiration medium was prepared by replacing glucose with non-fermentable glycerol as the sole carbon source in LSM (LSM-glycerol)[242]. We observed that Δ*pstA* mutants grew more slowly and had significantly longer doubling times compared to WT and pstA over-expression (P_{spac}-*pstA*) strain, despite their having the same growth rate in normal LSM (LSM-glucose) (**Fig. 3.1A-B**). These data indicate that PstA is crucial for either aerobic metabolism or, specifically, glycerol metabolism. We then investigated whether the growth defect of the Δ*pstA* mutant on LSM-glycerol affects its β-lactam resistance. Since PstA shows a stronger phenotype in low c-di-AMP background, we tested the cefuroxime sensitivity of *c-dacA*, *c-dacA* Δ*pstA*, and *c-dacA* P_{spac}-*pstA* mutants by plate spotting on LSM-glycerol with 1.25μg/mL of cefuroxime (**Fig. 3.1C**). Results showed that *c-dacA* Δ*pstA* still formed smaller colonies compared to *c-dacA* and *c-dacA* P_{spac}-*pstA*, consistent with the phenotype observed in WT background. Although it still exhibits a 1-log plating increase to *c-dacA*. And as expected, *c-dacA* P_{spac}-*pstA* mutants were defective by >2-log compared to *c-dacA*. These data suggest that the growth defect of the Δ*pstA* mutant on LSM-glycerol is independent of its susceptibility to β-lactams, indicating that PstA may have different functions in *L. monocytogenes*.

3.3.2 Deletion of PstA increased *Listeria* gentamicin resistance

In addition to β-lactam antibiotics, which specifically target bacterial cell wall, we also accessed the Δ*dacA* and Δ*pstA* mutants with other types of antibiotics such as gentamicin. Gentamicin is an aminoglycoside antibiotic that works primarily by binding to the bacterial 30S ribosomal subunit, interfering with protein synthesis and ultimately causing errors in the genetic code translation which leads to bacterial death. Therefore, gentamicin needs

to cross the bacterial cell envelope and reach the ribosomes located in the cytoplasm to exert its antibacterial effects. In *L. monocytogenes*, the transport of gentamicin is not fully understood but is thought to involve passive diffusion or energy-dependent transport. Bacteria with lower osmotic stress or higher membrane potential would be more sensitive to gentamycin. As expected, in contrast to cefuroxime susceptibility, the *c-dacA* mutant exhibited remarkably increased gentamicin resistance (**Fig. 3.2**). Since c-di-AMP negatively regulates both potassium and osmoprotectant transport, low level of c-di-AMP in *c-dacA* mutant result in increased potassium and osmoprotectant imports and therefore increase the intracellular osmotic stress, restricting the diffusion of gentamicin into cells. Interestingly, we also found that deletion of *pstA* also significantly increased the gentamicin resistance compared to WT. When grown in LSM with 75μg/mL of gentamicin, we still observed a modestly increased resistance in Δ*pstA* mutant and increased susceptibility when *pstA* is over-expressed in both WT and *c-dacA* background (**Fig. 3.2**). These results suggests that pstA deletion may causes low membrane potential, suggesting the role of PstA in bacteria aerobic metabolism.

3.3.3 PstA protein-protein interactions.

PstA belongs to the PII-like protein family, known for protein-protein interactions that disassemble upon binding with specific metabolites like α-ketoglutarate (αKG) and ATP. Crystallographic information indicates that binding of PstA with c-di-AMP decreases its “B-loop” accessibility and interrupts interactions with other proteins[148]. Additionally, my previous data showed that PstA largely functions in the apo form in both the WT and Δ*dacA* background, and the apo form of PstA is toxic for β-lactam resistance. I hypothesized that in the absence of c-di-AMP, PstA-protein interactions were stabilized leading to susceptibility to cefuroxime. To completely eliminate the interference of c-di-AMP on PstA binding with other proteins, I performed SPINE affinity purification of PstA in a low c-di-AMP background to identify PstA-interacting proteins.

I first constructed PstA with an N-terminal Flag-tag fusion linked by a GGS linker (Flag-PstA) (**Fig. 3.3A**) and introduced it into the *c-dacA* Δ*pstA L. monocytogenes* mutant. The Δ*pstA* mutation in the *c-dacA* background can be complemented by both over-expressing *pstA* or Flag-*pstA* (**Fig. 3.4, Table 3.2**), suggesting that Falg-PstA retained its biological

function. Affinity purifications from the lysates of *L. monocytogenes* Δ*dacA* Δ*pstA* P_{spac}-Flag-*pstA* mutant were compared to the purifications from Δ*dacA* Δ*pstA* lysates. Western blot analysis showed that Flag-PstA is well expressed (**Fig. 3.5**). However, even after incubating Listeria cell lysates with Anti-Flag beads for 4 hours or overnight, we failed to capture any specific PstA-binding proteins, as visualized by SDS-PAGE and silver staining (**Fig. 3.6**). We hypothesized that the endogenous expression level of Flag-PstA might not be adequate to recruit enough binding proteins detectable by silver staining. Therefore, we cloned Flag-GGS-PstA into pET20b (**Fig. 3.3C**), and over-expressed Flag-PstA in Rosetta. The Anti-FLAG® M2 Magnetic Beads were mixed with sonicated lysed Rosetta for 2 hours, and then mixed with Δ*pstA*, *c-dacA* Δ*pstA Listeria* cell lysates. The Rosetta cells containing empty pET20b plasmid served as a control. However, we still did not observe any specific PstA-binding proteins (**Fig. 3.6**). We also constructed PstA with a C-terminal StrepII-tag fusion linked by AAAS linker (**Fig. 3.3B**). Although over-expressing PstA-StrepII could complement the Δ*pstA* mutation in *c-dacA* background in terms of cefuroxime resistance (**Fig. 3.4**), we could not purify PstA-StrepII, and most of the proteins are adhered to the resins (**Fig 3.7**). This could result from the intrinsic binding affinity of PstA to Strep-Tactin resins.

3.3.4 Testing the interaction of PstA and type II-NADH dehydrogenase

In 2015, a chemical proteomics approach was performed to identify the c-di-AMP interactome of *L. monocytogenes*[154]. They identified 12 proteins that were statistically significant compared to control group, and 6 of them (PstA, CbpA, CbpB, PdeA, NrdR and PycA) were confirmed to directly bind with c-di-AMP. NADH dehydrogenase Ndh2 (Lmo2638) was also on the top hits, but the interaction between c-di-AMP and Ndh2 was not confirmed. Moreover, Aaron Whitely previously performed three different methods, including pull-down assays, immunoprecipitation, and yeast two-hybrid assays to identify PstA binding proteins, and Ndh2 appeared to show interactions with PstA in all three experiments. Furthermore, we also observed that deletion of *ndh2* significantly increases listeria b-lactam sensitivity in WT (**Table 3.2**). In addition to the conclusion from our previous research that PstA may induce *L. monocytogenes* aerobic metabolism, I hypothesize that PstA binds Ndh2 and regulates its activity.

To determine whether PstA interacts directly with Ndh2, I employed a bacterial two-hybrid analysis (BATCH). Since Ndh2 is a membrane protein, and PstA is a cytosolic protein, I suspected that PstA interacts with the inner part of Ndh2, specifically the NDH II domain. Genes encoding both full length Ndh2 and NDH II domain, as well as full length PstA, were cloned in fusion with T18 and T25 domains of adenylate cyclase. All combinations of interacting pairs were tested in assays. As a control, I also tested PstA binding with itself since PstA can form a homotrimer. The PstA was shown to bind to itself in all combinations, suggesting that the PstA protein is well expressed and folded, However, our experiments did not reveal a significant interaction between PstA and either full length Ndh2 or NDH II domain (**Fig. 3.8**). Additionally, I also performed a pull-down assay using N-terminal His-tagged PstA (His-PstA). The His-PstA protein was purified using pET20b, and the glutathione S-transferase tagged NDH II domain (GST-NDH II domain) was expressed and purified using a pGEX-6P plasmid. The GST tag was then cleaved off by PreScission Protease. We found that the pure NDH II domain was able to directly bind with Ni-NTA resin (**Fig. 3.9**). In conclusion, bindings between PstA and Ndh2 or NDH II domain were still not verified.

Next, we tested whether PstA regulates Ndh2 function, and how it contributes to *L. monocytogenes* β-lactam resistance. NADH dehydrogenase functions as part of the respiratory processes, playing a crucial role in catalyzing electron exchange from cytosolic NADH to a lipid-soluble quinone derivative. *In L. monocytogenes*, there are two distinct type II NADH dehydrogenases, Ndh1 and Ndh2. Ndh1 is a smaller enzyme that is part of the classical respiratory chain. It plays a major role in aerobic respiration, transferring electrons from NADH to ubiquinone and contributing significantly to the proton motive force used for ATP synthesis. Ndh2 is a larger, multi-subunit enzyme that does not contribute to proton pumping. Ndh2 is more flexible compared to Ndh1, as it can function under both aerobic and anaerobic conditions. It is crucial in a specialized flavin-based extracellular electron transfer (EET) mechanism, which transfers electrons from NADH directly to quinones and then directly to extracellular acceptors, even in the absence of oxygen. Mutations in *ndh2* will result in the impairment of extracellular electron transfer, and significantly reduce Ferric iron reductase activity[242].

To test if PstA regulates EET through Ndh2, we performed ferrozine assays for *pstA* mutants in both WT and *c-dacA* backgrounds. In this assay, *L. monocytogenes* mutants were exposed to an iron (III) source, and any iron (II) produced as a result of bacterial EET was quantitatively measured using ferrozine, a compound that specifically reacts with iron (II) to form a purple complex. The colorimetric changes were then measured spectrophotometrically using a plate reader. We found that neither deletion nor over-expression of *pstA* significantly changed their EET activity. However, *c-dacA* mutants showed decreased EET activity compared to WT. Interestingly, in *c-dacA* background, we found that deletion of *pstA* significantly restored its EET activity, while *c-dacA* P_{spac}-*pstA* abolished EET activity, almost the same as *ndh2* mutant control (**Fig. 3.10**). All these data suggest that PstA has a modest effect on bacteria extracellular electron transfer, but the regulation of PstA on Ndh2 remains unclear.

3.3.5 PstA reduces *L. monocytogenes* intracellular growth in low c-di-AMP background.

Previous studies have shown that the *Listeria c-dacA* mutant exhibits a growth defect in macrophages, and deletion of *pstA* in the *c-dacA* background resulted in a small but reproducible mitigation of the growth defect exerted by the loss of c-di-AMP production. The *c-dacA* Δ*pstA* mutant was reported to have slightly higher levels of intracellular growth in macrophages, and increased plaque formation in fibroblasts compared to the *c-dacA* strain[148]. These data indicate that PstA has a negative impact on bacterial intracellular growth and survival.

To further explore the function of PstA on *L. monocytogenes* intracellular growth, we tested the intracellular growth in macrophages and plaque formation in fibroblasts for both deletion and over-expression of *pstA* in WT and *c-dacA* background. Consistent with previous reports, we found that Δ*pstA* and P_{spac}-*pstA* mutants exhibited the same growth in macrophages and same plaque size compared to WT (**Fig. 3.10A&D**). In the *c-dacA* background, deletion of *pstA* modestly restored the intracellular growth defect and plaque formation for *c-dacA*. Over-expression of *pstA* in the *c-dacA* background resulted in reduced levels of intracellular growth, as well as the formation of plaques (**Fig. 3.10B&D**). Interestingly, we noticed that the growth rate in macrophages between 2 to 8 hours for the

c-dacA P_{spac}-*pstA* mutant is comparable to *c-dacA*, but it has significantly lower CFU counts compared to *c-dacA* at 2 hours post-infection. When *L. monocytogenes* infects macrophages, the bacteria are initially engulfed through phagocytosis, leading to their containment within vacuoles, specifically phagosomes. During the first hour or two post-infections, *Listeria* primarily remains within these vacuoles[258]. Therefore, we suspected that the *c-dacA* P_{spac}-*pstA* may have a defect in vacuole survival. To test this hypothesis, we deleted *hly* gene in WT, *c-dacA*, and *c-dacA* P_{spac}-*pstA* background. The *hly* gene encodes listeriolysin O, a pore-forming toxin that enables the bacterium to escape from the vacuole into the cytoplasm of host cells. When all the mutants are trapped in the vacuole, we expected that *c-dacA* P_{spac}-*pstA* mutant would have lower CFU counts compared to *c-dacA*. However, we observed that both Δ*hly c-dacA* and Δ*hly c-dacA* P*spac-pstA* exhibited the same growth in macrophages, even were the same as Δ*hly* mutants (**Fig. 3.10C**). These data suggest that PstA does not exacerbate the vacuole survival for c-dacA mutants, and the reduced growth for c-dacA Pspac-pstA in macrophage could result from a defect in escaping from the vacuole or survival in the cytosol.

3.3.6 Suppressor screening of a *c-dacA* P_{spac}-*pstA* EMS library.

To further identify the role of PstA in *L. monocytogenes* cefuroxime resistance, we generated an EMS library for the *c-dacA* P_{spac}-*pstA* and performed genetic screening. EMS (ethyl methanesulfonate) is a chemical mutagen that induces random point mutations by alkylating guanine bases in DNA, leading to G/C to A/T transitions. By treating the *Listeria monocytogenes c-dacA* P_{spac}-*pstA* mutant with EMS for 30min, we created a *c-dacA* P_{spac}-*pstA* EMS library with a mutation frequency of 0.12 mutation/genome, assessed by rifampicin resistance test[259,260]. The EMS library was then plated on LSM containing 2.5μg/mL of cefuroxime to screen for suppressors. This concentration of cefuroxime allows *c-dacA* to form colonies on the plates but not *c-dacA* P_{spac}-*pstA*. As a result, 183 colonies were selected from the plates. We confirmed their phenotypes by testing their growth in BHI with 2.5 μg/mL and 5 μg/mL of cefuroxime for 16 hours. At these two concentrations, the growth difference between *c-dacA* and *c-dacA* P_{spac}-*pstA* mutants are the most significant. We observed that 180 mutants have significantly higher growth compared to *c-dacA* P_{spac}-*pstA*. However, most mutants even grew better than the *c-dacA* mutant. We suspected that these mutants may either contain mutations that contribute to

β-lactam resistance even in WT background, which is independent of PstA function, or contain mutations that can restore c-di-AMP to WT level. Therefore, we also tested these mutants the growth with cefuroxime sensitivity in the presence of IPTG, mutants that have increased cefuroxime resistance when treated with IPTG, suggesting that the c-di-AMP level of these mutants remain low and can be induced. Finally, 5 mutants were further verified to be resistant to cefuroxime at the *c-dacA* mutant level, and they were still maintaining low c-di-AMP levels. This suggests that these suppressor mutants specifically alleviated the toxicity of PstA for cefuroxime susceptibility. We selected 3 suppressors for whole genome sequencing. However, we found that each mutant contained more than 10 gene mutations (**Table 3.3**), making it difficult to determine which gene is crucial for PstA-induced cefuroxime sensitivity. These results indicate that 30min of EMS treatment is too long for *c-dacA* P_{spac}-*pstA* strain. A better EMS library with shorter EMS treating time is needed for effective suppressor screening.

3.4 Methods

3.4.1 Bacterial strains and culture conditions

L. monocytogenes and *E. coli* strains in this study are listed in **Table 3.1**. *L. monocytogenes* cultures were grown in Brain Heart Infusion (BHI) broth at 37°C and improved *Listeria* synthetic medium (LSM)[193]. The *dacA* conditional deletion mutant (c-*dacA*) mutant and its derivatives were maintained in BHI + 0.5mM IPTG agar, and IPTG was removed in BHI broth cultures, as previously described[226].

3.4.2 Antibiotic susceptibility assays

Antibiotic susceptibility in LSM was assessed by bacterial growth with shaking at 37°C for 16 hours. These cultures were inoculated to the same initial OD_{600} with overnight LSM cultures. For each strain, final OD_{600} in LSM + cefuroxime was normalized to OD_{600} in LSM only of the same strain.

3.4.3 Co-immunoprecipitation for Flag-PstA and Western-blot

Flag-PstA was over-expressed from a neutral locus in the strains indicated, and LSM cultures of *L. monocytogenes* were grown to mid-log. Bacteria cells were fixed in 0.4% paraformaldehyde for 20 min. The fixation was stopped with the addition of 0.5M glycine for 5 min. The *Listeria* cultures were washed twice with PBS and resuspended in TBS-T buffer (20mM Tris HCl, pH 7.4,150mM NaCl, 0.1% Tween-20, v/v), and then lysed by sonication. 20μL of Anti-FLAG® M2 magnetic beads (Thermo Fisher) were added into 1mL of bacteria cell lysates and rotated at 4°C for indicated time. The beads were then washed with TBS 3x 1mL and then eluted with Laemmli sample loading buffer. The samples were analyzed by SDS-PAGE using 10% polyacrylamide gel and visualized via silver staining.

For Western-blot, 10μL of eluted samples were resolved by using 10% of SDS-PAGE. After transferring, blots of nitrocellulose membrane were blocked in 5% fat-free milk in TBS-T, and then incubated with anti-Falg antibody (1:2000 dilution), at 4°C overnight. After TBS-T washing, these blots were incubated with corresponding secondary antibody (1:5000 dilutions) and detected and visualized by ECL Western Blotting Substrate (Thermo Fisher).

3.4.4 Flag-PstA pull-down

Flag-PstA was over-expressed in *E. coli* using pET20b-Flag-GGS-*pstA*. An empty pET20b plasmid was also introduced in E. coli as a control. The *E. coli*. cultures were grown to mid-log phase, The bacteria cells were then washed with PBS and lysed by sonication in TBS-T buffer. 20μL of Anti-FLAG M2 magnetic beads were added into 1mL of *E. coli* lysates and incubating for 2 hours at 4°C. In the meantime, the *Listeria* strains indicated were grown in LSM to mid-log phase, washed with PBS, and then lysed by sonication in TBS-T buffer. The Anti-FLAG M2 magnetic beads from *E. coli* lysates were next washed with TBS 3x1mL and then mixed with *Listeria* cell lysates, incubating for 4 hours. The beads were washed with TBS 3x 1mL again and eluted with Laemmli sample loading buffer. Samples were analyzed by SDS-PAGE and visualized via Coomassi Blue Staining.

3.4.5 Pull-down assay for PstA-NDH II domain binding

Protein Expression and Purification:

Both Recombinant His-PstA and GST-NDH II domain were expressed in *E. coli* Rosetta cells. Cells were grown in LB medium supplemented with 100 μg/mL ampicillin at 37°C until the OD_{600} reached 0.6. Protein expressions were induced with 0.5 mM isopropyl β-D-1-thiogalactopyranoside (IPTG) at 16°C overnight. Cells were harvested, resuspended in PBS buffer containing 1 mM phenylmethylsulfonyl fluoride (PMSF), and lysed using sonication. The lysates were centrifuged at 12,000 × g for 20 minutes, and the supernatant was applied with Ni-NTA resins (Sigma-Aldrich) for His-PstA and glutathione agarose (Sigma-Aldrich) resins for GST-NDH II domain. For His-PstA, resins were washed three times with phosphate buffer (30mM KH_2PO_4/K_2HPO_4 pH 8.0, 300mM NaCl) + 30mM imidazole, and with 300 mM imidazole in phosphate buffer. For the GST-NDH II domain, resins were washed three times with phosphate buffer, and the PreScission Protease (0.05mg protease for every 1mg protein) was added to the resins in phosphate buffer and incubated overnight at 4°C for cutting the link between GST and NDHII. NDH II protein was collected by removing the resins by spinning.

Pull-down assay:

The His-PstA protein was mixed with NDH II domain in phosphate buffer for 3 hours at 4°C with gentle rotation, then the Ni-NTA resins were applied into the protein mix for another 4 hours at 4°C with gentle rotation. After incubation, the resins were washed 3 times with phosphate buffer + 30mM imidazole. The protein complexes were eluted from the resins with Laemmli sample loading buffer and analyzed by SDS-PAGE.

3.4.6 Bacterial two-hybrid assay

Clone the genes encoding PstA, Ndh2 and Ndh2 NDH II domain into the two sets of BACTH (Bacterial Adenylate Cyclase-Based Two-Hybrid) vectors (pKT25 or pKNT25 and pUT18C or pUT18) using standard molecular biology techniques[261]. Co-transform the recombinant plasmid harboring pKT25 and pUT18 indicated into *E. coli* BTH101 cells, and transformed derivatives were then grown overnight in LB with appropriate antibiotics + 0.5 mM IPTG at 30°C, 2 μL of each overnight culture were plated onto an indicator plate (LB + 100μg/mL Amp + 50μg/mL Kan + 40μg/mL X-gal + 0.5mM IPTG). Incubate plates at 30°C check plates, and take pictures at 24 hours.

3.4.7 Ferrozine assay

Listeria monocytogenes cells, cultivated to mid-log phase in LSM, were washed twice and adjusted to an OD_{600} of 0.5, then suspended in fresh LSM containing 4 mM ferrozine. The assay commenced by introducing 100μL of the cell suspension into an equal volume of either 50mM ferric ammonium citrate or ferric (hydr)oxide. These experiments were performed in triplicate at 37°C using a 96-well plate format and a plate reader. Absorbance at 562 nm (OD562) was recorded every 1 minute for a duration of one hour. Maximal rates (typically over 25 min) calculated from Fe^{2+} standard curves are reported.

3.4.8 Generation of *c-dacA* P_{spac}-*pstA* EMS library

The *Listeria monocytogenes c-dacA* P_{spac}-*pstA* culture was grown in BHI with 0.5 mM IPTG to OD_{600} of 0.9. Bacteria cells were then washed twice with PBS and resuspended in Tryptic soy broth (TSB) to reach the cell concentration of $2x10^9$ CFU/mL. EMS was added to the suspended culture (1.5% v/v) and incubated at 37°C for 30min (The incubation time can be adjusted based on the mutation rate). After incubation, cells were washed twice with TSB to remove EMS, and stocked in BHI + 40% glycerol at -80°C.

3.4.9 Assess mutation frequency by rifampicin resistance

Thaw 100μL aliquot of library and make serial dilutions from 10^0 to 10^{-7} in BHI. Then plate dilutions onto both BHI and BHI + 5μg/mL rifampicin plates. The rifampicin-resistant frequency is calculated by the counts of rifampicin-resistant isolates from BHI rifampicin plates divided by the total population from BHI plates, and the mutation rate (mutations/genome) can be calculated via equations from Kari et al. (2011)[260].

3.5 Figures and tables

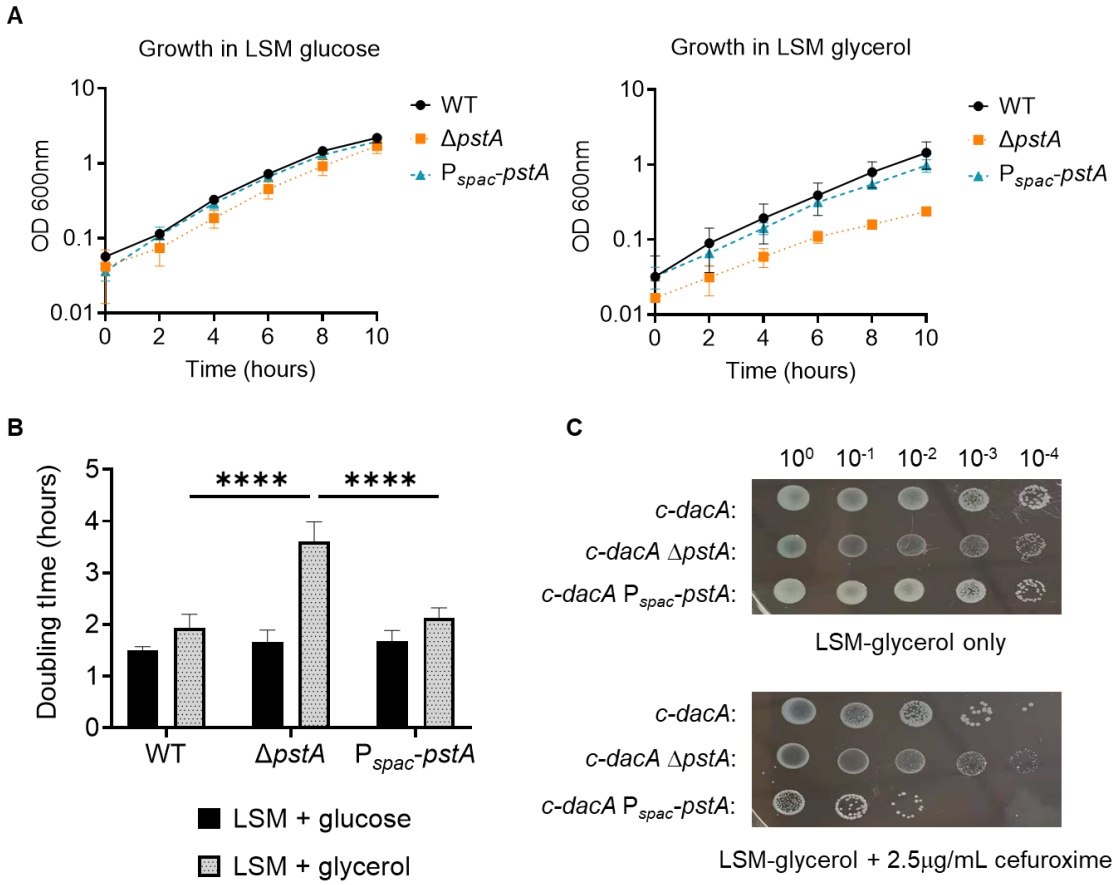

Figure 3.1 Deletion of PstA impaired Listeria growth in LSM-glycerol. (**A**) *L. monocytogenes* cultures were grown in LSM containing glucose (left) or glycerol (right) as the sole carbon source shaking at 37°C. Data are average of three experiments. (**B**) Growth doubling time of each mutant strain grown in LSM-glucose or LSM-glycerol. (**C**) Agar plate spotting of *Listeria* mutant stains in serial 10-fold dilutions on LSM-glycerol containing 0 μg/mL (top) or 2.5 μg/mL (bottom) of cefuroxime. Error bars represent standard deviations. Statistics: two-way ANOVA. ****, P<0.0001.

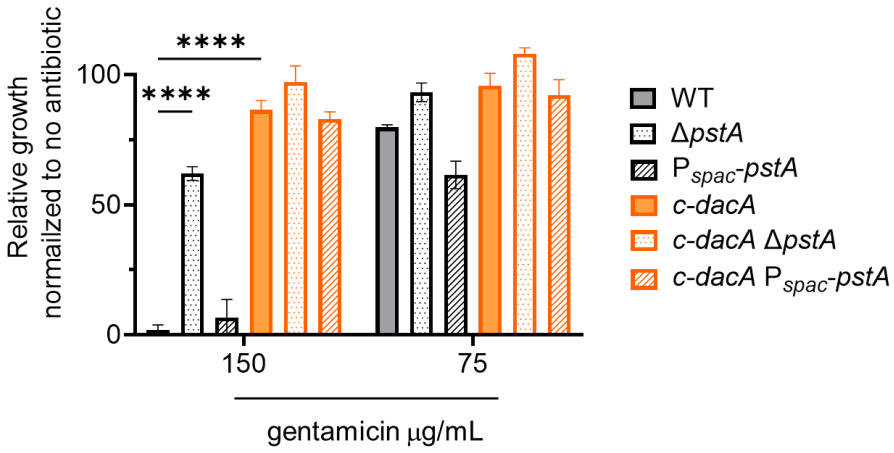

Figure 3.2 Deletion of PstA increased *Listeria* gentamicin resistance. *L. monocytogenes* cultures were grown with shaking in LSM with varying gentamicin concentrations for 16 hours. For each strain, OD_{600} of cultures grown in gentamicin were normalized to OD_{600} of the same strain grown in LSM only. Data are the average of two independent experiments. Error bars represent standard deviations. Statistics: two-way ANOVA; ****, P<0.0001.

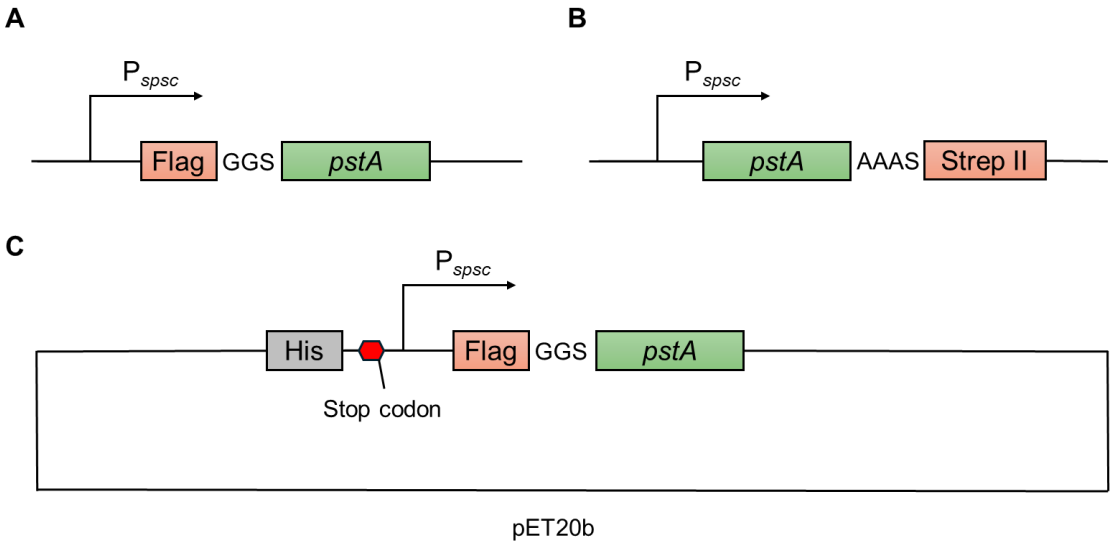

Figure 3.3 Schematic of PstA constructs. (**A-B**) Genes encoding Flag-PstA, PstA-Strep II were cloned into pPL1 plasmid. The genes were driven by P_{spac} promoter. The Flag tag is at the N-terminal of PstA and 3 amino acids GGS are used to link Flag and PstA. The Strep II tag is at the C-terminal of PteA and 4 amino acids AAAS are used to link PstA and Strep II. (**C**) For overexpressing Flag-PstA in *E. coli*, the Flag tag is also at the N-terminal of PstA and linked by GGS. And the inserts were cloned into pET20b. Since there is a His tag on the backbone of pET20b, I added a stop codon at the end of His tag to prevent His tag linking to PstA.

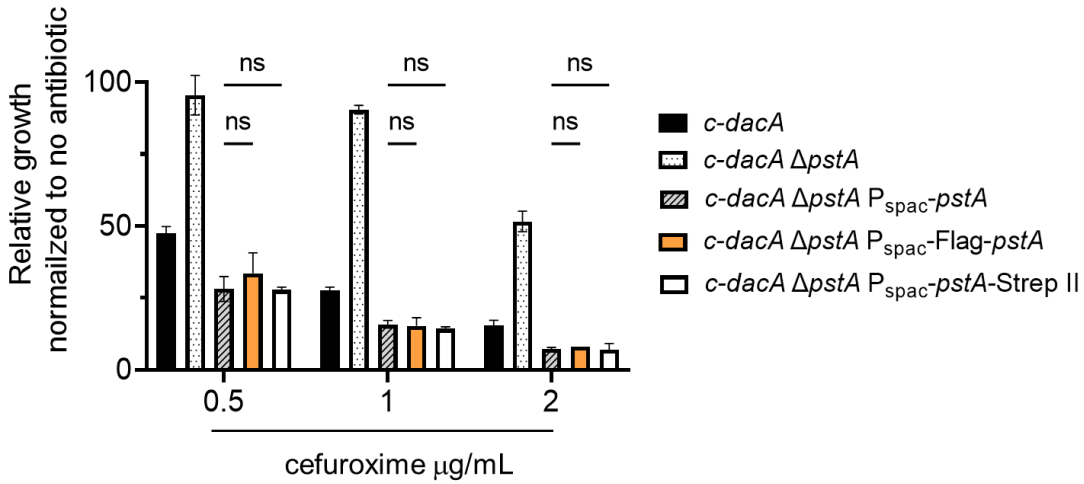

Figure 3.4 Expression of Flag-PstA or PstA-Strep II complement deletion of *pstA* in *c-dacA* mutant. *L. monocytogenes* cultures were grown with shaking in LSM with varying cefuroxime concentrations for 16 hours. For each strain, OD_{600} of cultures grown in cefuroxime were normalized to OD_{600} of the same strain grown in LSM only. The over-expression of Flag-PstA and PstA -Strep II have the same growth rate as over-expressing PstA only. Which complement deletion of pstA in c-dacA mutant. Data are the average of two independent experiments. Error bars represent standard deviations. Statistics: two-way ANOVA; ns, non-significant.

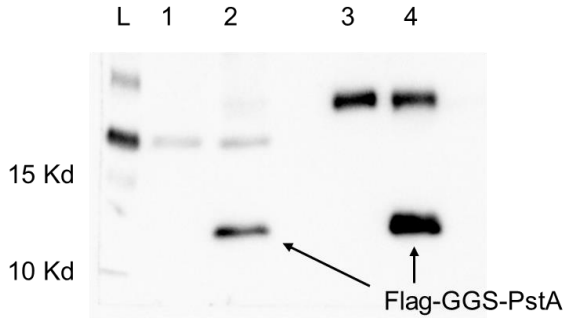

1: *Listeria* cell lysates for *c-dacA* Δ*pstA*

2: *Listeria* cell lysates for *c-dacA* ΔpstA P_{spac}-*flag-pstA*

3: Eluates for *c-dacA* Δ*pstA* after Anti-Flag beads binding.

4: Eluates for *c-dacA* P_{spac}-*flag-pstA* Δ*pstA* after Anti-Flag beads binding.

Figure 3.5 Flag-PstA was well expressed in *L. monocytogenes* mutant strains. Western blot showing the detection of FLAG-PstA using an anti-FLAG antibody (lane 2 and 4). An isogenic strain expressing untagged PstA was examined as a control (lane 1 and 3).

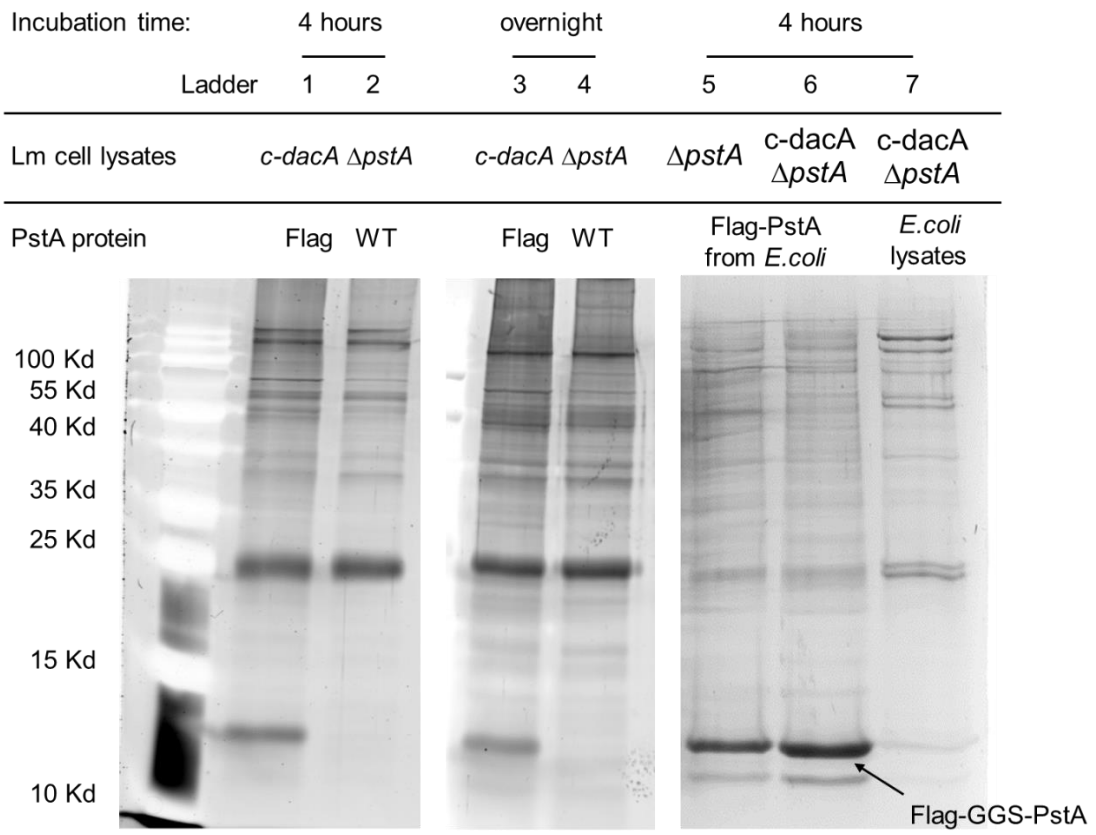

Figure 3.6 Pull-down of Flag-PstA from *L. monocytogenes*. In **1-4,** Flag-PstA was over-expressed from a neutral locus in the indicated *Listeria* strains, and LSM cultures of *L. monocytogenes* were grown to mid-log phase. Bacteria were then fixed in 0.4% paraformaldehyde (PFA) for 20 min. The fixation was stopped by adding 0.5M glycine for 5 min. Bacteria were lysed by sonication in TBS-T buffer and applied to 20μL of Anti-FLAG M2 magnetic beads, incubating for 4 hours (**1** and **2**) or overnight (**3** and **4**). The beads were washed with TBS 3x 1mL and then eluted with Laemmli sample loading buffer. The samples were analyzed by SDS-PAGE. In **5, 6** and **7,** Flag-PstA was over-expressed in *E. coli*. *E. coli* cells were lysed by sonication in TBS-T buffer and applied to 20μL of Anti-FLAG M2 magnetic beads, incubating for 2 hours. The beads were washed with TBS 3x1mL and then mixed with *Listeria* cell lysates, incubating for 4 hours. The beads were washed with TBS 3x 1mL again and eluted with Laemmli sample loading buffer. Samples were analyzed by SDS-PAGE.

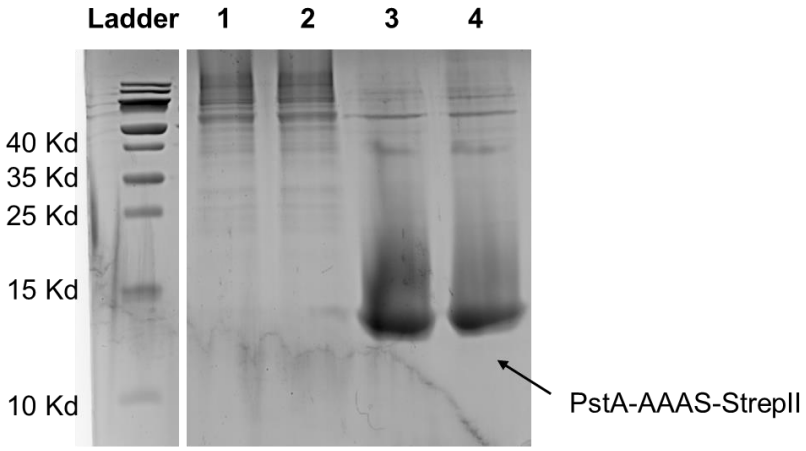

Lane1: Eluates for *c-dacA* Δ*pstA* + P_{spac}-*pstA*

Lane2: Eluates for *c-dacA* Δ*pstA* + P_{spac}-*pstA-strepII*

Lane3: Resins for *c-dacA* Δ*pstA* + P_{spac}-*pstA*

Lane4: Resins for *c-dacA* Δ*pstA* + P_{spac}-pstA-*strepII*

Figure 3.7 Pull-down of PstA-StrepII from *L. monocytogenes*. PstA-StrepII was over-expressed from a neutral locus in the indicated *Listeria* strains, and LSM cultures of *L. monocytogenes* were grown to the mid-log phase. Bacteria were then resuspended in PBS and fixed in 0.4% paraformaldehyde for 20 min. The fixation was stopped with adding 0.5M glycine for 5 min. Bacteria were lysed by sonication in TBS-T buffer and applied to 200 μL Streptactin resin (IBA). The beads were washed and eluted as per manufacturer's instructions. Both eluates and resins were mixed with Laemmli sample loading buffer, heated at 56°C for 20min. Samples were analyzed by SDS-PAGE.

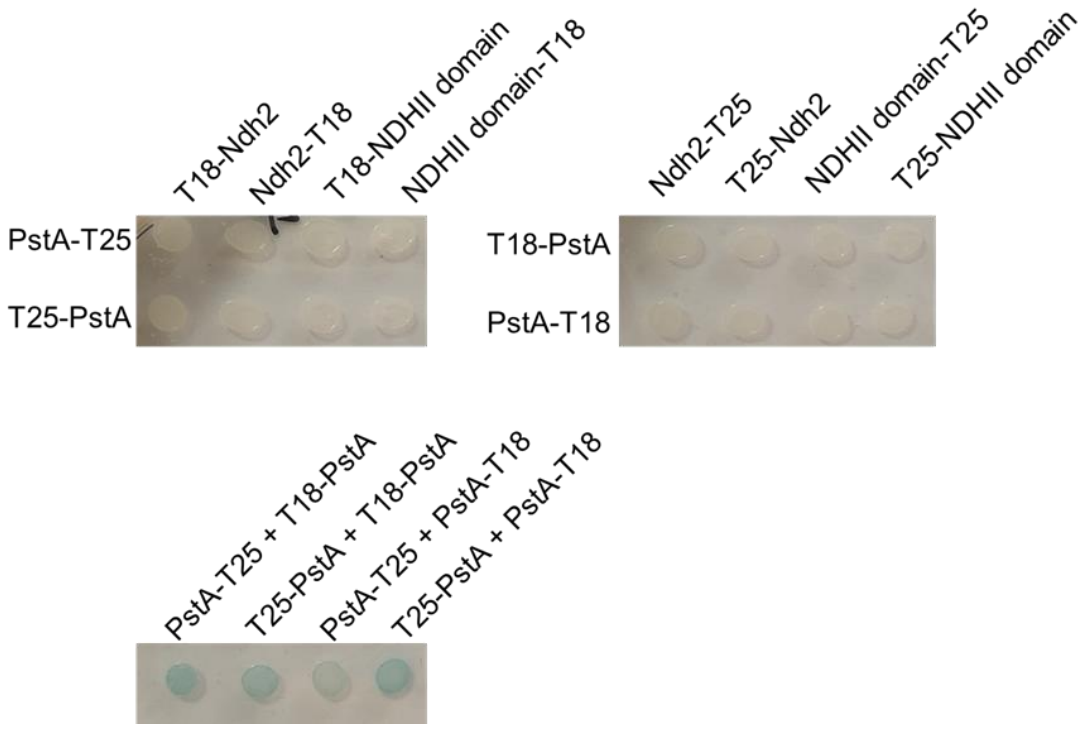

Figure 3.8 Bacteria two-hybrid analysis of PstA - Ndh2/NDH II domain protein-protein interactions. *E. coli* strain BTH101 was co-transformed with plasmids encoding the indicated fusions to adenylate cyclase fragments T18 and T25, 10 μL of the co-transformant cell suspensions were spotted onto the LB agar plates containing IPTG and X-Gal. Blue staining indicates a positive interaction between each pair of fusion proteins.

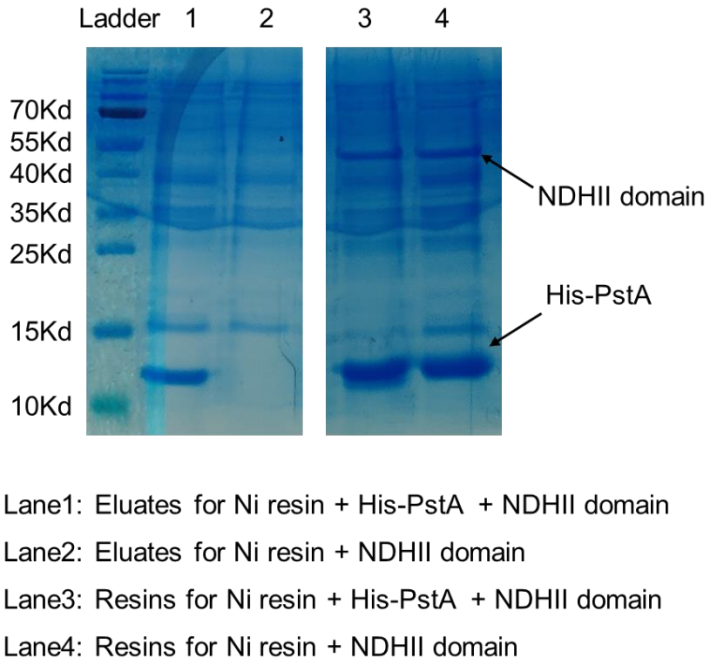

Figure 3.9 Pull-down assays for His-PstA-NDH II domain interaction. Hexa Histidine tag-based pull-down assays were carried out to demonstrate protein-protein interactions in vitro. The purified His-PstA and NDH II domain proteins were first incubated together for 30 hours; then the proteins mix was applied onto the Ni resin for pull-down assay. Both eluates and resins were treated with Laemmli sample loading buffer and heated at 56°C for 20min. Samples were analyzed by SDS-PAGE.

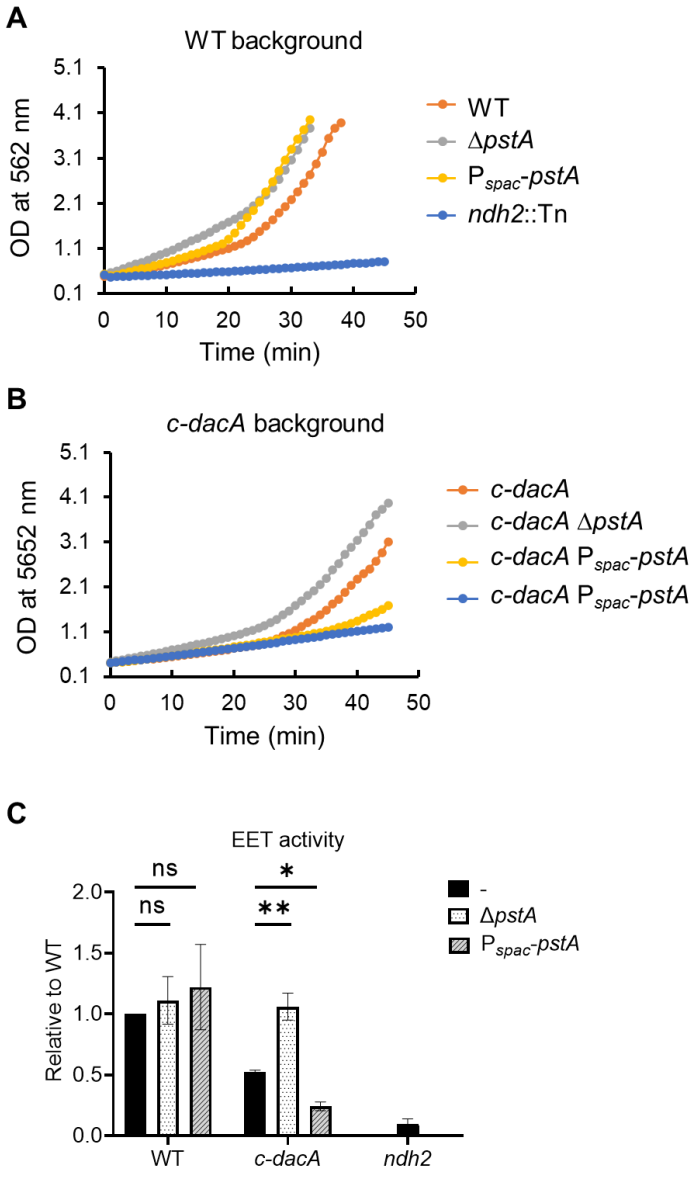

Figure 3.10 PstA regulates *L. monocytogenes* Extracellular electron transfer (EET) activity, particularly in a *c-dacA* background. EET was assessed by the colorimetric ferrozine-based assay. Bacteria cultures were grown in LSM to mid-log phase and normalized to OD_{600} =1 with LSM + 2mM ferrozine, then the bacteria suspensions were mixed with 50mM ferric ammonium citrate and absorbance at 562nm were observed (**A-B**). The maximal rates (typically over 25 min) were calculated normalized to that of WT in each experiment. Data are the average of two experiments. Statistics: one-way ANOVA; ns, non-significant; *, P<0.05; **, P<0.01.

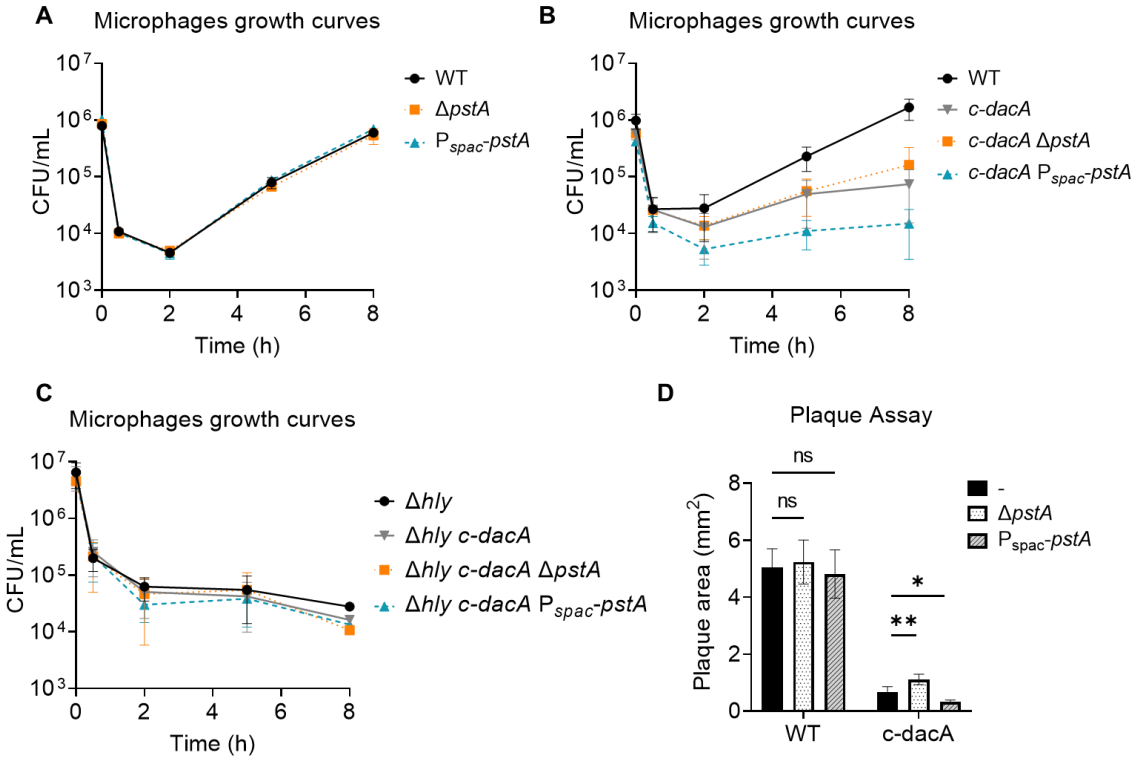

Figure 3.11 PstA reduces *L. monocytogenes* intracellular growth in low c-di-AMP background. A-C. Immortalized bone marrow-derived macrophages (iBMMs) were infected with indicated *L. monocytogenes* strains and CFU were enumerated at various times post-infection. **D**. Plaque area from mouse fibroblasts (L2 cells) infected with indicated strains for three days and normalized to wild type (WT). Statistics: one -way and two-way ANOVA; *, P<0.05; **, P<0.01.

Table 3.1: Strains used in this study

Strain number	Genotype	Source
L. monocytogenes (derivatives of strain 10403S)		
TNHL262	*c-dacA*	(226)
TNHL951	*dacA*::kan (Δ*dacA*)	(136)
TNHL349	Δ*pstA*	This study
TNHL387	P_{spac}-*pstA*	This study
TNHL345	*c-dacA* Δ*pstA*	This study
TNHL408	*c-dacA* P_{spac}-*pstA*	This study
TNHL989	*c-dacA* Δ*pstA* P_{spac}-*pstA*	This study
TNHL996	*c-dacA* Δ*pstA* P_{spac}-Flag-GGS-*pstA*	This study
TNHL617	*c-dacA* Δ*pstA* P_{spac}-*pstA*-AAAS-Strep II	This study
TNHL377	*ndh2*::Tn	This study
TNHL635	*ndh2*::Tn Δ*pstA*	This study
TNHL636	*ndh2*::Tn P_{spac}-*pstA*	This study
TNHL357	*ndh2*::Tn *c-dacA*	This study
TNHL356	*ndh2*::Tn *c-dacA* Δ*pstA*	This study
TNHL468	*ndh2*::Tn *c-dacA* P_{spac}-*pstA*	This study
E. coli		
TNH581	pPL1-P_{spac}-*hly* 5'UTR-Flag-GGS-*pstA* in XL1B	This study
TNH724	pPL1-P_{spac}-*hly* 5'UTR-*pstA*-AAAS-Strep II in XL1B	This study
TNH324	pET20b in XL1B	This study
TNH411	pET20b-*pstA* in XL1B in XL1B	This study
TNH513	pGEX-6P-*ndh2,* NDH II domain (aa. 1-410) in XL1B	This study
TNH839	pET20b-Flag-GGS-*pstA* in XL1B	This study
TNH406	pKT25-*pstA* in XL1B	This study
TNH407	pKNT25-*pstA* in XL1B	This study
TNH408	pUT18-*pstA* in XL1B	This study
TNH409	pUT18C-*pstA* in XL1B	This study
TNH450	pKT25-*ndh2* in XL1B	This study
TNH449	pKNT25-*ndh2* in XL1B	This study
TNH451	pUT18-*ndh2* in XL1B	This study
TNH452	pUT18C-*ndh2* in XL1B	This study
TNH582	pKT25-*ndh2*, NDH II domain (aa. 1-410) in XL1B	This study
TNH583	pKNT25-*ndh2*, NDH II domain (aa. 1-410) in XL1B	This study
TNH584	pUT18-*ndh2*, NDH II domain (aa. 1-410) in XL1B	This study
TNH585	pUT18C-*ndh2*, NDH II domain (aa. 1-410) in XL1B	This study
TNH637	pKT25-*pstA*, pUT18-*pstA* in BTH101	This study
TNH638	pKTN25-*pstA*, pUT18-*pstA* in BTH101	This study
TNH639	pKT25-*pstA*, pUTC18-*pstA* in BTH101	This study

Table 3.1 (Continued)

Strain number	Genotype	Source
E. coli		
TNH640	pKTN25-*pstA*, pUTC18-*pstA* in BTH101	This study
TNH822	pKT25-*pstA* & pUT18-*ndh2* in BTH101	This study
TNH823	pKT25-*pstA* & pUT18C-*ndh2* in BTH101	This study
TNH824	pKT25-*pstA* & pUT18-NDH II domain in BTH101	This study
TNH825	pKT25-*pstA* & pUT18C-NDH II domain in BTH101	This study
TNH826	pKNT25-*pstA* & pUT18-*ndh2* in BTH101	This study
TNH827	pKNT25-*pstA* & pUT18C-*ndh2* in BTH101	This study
TNH828	pKNT25-*pstA* & pUT18-NDH II domain in BTH101	This study
TNH829	pKNT25-*pstA* & pUT18C-NDH II domain in BTH101	This study
TNH830	pUT18-*pstA* & pKT25-*ndh2* in BTH101	This study
TNH831	pUT18-*pstA* & pKNT-*ndh2* in BTH101	This study
TNH832	pUT18-*pstA* & pKT25-NDH II domain in BTH101	This study
TNH833	pUT18-*pstA* & pKNT25-NDH II domain in BTH101	This study
TNH834	pUT18C-*pstA* & pKT25-*ndh2* in BTH101	This study
TNH835	pUT18C-*pstA* & pKNT-*ndh2* in BTH101	This study
TNH836	pUT18C-*pstA* + pKT25-NDH II domain in BTH101	This study
TNH837	pUT18C-*pstA* + pKNT25-NDH II domain in BTH101	This study

Table 3.2: Cefuroxime MICs for indicated listeria mutants

Strain	Cefuroxime MIC[a]s (μg/mL)
WT	128
Ndh2::Tn	64
c-dacA	2
c-dacA Δ*pstA*	64
c-dacA Δ*pstA* + P_{spac}-*pstA*	1 - 2
c-dacA Δ*pstA* + P_{spac}-Flag-*pstA*	1 - 2
c-dacA Δ*pstA* + P_{spac}-*pstA*-Strep II	1 - 2

[a]The lowest concentration of an antibiotic that inhibits the growth of a given strain of bacteria.

Table 3.3: Suppressor mutations identified in *c-dacA* P_{spac}-*pstA* mutants that resistant to cefuroxime

10403S Locus	EGD-e Locus	Description	Ref base	Pos base	Ref AA.	Pos AA.
P1-G5						
lmo1496	*LMRG_01474*	transcription elongation factor GreA	G	A	Ala (G**C**C)	Val (G**T**C)
lmo1024	*LMRG_02373*	hypothetical protein	G	A	Thr (A**C**A)	Ile (A**T**A)
lmo0626	*LMRG_00309*	membrane protein	C	T	Arg (C**G**G)	Gln (CAG)
lmo0689	*LMRG_00377*	chemotaxis protein CheV	G	A	Ala (**G**CA)	Thr (**A**CA)
lmo0974	*LMRG_02073*	D-alanine--poly(phosphoribitol) ligase subunit 1	G	A	Ala (G**C**T)	Val (G**T**T)
lmo1029	*LMRG_02129*	Cof-type HAD-IIB family hydrolase	C	T	Ser (T**C**G)	Leu (T**T**G)
lmo1153	*LMRG_00596*	propanediol/glycerol family dehydratase large subunit	G	A	Glu (**G**AA)	Lys (**A**AA)
lmo1193	*LMRG_00639*	cobalt-precorrin-8 methylmutase	G	A	Asp (**G**AT)	Asn (**A**AT)
lmo1575	*LMRG_01392*	oligoribonuclease	C	T	Glu (**G**AA)	Lys (**A**AA)
lmo1625	*LMRG_01341*	Membrane protein involved in the export of O-antigen, teichoic acid lipoteichoic acids	C	T	Gly (**G**GG)	Arg (**A**GG)
lmo2495	*LMRG_01753*	phosphate import ATP-binding protein PstB 1	C	T	Arg (A**G**A)	Lys (A**A**A)
P1-D10						
lmo1496	*LMRG_01474*	transcription elongation factor GreA	G	A	Ala (G**C**C)	Val (G**T**C)
lmo0085	*LMRG_02334*	hypothetical protein	G	A	Asp (**G**AC)	Asn (**A**AC)
lmo1055	*LMRG_00517*	dihydrolipoamide dehydrogenase	G	A	Glu (**G**AA)	Lys (**A**AA)
lmo1171	*LMRG_00617*	Alcohol dehydrogenase	C	T	His (**C**AC)	Tyr (**T**AC)
lmo1821	*LMRG_00968*	Protein serine/threonine phosphatase PrpC, regulation of stationary phase	G	A	Ser (T**C**C)	Phe (T**T**C)
lmo1825	*LMRG_00972*	Phosphopantothenoylcysteine decarboxylase/ Phosphopantothenoylcysteine synthetase	G	A	Arg (**C**GT)	Cys (**T**GT)
lmo1928	*LMRG_01075*	chorismate synthase	C	T	Gly (**G**GC)	Ser (**A**GC)
lmo2267	*LMRG_02922*	ATP-dependent helicase (addA)	G	A	Arg (**C**GT)	Cys (**T**GT)

lmo2833	*LMRG_01865*	glycoside hydrolase family 65 protein	G	A	Leu (**C**TT)	Phe (**T**TT)
P2-E7						
lmo0596	*LMRG_00279*	LPXTG cell wall anchor domain-containing protein	G	A	Ser (T**C**T)	Phe (T**T**T)
lmo0752	*LMRG_00440*	alpha/beta hydrolase	C	T	Ala (G**C**A)	Val (G**T**A)
lmo0849	*LMRG_02272*	amidase	C	T	Gly (**G**GC)	Ser (**A**GC)
lmo1021	*LMRG_02121*	response regulator transcription factor (lias)	G	A	Val (**G**TA)	Ile (**A**TA)
lmo1072	*LMRG_00534*	pyruvate carboxylase	G	A	Val (**G**TT)	Ile (**A**TT)
lmo1349	*LMRG_00799*	glycine dehydrogenase subunit 1	G	A	Gly (G**G**G)	Glu (G**A**G)
lmo1652	*LMRG_01315*	ATP-binding cassette domain-containing protein	C	T	Gly (**G**GC)	Ser (**A**GC)
lmo1804	*LMRG_00951*	chromosome segregation protein SMC	C	T	Arg (A**G**A)	Lys (A**A**A)
lmo1896	*LMRG_01043*	asparagine--tRNA ligase	C	T	Gly (**G**GA)	Arg (**A**GA)

Chapter 4

Understanding the coordination between MreB and c-di-AMP in *Listeria monocytogenes* β-lactam resistance and pathogenesis

Contributions:

Tu Z. designed and performed the experiments for figure 4.1-4.9, wrote the manuscript.

Huynh TN. secured funding, conceived, designed, and supervised the study, and critically revised the manuscript.

4. UNDERSTANDING THE COORDINATION BETWEEN MREB AND C-DI-AMP IN *LISTERIA MONOCYTOGENES* β-LACTAM RESISTANCE AND PATHOGENESIS

4.1 Abstract

Bacterial adaptation relies on signal transduction pathways that facilitate changes in lifestyle across environmental and infectious niches. c-di-AMP is an essential signal nucleotide that regulates a wide variety of prokaryotic physiological functions, including β-lactam antibiotic susceptibility. In food-borne pathogen *Listeria monocytogenes*, either low or unregulated accumulation of c-di-AMP in bacteria will significantly increase its susceptibility to β-lactams. Our lab previously demonstrated that accumulation of c-di-AMP in *L. monocytogenes* exhibits less production of peptidoglycan, and reduced cell wall thickness, suggesting that c-di-AMP regulates *L. monocytogenes* β-lactam resistance by diminishing bacterial cell wall integrity. However, the mechanism of how c-di-AMP regulates bacterial cell wall homeostasis is still unclear. Here in my study, we generated an EMS library for c-di-AMP accumulating mutant (ΔPDE), and selected suppressor mutants that is resistant to b-lactams while maintaining high c-di-AMP level. We identified that mutations on MreB, a cytoskeletal protein that determines cell shape guiding the synthesis of the PG, not only restored ΔPDE mutant β-lactam susceptibility, but also its attenuated virulence. Further studies proved that these mutations on MreB reduced its activity. In addition, we also found that mutation in MreB rescues ΔPDE mutant bacterial cell wall synthesis as well as induced autolysis specifically under the cell wall stress condition. Collectively, our work laid a foundation to further characterize the function of c-di-AMP on bacterial cell wall integrity to unravel the regulation of c-di-AMP on bacteria β-lactam susceptibility.

4.2 Introduction

Many bacteria consistently maintain specific cell shapes during their growth phase[262]. In the majority of these bacteria, the peptidoglycan (PG) layer of the cell wall provides the structural support necessary for maintaining these various shapes. On the other hand, the bacterial cytoskeleton is also crucial in determining and maintaining cell shape[263]. MreB is a bacterial cytoskeleton protein that has been widely studied and is associated with the determination of rod shape as well as important subcellular processes including cell division, chromosome segregation, cell wall morphogenesis, and cell polarity[47,264]. There are three major paralogs in various bacterial species: MreB, Mbl (MreB-like protein), and MreBH[265]. The Mbl was shown to be required for lateral wall expansion (elongation) by directing the helical insertion of new PG into the lateral cell wall[266]. And MreBH, was also shown to form helical filaments, and depletion of the protein led to a mild morphological defect[267]. And MreB is essential under normal growth conditions and has a role in the control of cell width[268]. Once bind with ATP, individual MreB monomers undergo a conformational change, and interact with each other to form a filamentous structure on cell membrane and moves in a direction perpendicular to the cell axis, coupling with PG synthesis[269]. During PG synthesis, MreB, MreC, MreD, RodA, PBP2, and RodZ formed a Rod complex, orchestrating the insertion of new glycan strands and peptide cross-links into the existing cell wall. Each component of the Rod complex has a specific role in this process, with MreB guiding the overall spatial organization of cell wall growth, MreC and MreD possibly linking membrane proteins to peptidoglycan synthesis enzymes[50], RodA functioning as a glycosyltransferase[46], PBP2 facilitating the cross-linking of peptidoglycan strands[48], and RodZ aligning the activities of the Rod complex with the cell's cytoskeletal elements[47]. These proteins ensure precise and effective growth of the cell wall, which is crucial for the bacteria's structural integrity and ability to divide properly.

To date, the relationship between c-di-AMP signaling and the stability of bacterial cell walls in *Firmicutes* is well-studied, particularly focusing on the context of c-di-AMP depletion. A prevailing theory suggests that c-di-AMP regulates bacterial turgor pressure, with cell wall stability being a secondary effect resulting from the maintenance of turgor balance[169]. This theory is supported by extensive experiments across multiple species. First, c-di-AMP inhibits osmolyte transport by binding to various potassium and osmolyte

transporters and controlling the gene expression of these transporters. Deleting potassium transporters or removing potassium from the medium can mitigate the bacterial lysis of c-di-AMP-depleted mutants[184,270]. Additionally, the increased antibiotic susceptibility observed in these mutants can be alleviated by adding osmoprotectants like NaCl or sucrose to their growth media[211]. This turgor regulation theory suggests that c-di-AMP accumulation would confer resistance to β-lactams. However, many studies in *L. monocytogenes* showed that ΔPDE mutants, which accumulates c-di-AMP within the bacteria, are still highly sensitive to a lot of stress conditions including β-lactams, and greatly attenuated for virulence[136]. In addition, similar phenotypes affecting growth, stress response, or virulence have been also reported in c-di-AMP-accumulating mutants across a diverse range of bacteria, including *Bacillus subtilis*, *Bacillus anthracis*, *Mycobacterium tuberculosis*, *Streptococcus pneumoniae*, and *Streptomyces venezuelae*[127,135,217]. Thus, the toxicity of c-di-AMP accumulation for bacterial physiology and pathogenesis is a widespread phenomenon.

Our previous study showed that c-di-AMP accumulation diminished cell wall integrity in *L. monocytogenes*, causing reduced peptidoglycan content[189]. We found that ΔPDE mutant was deficient for two crucial muropeptides precursors UDP-N-acetylmuramic acid (MurNAc) and D-Ala-D-Ala. Additionally, we found that the activity of D-Ala ligase (Ddl), which synthesizes D-Ala-D-Ala, was compromised in ΔPDE mutant. This impairment was partly linked to a deficiency in potassium (K^+) concurrent with high levels of c-di-AMP. However, how exactly c-di-AMP regulates bacterial cell wall integrity is still unclear. Here, we reported the isolations and characterization of suppressor mutations that allow *L. monocytogenes* to be resistant to cefuroxime, a β-lactams, when c-di-AMP is accumulated. We found that mutations on MreB, a cytoskeletal protein that determines cell shape by guiding the synthesis of the cell wall, restored ΔPDE mutants for cefuroxime sensitivity as well as virulence. Further studies demonstrated that inhibition of MreB restored ΔPDE strains resistance to β-lactams as well as PG synthesis. Moreover, we also found that the accumulation of c-di-AMP also exhibited significantly higher autolysin activity, which is likely independent of MreB function, suggesting another role of c-di-AMP in bacterial cell wall integrity. Our findings laid a foundation to further characterize the complex function of

c-di-AMP in regulating both bacteria wall synthesis and hydrolysis, providing insight into the toxic effect of c-di-AMP imbalance on bacterial cell wall integrity as well as virulence.

4.3 Results

4.3.1 Suppressor mutations restore β-lactam resistance in ΔPDE but do not increase resistance in WT

The defect of ΔPDE mutants for growth on Brain Heart Infusion (BHI) plates with cefuroxime provided a perfect condition for screening. To get more insight into the function of c-di-AMP on bacterial cell wall integrity. We generated an EMS library for ΔPDE mutant and isolated, characterized suppressor mutants that can overcome the β-lactam stress on the plate even with the accumulation of c-di-AMP. In addition, we also excluded the mutants that are still resistant to cefuroxime when intracellular c-di-AMP levels were reduced to WT level by complementing them with *pgpH* allele. Thus, the mutations that restored ΔPDE cefuroxime sensitivity are specifically related to c-di-AMP regulations.

Ten suppressor mutants, numbered S1-S10, were chosen for initial characterization. As expected, these mutants have a significantly higher growth rate compared to ΔPDE when grew in BHI broth with cefuroxime, while have similar growth as WT (**Fig. 4.1A-B**). In addition, complementation of these suppressor mutants with *pgpH* allele did not remarkably increase their cefuroxime resistance, which have been observed in ΔPDE strain (**Fig. 4.1C-D**). We hypothesized that high c-di-AMP level impaired bacterial cell wall integrity, but these ΔPDE strains contained with suppressor mutations by passed the toxic effects of c-di-AMP. As a cell wall targeting antibiotics, β-lactams bind with penicillin-binding proteins (PBPs) and inhibit their function specifically in formation of cross-linking between glycan chains during PG synthesis. To further explore the effect of high c-di-AMP levels on cell wall integrity, and how these suppressor mutations contribute to it, we tested their susceptibility to Moenomycin, another cell wall targeting antibiotics that directly inhibit bacterial peptidoglycan glycosyltransferases. These enzymes are responsible for the extension of the glycan chain, a process that occurs before glycan chain cross-linking in peptidoglycan synthesis. We found that ΔPDE strains exhibited the same growth rate as WT in the present of Moenomycin (**Fig. 4.2**), suggesting that c-di-AMP accumulation does

not affect the elongation of glycan chains during PG synthesis. The effect of c-di-AMP on cell wall synthesis may be specifically on PG cross-lining (Transpeptidation). Surprisingly, we noticed that most suppressor mutants except S10 are even more resistant to Moenomycin. Suggesting that these suppressor mutants are also involved in regulating bacterial cell wall synthesis.

4.3.2 Suppressor mutations likely reduce MreB activity

The whole genome sequencing was performed for the 10 suppressor mutants (S1-S10) and confirmed that both *pdeA* and *pgpH* were absent. Interestingly, 8 out of 10 strains contain mutations in *mreB* gene, encoding a cell shape-determining protein MreB (**Table 4.1**). It is worth noting that S3, S6 and S8 only contain mutations on MreB with amino acid substitution at A46V, G108E and V47I respectively, suggesting that MreB plays a critical role in mediating the regulation of c-di-AMP on bacteria β-lactam susceptibility. The S9 contains a sole mutation with T334A in *rpoD*, encoding an RNA polymerase sigma factor, and the S10 got mutations on *walR* E25G and *pdhA* T207C. WalR protein is a part of WlaRK two-component system that regulates bacterial cell wall hydrolysis[271] while *pdhA* encodes the E1α subunit of the pyruvate dehydrogenase (PDH) complex that catalyzes the conversion of pyruvate to acetyl-CoA during glycolysis[272]. MreB is a bacterial actin-like protein that plays a crucial role in determining cell shape and supporting bacteria elongation. In *L. monocytogenes* and many other rod-shaped bacteria, MreB is essential for maintaining the cell cylindrical shape by directing the synthesis and placement of cell wall components[273]. One study also proved that reducing *mreB* expression level will significantly increase its bacteria cell width[274]. Therefore, we hypothesized that those suppressor mutants containing *mreB* mutations also have changed bacteria cell morphology.

Therefore, we used wheat germ agglutinin (WGA) to stain the bacterial cell membrane of *L. monocytogenes* WT, ΔPDE strains and the suppressor mutants, particularly S1, S3, S6, S7 and S8 that contain different mutation sites in *mreB*, and measured their cell length and width. The S9 and S10 mutants that possess a functional MreB is served as controls. As the result shows, ΔPDE strain has significantly reduced cell width compared to WT, while all the suppressor mutants have increased cell width compared to ΔPDE, except the

control strains which do not contain *mreB* mutations (**Fig. 4.4A**). The S9 have the same width as the ΔPDE, and S10 mutant is even shorter than ΔPDE strain. These data suggest that the suppressor mutants that contain *mreB* mutations likely have reduced MreB activity. Interestingly, when complemented with *pgpH*, which reduced the c-di-AMP to normal level, the cell width of ΔPDE and suppressor mutants were significantly increased, including S9 and S10 mutants (**Fig. 4.4B**), suggesting that c-di-AMP also plays a role in regulating bacteria cell width, and this regulation could be independent of MreB function.

In terms of bacteria cell length, there was no remarkable difference between WT, ΔPDE and S9, and S10 strain only has slightly reduced in cell length. Howvever, the suppressor mutants containing *mreB* mutations were significantly shorter than WT and ΔPDE (**Fig. 4.5A**). We suspected that the changes in length could result from reduced MreB activity, which impairs bacterial cell wall elongation, and c-di-AMP does not regulate bacteria elongation. In addition, complementation of *pgpH* did not change their cell length in ΔPDE and most *mreB* mutation suppressors (**Fig. 4.5B**), further supporting our hypothesis that c-di-AMP level is independent of regulating bacteria cell length. As for S7, complementation of *pgpH* results in an even shorter cell width, this could be related to the mutation of a functional unknown transcriptional factor Lmo0659. Taken together, these results indicate the connection of c-di-AMP level with bacteria cell morphology, specifically, increasing c-di-AMP level will reduce bacterial cell width, while decreased MreB activity restores it.

4.3.3 MreB inhibitor compounds A22 and MP265 restore β-lactam resistance in ΔPDE but not in WT

To verify our hypothesis that mutations on *mreB* form those suppressor mutants reduce MreB activity, we directly treated ΔPDE strain with MreB inhibitors. During bacterial cell wall synthesis, MreB polymerizes into an antiparallel double-stranded filament. This polymerization is dependent on the binding of nucleotides, such as ATP and GTP[275]. The MreB inhibitor S-(3, 4-dichlorobenzyl) isothiourea (A22) and its less cytotoxic and much more water-soluble derivative MP265 have been used extensively since they act as an ATP-competitive inhibitor, and binds to the nucleotide binding site of MreB, and thus perturb cell morphology reminiscent of an MreB knock-out[264,276]. Our results showed that

treatment of A22 or MP265 significantly reduced WT strains cefuroxime resistance (**Fig. 4.6A-B**). This is consistent with our expectation that MreB inhibitors and β-lactams could have a synergistic effect since they both target bacterial cell wall synthesis in different processes. In contrast, in c-di-AMP accumulated background, adding A22 or MP265 significantly restored ΔPDE susceptibility to cefuroxime, consisting with the phenotypes of all suppressor mutants (S1-S8) (**Fig. 4.6A-B**). These results further confirmed that those suppressor mutants containing *mreB* mutations confer a reduced MreB activity. And furthermore, we hypothesize that accumulation of c-di-AMP disrupts bacterial cell wall homeostasis by hyperactivating MreB under cell wall stress.

4.3.4 MreB mutation rescue ΔPDE PG synthesis upon β-lactam stress.

During cell wall elongation, the MreB filament acts as a guide, directing the Rod complex to specific sites along the cell membrane and coordinating the insertion of new peptidoglycan fragments. To test the effect of high c-di-AMP on MreB activity, we quantified the PG synthesis by examining the uptake of [^{14}C] GlcNAc, an essential component of PG, in ΔPDE mutant. I also tested the strain S6 and S6 complemented by *pgpH* as representative suppressor mutant that only contains *mreB* mutation. The WT *L. monocytogenes* strain as well as other mutant strains were grown in BHI broth or BHI broth with 0.5XMIC cefuroxime. The [^{14}C] GlcNAc uptake activities were quantified by calculating the increasing radioactivity rate between 15 – 30 min. As the result, we noticed that ΔPDE mutant has decreased [^{14}C] GlcNAc uptake activity compared to WT, suggesting that high c-di-AMP level impaired bacteria PG synthesis (**Fig. 4.7**). This observation is consistent with our previous observation that c-di-AMP accumulation led to a reduction in peptidoglycan (PG) content as well as decreased cell wall thickness [189]. Furthermore, the S6 + P*spac-pgpH* mutant, equivalent to *mreB* mutation in WT background, showed the same reduced [^{14}C] GlcNAc uptake activity as ΔPDE, indicating that both accumulated c-di-AMP level and reduced MreB activity have the same effect in diminishing bacterial cell wall synthesis. However, combining these two factors (mreB mutations in accumulated c-di-AMP background) did not exhibit an additive effect, as the [^{14}C] GlcNAc uptake activity of S6 strain is similar to ΔPDE and S6 + P*spac-pgpH* strains. This data suggests that c-di-AMP may be in the same pathway of *mreB* in regulating [^{14}C]

GlcNAc uptake and PG synthesis. On the other hand, as expected, given that β-lactams inhibit bacterial cell wall synthesis, all strains grown with cefuroxime exhibited decreased peptidoglycan (PG) synthesis, with their [^{14}C] GlcNAc uptake activities being significantly lower than when they were grown in BHI broth. Interestingly, in the present of cefuroxime, we observed that the reduction of [^{14}C] GlcNAc uptake activity in the ΔPDE mutant is significantly less than that in the WT. Furthermore, the mutation in *mreB* within the ΔPDE strain restored this activity to WT level, whereas the mreB mutation alone (S6 + P*spac*-*pgpH*) did not affect PG synthesis activity. Taken together, these results suggest that c-di-AMP in ΔPDE strains impaired bacterial cell wall synthesis, particularly under the cell wall stress, and the regulation of c-di-AMP under β-lactam stress can be bypassed by reducing MreB activity.

4.3.5 ΔPDE have increased autolysins activity while MreB mutations have modest effect on them.

The integrity of the bacterial cell wall is maintained through a delicate balance between PG synthesis and PG hydrolysis. Unlike the process of PG synthesis, where enzymes are required to continuously add new glycan strands and peptide cross-links to the cell wall, PG hydrolysis involves hydrolases or autolysins, which break down old or damaged parts of the peptidoglycan layer[277]. We wonder if ci-di-AMP also affects bacterial cell wall hydrolysis by regulating the activity of autolysins. Therefore, we tested bacteria induced autolysis activity by treating *L. monocytogenes* with TritonX-100[278]. The non-ionic surfactants TritonX-100 destroys bacterial membranes, and the disrupted plasma membrane will induce cell autolysis - the hydrolysis of PG layer by cellular autolysins. Here, we monitored the OD_{600} of each *L. monocytogenes* strain after treatment with TritonX-100. The reduction in OD_{600} at certain time indicates the rate of bacteria lysis, which reflects the activity of autolysins. Our results showed that ΔPDE mutant exhibited significantly increased bacterial lysis rate compared to WT (**Fig 4.8A**), suggesting that accumulated c-di-AMP may induce bacteria autolysins activity. The suppressors that containing *mreB* mutations also exhibit the same lysis rate as ΔPDE (**Fig 4.8B**). Moreover, complementation of *pgpH* in these strains reduced their autolysins activity to WT level, including ΔPDE. Besides, I included another cell wall synthesis deficient mutant (Δ*pgdA*

Δ*oatA*) as a control, and autolysins activity of this mutant is still the same as WT. These results imply that MreB activity as well as bacterial cell wall synthesis is independent of bacterial autolysins activity. Next, we also tested the autolysins activity of these strains after growing in the presence of cefuroxime, the WT strains showed a significant increase in lysis rate after cefuroxime treatment (**Fig 4.8A**). This could be explained by either cefuroxime induced autolysins activity or the cefuroxime treatment already impaired bacterial cell wall before the assay, and therefore exhibited increased OD_{600} reduction. However, the ΔPDE strains treated with cefuroxime exhibited a similar lysis curve to that of the untreated strains. This result eliminates the possibility that the increased lysis rate is due to the impaired cell wall integrity caused by pretreating with cefuroxime, and the ΔPDE mutant may possess highly active autolysins that cannot be further induced by β-lactams. Moreover, all suppressor mutants complemented with *pgpH*, as well as all the Δ*pgdA* Δ*oatA* strain, exhibited the similar induced autolysins activity to WT when they are pretreated with cefuroxime (**Fig 4.8B**), consistent with our conclusion that MreB do not regulate the activity of autolysins. However, interestingly, in c-di-AMP accumulated background, all the *mreB* mutation suppressors and S10 have reduced lysis activity when they were pretreated with cefuroxime. This data provides a hypothesis, that MreB mutation may still be able to affect bacterial autolysins activity directly or indirectly, but only in the present of accumulated c-di-AMP and under the cell wall stress condition. In addition, since we know that S10 contains WalR mutation, and this mutation also results in an induced bacterial lysis since S10 + P_{spapc}-*pgpH* strain showed lower relative OD_{600} than WT at 2 hours post treatment with TritonX-100. The effect of MreB mutation on bacterial autolysins is the same as WalR mutation, which is inducing their activity.

4.3.6 Suppressor mutations rescue ΔPDE in ex-vivo infection

The bacteria cell wall not only provides physical protection and shape to the bacterium but also plays a critical role in the interaction between pathogens and their hosts. Components of the cell wall, such asPG in *L. monocytogenes*, can trigger immune responses. Additionally, the cell wall's integrity and metabolism are essential for the processes of adhesion, invasion, and evasion of host immune defenses, making it a pivotal factor in bacterial pathogenicity. C-di-AMP has been reported to affect bacterial virulence; accumulation of c-di-AMP resulted in a reduced plaque formation in plaque

assay, an ex-vivo infection model that serves as a surrogate for virulence[203]. We wonder if c-di-AMP regulates bacteria infection through regulating the cell wall homeostasis. In the plaque assay, confluent mammalian fibroblasts are infected with *L. monocytogenes*. The intracellular growth and cell-to-cell spread of the bacteria result in a quantifiable zone of clearance (plaque), allowing for quantification[279]. Small plaques often correlate to virulence defect in vivo, and the ΔPDE mutant strains produced remarkably smaller plaques that were 40% the area of WT plaques. Interestingly, we found that all suppressor mutants that containing *mreB* mutations were also restored for plaque formation, indicating that these mutations rescue the attenuated virulence coffered by high c-di-AMP (**Fig. 4.9A**), suggesting a potential connection between bacterial cell wall integrity and its virulence.

Then, we also tested the intracellular growth of the suppressor mutants and the strains complemented with *pgpH*. The S3 and S6, which only contained *mreB* mutations, were selected for the preliminary test. Strikingly, although we observed a significant decrease of growth for ΔPDE mutants compared to WT, the S3 or S6 did not restore this defect for ΔPDE (**Fig. 4.9B**). In addition, when complemented with *pgpH*, which reduces the c-di-AMP to a normal level, the growth defects conferred by ΔPDE also have disappeared. There is no difference between WT, S3+P_{spac}-*pgpH*, S6+P_{spac}-*pgph* for growth in L2 cells, these results suggest that the rescue effect of plaque formation for suppressor mutant on ΔPDE is not related to intracellular growth.

4.4 Discussion

C-di-AMP has been known to regulate bacterial susceptibility to cell wall-targeting antibiotics, such as b-lactams, for decades. Both depletion and unregulated accumulation of c-di-AMP significantly reduce bacterial resistance to b-lactams. However, despite extensive research in various bacteria[193,280], the molecular mechanisms by which c-di-AMP influences bacteria β-lactam susceptibility remain elusive. Our studies specifically focused on the effects of c-di-AMP accumulation on *L. monocytogenes* β-lactams sensitivity. We identified that inhibition of MreB, the rod-shape determining protein, restored cefuroxime resistance in *L. monocytogenes* ΔPDE mutants (high c-di-AMP) to WT level. Further, we also found that mutation in MreB rescues ΔPDE mutant bacterial cell wall synthesis as well as induced autolysis specifically under the cell wall stress condition. Our findings highlight the role of c-di-AMP in bacterial cell wall homeostasis, a relationship that has not been previously reported.

Besides cefuroxime, we also tested *L. monocytogenes* mutants with another cell wall targeting antibiotics, moenomycin. Cefuroxime binds to and inactivates penicillin-binding proteins (PBPs). These PBPs are responsible for the cross-linking of the peptidoglycan layer, which involves the final steps of peptidoglycan synthesis. However, moenomycin acts at an earlier step in peptidoglycan synthesis compared to β-lactams, it directly inhibits the function of transglycosylase enzymes, which are responsible for polymerizing the glycan strands of peptidoglycan. Our data showed that ΔPDE strains are susceptible to β-lactams but not to moenomycin, suggesting that initial synthesis of glycan strands may remain unaffected by c-di-AMP levels, ΔPDE mutants may have defect in bacteria PG cross-linking. Previous studies have demonstrated that c-di-AMP bind and inhibit the activity of pyruvate carboxylase (PycA)[192]. The increased c-di-AMP level reduces the activity of TCA cycle, thus affecting the efficiency of generating energy (ATP) for biosynthesis pathways and providing precursors for amino acids like glutamate and aspartate. These amino acids are critical for synthesizing the peptidoglycan subunits that form the bacterial cell wall. It is worth noting that mutations on mreB, which decrease MreB activity, significantly increase ΔPDE mutant resistance to moenomycin. It is possible that the inhibition of MreB results in the altered organization and localization of glycosyltransferase due to the lack of structural guidance provided by MreB filaments. This

mis-localization can result in less efficient interaction between the enzymes and moenomycin. On the other hand, bacteria might also trigger adaptive responses to MreB inhibition that fortify the cell wall against external threats, including antibiotics. This could involve the upregulation of alternative pathways or enzymes that compensate for the disrupted function of MreB.

In addition to mutations on *mreB*, *rpoD* and *walR* were also identified from the suppressor mutants. The *rpoD* gene encodes the sigma factor sigma 70 in bacteria, which is essential for initiating the transcription of most bacterial genes during the exponential growth phase[281]. The sigma factors could bind to RNA polymerase and direct it to specific promoter regions of DNA to start transcription of genes encoding enzymes like peptidoglycan synthases, penicillin-binding proteins (PBPs), stress response proteins, and enzymes involved in lipid metabolism and amino acid synthesis. These enzymes are crucial for various cellular functions, including cell wall construction and repair, response to environmental stresses, and overall metabolic regulation. The mutation of RpoD can in some way restore the negative effect of c-di-AMP on bacterial cell wall, metabolism, stress response or directly on gene transcription. The WalR is a response regulator protein that is part of the WalRK two-component system. WalK (also referred to as YycG, VicK, or MicA) is a membrane-anchored sensor kinase and WalR (also called YycF, VicR, or MicB) is a DNA binding response regulator of the OmpR family[271]. Once phosphorylated, WalR undergoes a conformational change that enhances its DNA-binding capability, acting as a transcriptional activator and inducing the synthesis of several cell wall hydrolases, which are essential for maintaining bacterial cell wall homeostasis. Our TritonX-100 induced cell autolysis assay demonstrated that mutation of WalR induces bacteria autolysins activity, suggesting that increasing cell wall hydrolysis can also restore ΔPDE mutant cefuroxime sensitivity. On the other hand, we observed that ΔPDE strains have reduced cell width, although reduced MreB activity was reported to increase cell width[274], there is no evidence showed that hyperactive MreB decreases cell width. Since S10 as well as S10 + P_{spac}+*pgpH* mutants also exhibit decreased cell width, and later experiments also demonstrated that ΔPDE strains processes induced autolysins. I have grounds to hypothesize that reduced cell width in ΔPDE strain is caused by its overactive autolysins. While. All these clues highlight the role of c-di-AMP in bacterial cell wall homeostasis.

We observed that mutations on *mreB* not only rescue ΔPDE mutants β-lactam susceptibility, but also restored the ΔPDE infectivity. All suppressors formed significantly larger plaque than ΔPDE mutant. This data suggests that the reduced virulence of ΔPDE is caused by its impaired bacterial cell wall. Although the mechanism of how bacterial cell wall affect its virulence remains elusive. The connection between cell wall and virulence is obvious. Firstly, the cell wall provides structural integrity and protection to bacteria, enabling them to withstand hostile conditions, including osmotic changes and immune defenses. In addition, *bacterial* cell wall contains lipoteichoic acids (LTAs) and wall teichoic acids (WTAs), which play roles in adhesion to host cells and in modulating immune responses. These molecules can bind to host cell receptors, facilitating the invasion process. Moreover, many virulence factors are associated with the cell wall, for example, in *L. monocytogenes*, proteins such as Internalin A (InlA) and Internalin B (InlB) are anchored to the cell wall, they are crucial for the entry of *L. monocytogenes* into non-phagocytic cells. InlA interacts with E-cadherin on host cells, while InlB targets the hepatocyte growth factor receptor (c-Met), facilitating the internalization of the bacteria. Lastly, the cell wall components, particularly peptidoglycan and teichoic acid are recognized by pattern recognition receptors (PRRs) such as Toll-like receptors (TLRs) on host immune cells, increased cell wall lysis can induce stronger immune response, and result in severe clearance of bacteria. The role of c-di-AMP in regulating bacterial cell integrity and its impact on bacterial virulence and host interactions remains to be fully elucidated and warrants further investigation.

4.5 Materials and methods

4.5.1 Bacterial strains and culture conditions.

L. monocytogenes and *Escherichia coli* strains in this study are listed in **Table 4.2**. All *L. monocytogenes* strains were grown in Brain Heart Infusion (BHI) broth and *E. coli* strains in Lysogeny broth (LB) unless otherwise indicated, with appropriate antibiotics at 37°C with agitation. For solid media 1.5% weight/volume agar was added.

4.5.2 Antibiotic susceptibility assays

Antibiotic susceptibility in BHI was assessed by bacterial growth in 96-well plates containing 200 μL BHI only, or BHI plus two-fold dilutions of cefuroxime or moenomycin. For experiments that treated with MreB inhibitors, BHI broth was supplemented with 100μg/mL of MP265 (MedKoo) or 50μg/mL A22 (Cayman) prior adding two-fold dilutions of cefuroxime. Overnight cultures grown in BHI with shaking at 37°C was inoculated into each well, and bacterial growth was measured by OD_{600} at 37°C with intermittent shaking for 14 hours in a plate reader. For each strain, growth rates at each cefuroxime concentration were normalized to growth rate in BHI only of the same strain.

4.5.4 Mammalian L2 plaque assay

L2 fibroblasts cells were grown in DMEM - high glucose (Sigma) with 1% of sodium pyruvate and 1% of L-glutamine in the presence of 10% fetal bovine serum (FBS). Plaque formation upon *L. monocytogenes* infection of L2 cells was quantified as previously described[282]. Briefly, $1.2x10^6$ cells were infected with *L. monocytogenes* at multiplicity of infection (MOI) of 0.5. At 1 hour post infection, cells were washed, and fresh cell medium in 0.7% agarose was supplemented with 10μg/mL gentamicin to kill extracellular L. monocytogenes. At 5 days post infection, cells were stained with 0.3% crystal violet to visualize plaques. Plaque sizes were analyzed using ImageJ software.

4.5.5 Fluorescence Microscopy

L. monocytogenes strains were grown in BHI broth to OD_{600} ~0.5, bacteria cells were harvested by centrifugation, and washed with PBS. Next, 100μL of cell suspension was

incubated with 30μg/mL WGA for 10min in dark at room temperature. After incubation, 1.5μL of cell suspension was pipetted onto an agarose pad (1% agarose in PBS, placed on a microscopy slide), and sealed under a coverslip. Bacterial cells were imaged with a Nikon A1R Confocal (Nikon, Tokyo, Japan). The bacterial cell length and cell width were measured by MorphoSegger program created by Andres Florez from Github

4.5.6 Radioactive [^{14}C] GlcNAc Incorporation

L. monocytogenes strains were grown in BHI or BHI with 0.5xMIC of cefuroxime to mid-log phase. 0.32μL of [^{14}C] GlcNAc was added to 120μL of bacteria culture for a final concentration of 0.27mCi/mL. The sample was then incubated with shaking at 37°C. At time point 15min and 30min, the cells were collected on a 0.25μM filter paper and wash with PBS. The filter paper as well as bacteria cells were transferred into a pony vial containing 3 mL of scintillation fluid and the prepared sample will be analyzed for [^{14}C] GlcNAc using liquid scintillation analyzer (Tri-Carb 4910TR) as previously described[283].

4.5.7 Triton X-100–Induced Lysis

L. monocytogenes strains were grown to mid-log phase (OD_{600} ~0.5) in BHI or BHI + 0.5xMIC of cefuroxime, The bacteria cells were then washed by PBS, and resuspended in 0.1% volume/volume Triton X-100 in phosphate-buffered saline to a final OD_{600} of ~1. 200μL of bacteria suspension were transferred into a 96-wells plate and the cell lysis was monitored by OD_{600} measurements in a plate reader. The OD_{600} at each time points were normalized to OD_{600} in time zero of each strain.

4.6 Figures and tables

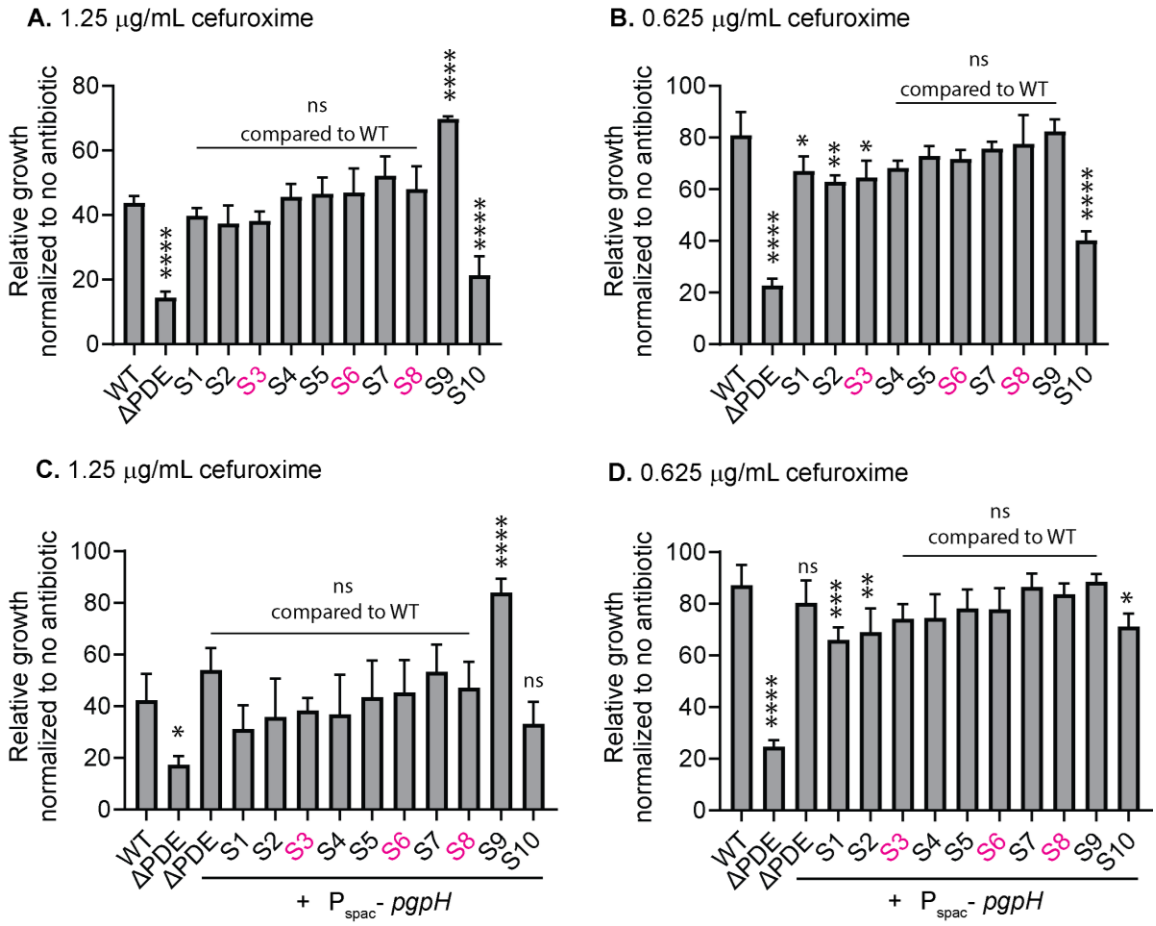

Figure 4.1 Suppressor mutations restore β-lactam resistance in ΔPDE but not in WT. *L. monocytogenes* cultures were grown in 96-well plate containing BHI only, or BHI plus 1.25μg/mL (**A, C**) or 0.625μg/mL (**B, D**) of cefuroxime, and bacterial growth was measured by OD_{600} at 37°C with intermittent shaking for 14 hours in a plate reader. For each strain, growth rates at each cefuroxime concentration were normalized to growth rate in BHI only of the same strain. Data are average of three independent experiments. Error bars represent standard deviations. Statistics: one-way ANOVA. ns, non-significant; *, P<0.05; **, P<0.01; ***, P<0.001; ****, P<0.0001.

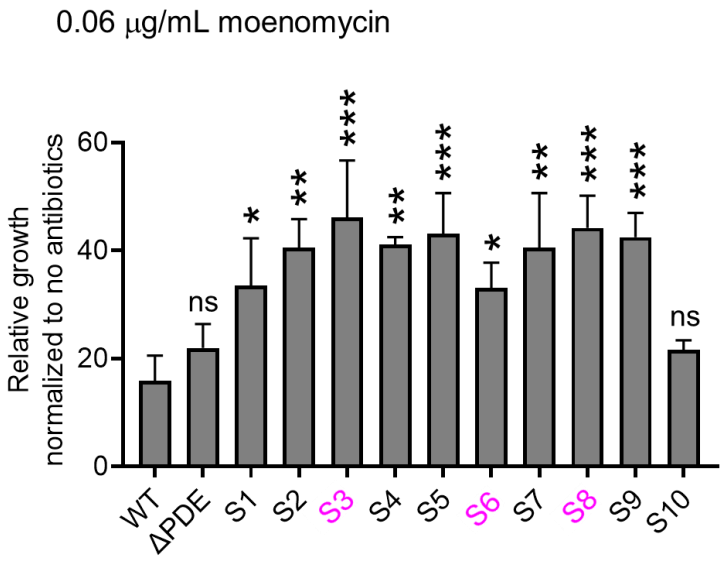

Figure 4.2 ΔPDE dose not sensitivity to Moenomycin while the suppressor mutants are more resistance to it. *L. monocytogenes* cultures were grown in 96-well plate containing BHI only, or BHI plus 0.06μg/mL of moenomycin, and bacterial growth was measured by OD_{600} at 37°C with intermittent shaking for 14 hours in a plate reader. For each strain, growth rates at 0.06 μg/mL moenomycin were normalized to growth rate in BHI only of the same strain. Data are average of three independent experiments. Error bars represent standard deviations. Statistics: one-way ANOVA. ns, non-significant; *, P<0.05; **, P<0.01; ***, P<0.001; ****, P<0.0001.

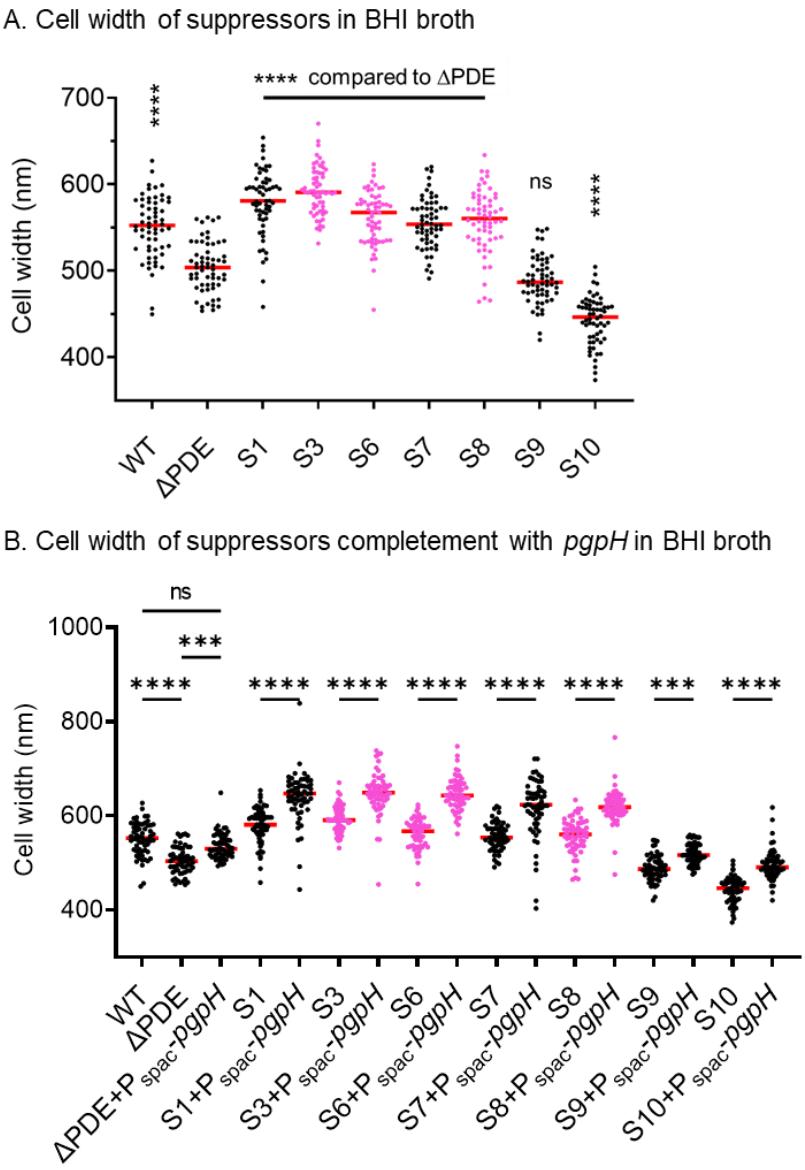

Figure 4.4 Mutations on MreB increased *L. monocytogenes* cell width. *Listeria* cultures were grown in BHI broth to mid-log phase. Bacteria cells were washed with PBS and stained with 30μg/mL of WGA for 10min. The Bacterial cells were imaged with a Nikon A1R Confocal (Nikon, Tokyo, Japan), and cell width were measured with MorphoSegger program. 50 representative measurements for suppressor mutants (**A**) and *pgph* complemented strains (**B**) are shown. The red dots indicate mutants that only contain MreB mutation. Statistics: one-way ANOVA. ns, non-significant; ***, P<0.001; ****, P<0.0001.

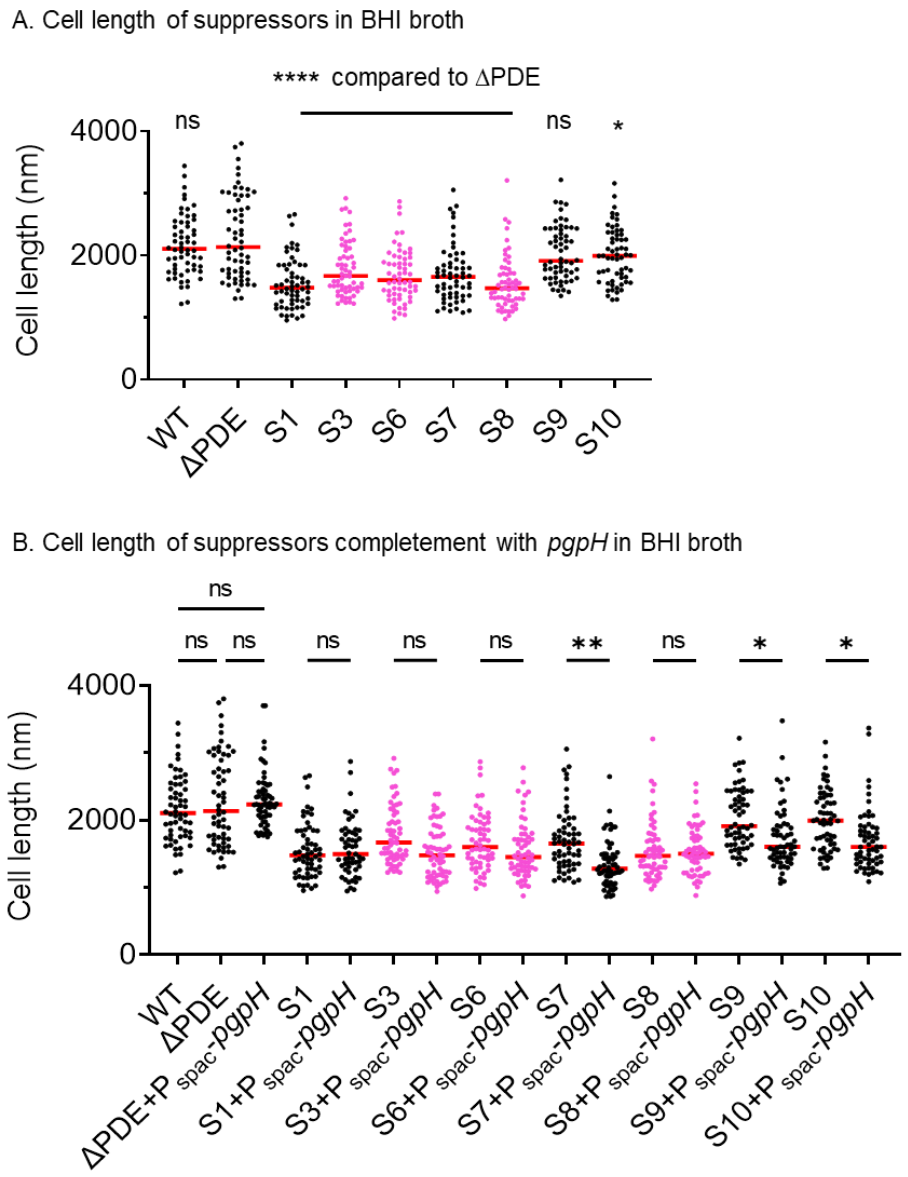

Figure 4.5 C-di-AMP level does not affect L. monocytogenes cell length. *Listeria* cultures were grown in BHI broth to mid-log phase. Bacteria cells were washed with PBS and stained with 30μg/mL of WGA for 10min. The bacterial cells were imaged with a Nikon A1R Confocal (Nikon, Tokyo, Japan), and cell length were measured with MorphoSegger program. 50 representative measurements for suppressor mutants (**A**) and *pgph* complemented strains (**B**) are shown. The red dots indicate mutants that only contain MreB mutation.Statistics: one-way ANOVA. ns, non-significant; *, P<0.05; **, P<0.01; ****, P<0.0001.

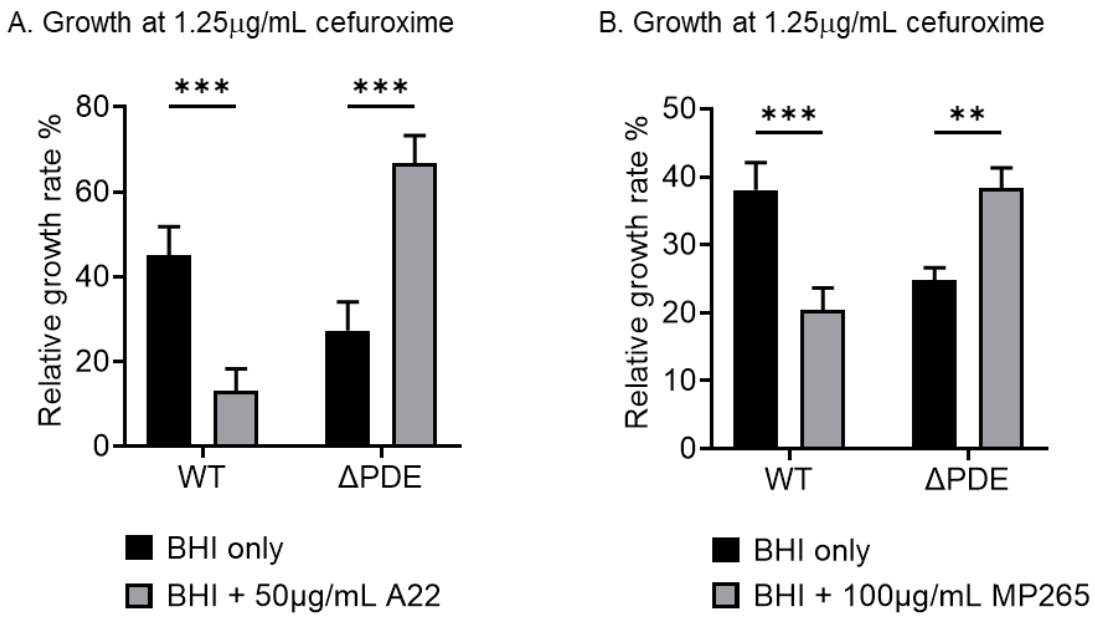

Figure 4.6 MreB inhibitor compounds restore β-lactam resistance for ΔPDE. *L. monocytogenes* cultures were grown in 96-well plate containing BHI only, BHI plus 1.25μg/mL of cefuroxime, The MreB inhibitor compounds A22 (**A**) or MP265 (**B**) were also added into the BHI broth or BHI plus cefuroxime at concentration of 50μg/mL, or 100μg/mL respectively. The bacterial growth was measured by OD_{600} at 37°C with intermittent shaking for 14 hours in a plate reader. For each strain, growth rates at each cefuroxime concentration were normalized to growth rate in corresponding broth without cefuroxime of the same strain. Data are average of three independent experiments. Error bars represent standard deviations. Statistics: two-way ANOVA. **, P<0.01; ***, P<0.001.

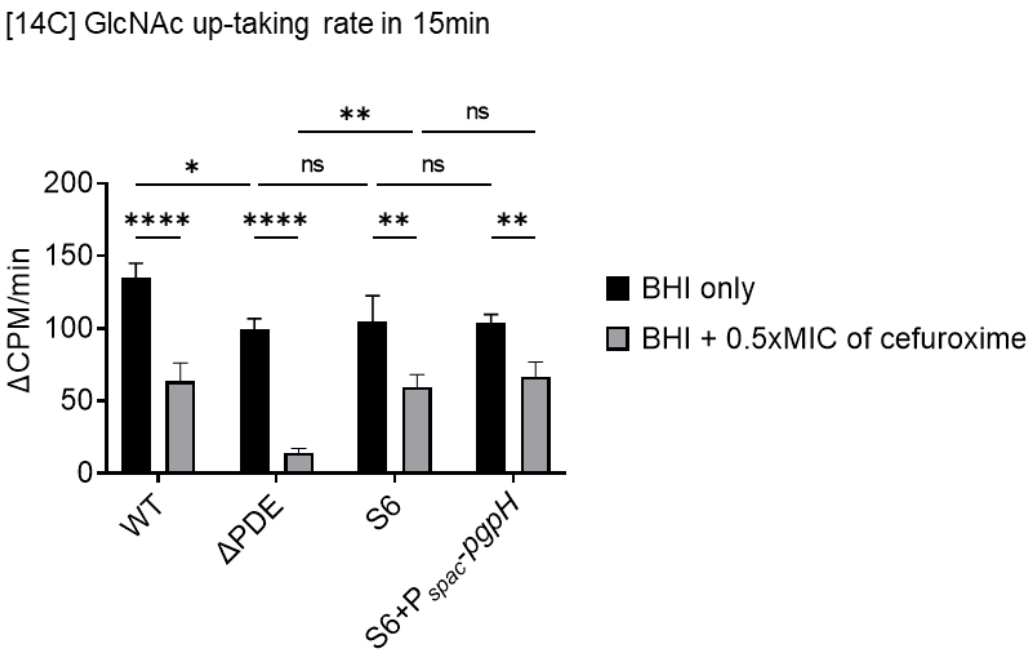

Figure 4.7 MreB mutation rescue ΔPDE PG synthesis upon β-lactam stress. *L. monocytogenes* cultures were grown in BHI, or BHI + 2.5μg/mL (WT and S6 + P_{spac}-*pgpH*) or 1.25μg/mL (ΔPDE and S6) of cefuroxime to mid-log phase. The [^{14}C] GlcNAc was then added to the bacteria cultures. Each sample was incubated with shaking at 37°C for 15min and 30min, the bacteria cells were collected, washed with PBS, and prepared for analysis of [^{14}C] GlcNAc using liquid scintillation analyzer (Tri-Carb 4910TR) as described[283]. Data are average of three independent experiments. Error bars represent standard deviations. Statistics: one-way ANOVA. ns, non-significant; *, P<0.05; **, P<0.01; ****, P<0.0001.

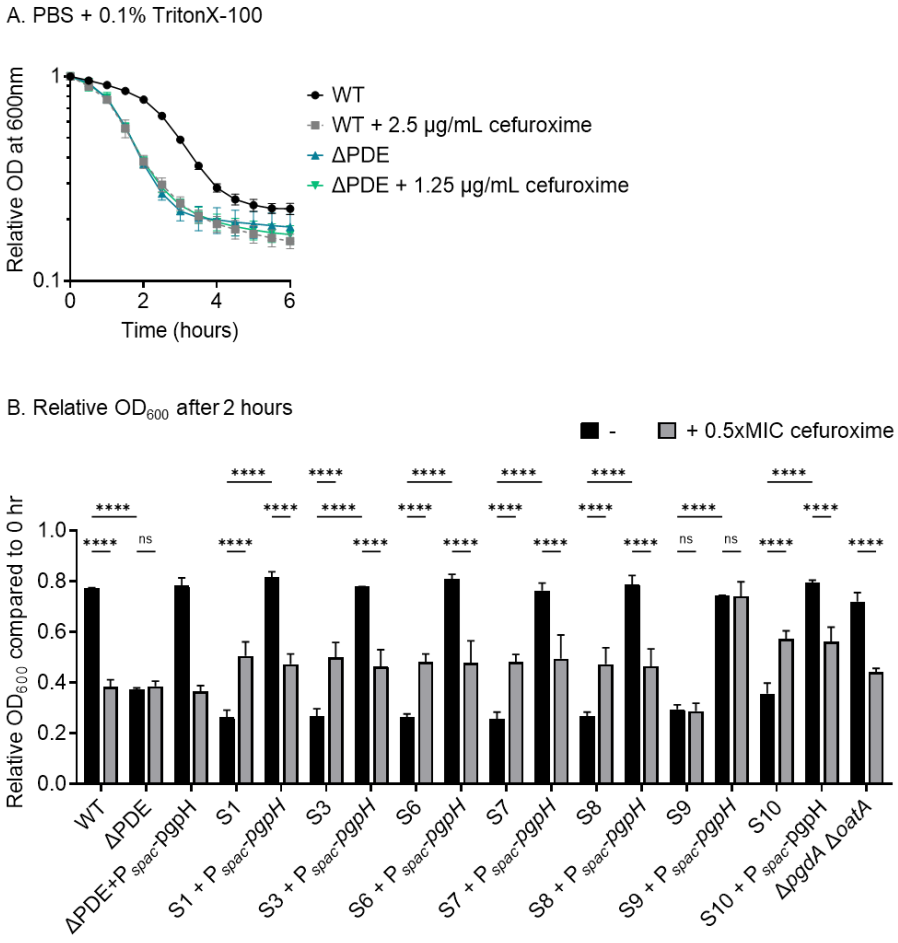

Figure 4.8 ΔPDE has increased autolysins activity while MreB mutations have modest effect on them. *L. monocytogenes* strains were grown to mid-log phase (OD_{600} ~0.5) BHI or BHI + 2.5mg/mL (WT) or 1.25mg/mL (ΔPDE) of cefuroxime, The bacteria cells were washed and resuspended in 0.1% volume/volume Triton X-100 in PBS to a final OD_{600} of ~1. 200µL of bacteria suspension were transferred into a 96-wells plate and the cell lysis was monitored by OD_{600} measurements in a plate reader. The OD_{600} at each time points were normalized to OD_{600} in time zero of each strain. (**A**) Lysis curves of WT and ΔPDE after grown in BHI or BHI + 2.5mg/mL (WT and S mutants + P_{spac}-*pgpH*) or 1.25mg/mL (ΔPDE and S mutants) of cefuroxime. (**B**) Relative OD_{600} after two hours treatment of TritonX-100. Data are average of three independent experiments. Error bars represent standard deviations. Statistics: one-way ANOVA. ns, non-significant; ***, P<0.001; ****, P<0.0001.

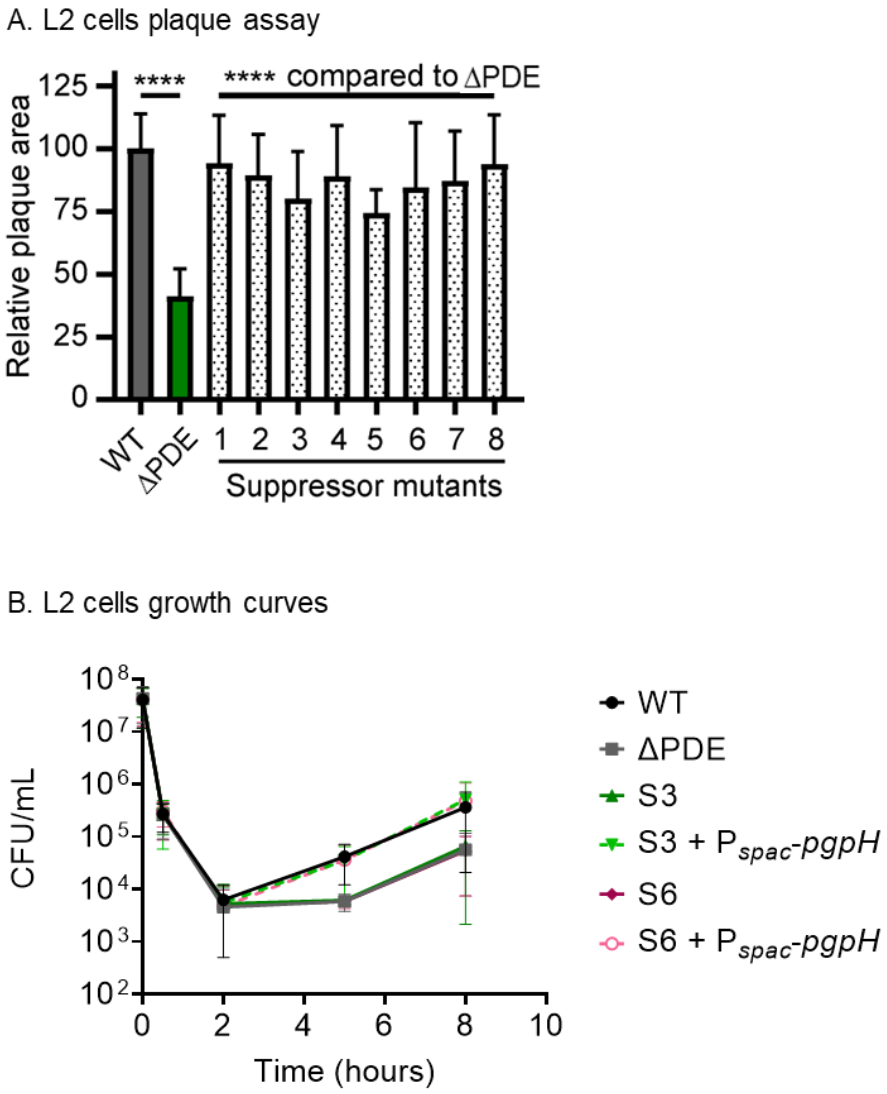

Figure 4.9 Suppressor mutations rescue ΔPDE in ex-vivo infection. (**A**)Plaque area from mouse fibroblasts (L2 cells) infected with indicated *L. monocytogenes* strains for three days and normalized to wild type (WT). (**B**) L2 cells were infected with indicated *L. monocytogenes* strains and CFUs were enumerated at various times post infection. Data are the average of two independent experiments. Error bars represent standard deviations. Statistics: one-way and two-way ANOVA; ****, P<0.0001.

Table 4.1 ΔPDE suppressor mutations. Nonsynonymous mutations resulting in amino acid changes are annotated from S1-S10.

Strains	Mutations	Gene annotations
S1	***mreB* (*mo1548*) A251V** *greA* (*lmo1496*) S46N	**rod-shape determinant** transcription elongation factor
S2	***mreB* G108E** *lmo0639* L93F *lmo2253* T88M	transcriptional regulator phosphoglucomutase
S3	***mreB* A46V**	
S4	***mreB* G108E** *lmo0723* A471V	chemotaxis protein
S5	***mreB* G108E** *atpF* (*lmo2533*) E70K	ATP synthase F(0) sector, subunit b
S6	***mreB* G108E**	
S7	***mreB* D8N** lmo0659 E98K	transcriptional regulator
S8	***mreB* V47I**	
S9	*rpoD* (*lmo1454*) T334A	control of cell wall metabolism
S10	*walR* (*lmo0287*) E25G *pdhA* (*lmo1052*) T207C	control of cell wall hydrolysis riboswitch preceding

Table 4.2 Strains used in this study

Strain number	Genotype	Source
L. monocytogenes (derivatives of strain 10403S)		
TNHL22	Δ*pdeA* Δ*pgpH* (ΔPDE)	(193)
TNHL376	S1	This study
TNHL392	S2	This study
TNHL393	S3	This study
TNHL394	S4	This study
TNHL418	S5	This study
TNHL414	S6	This study
TNHL416	S7	This study
TNHL417	S8	This study
TNHL395	S9	This study
TNHL396	S10	This study
TNHL29	ΔPDE + P_{spac}-*pgpH*	(193)
TNHL526	S1 + P_{spac}-*pgpH*	This study
TNHL527	S2 + P_{spac}-*pgpH*	This study
TNHL528	S3 + P_{spac}-*pgpH*	This study
TNHL529	S4 + P_{spac}-*pgpH*	This study
TNHL536	S5 + P_{spac}-*pgpH*	This study
TNHL532	S6 + P_{spac}-*pgpH*	This study
TNHL534	S7 + P_{spac}-*pgpH*	This study
TNHL535	S8 + P_{spac}-*pgpH*	This study
TNHL530	S9 + P_{spac}-*pgpH*	This study
TNHL531	S10 + P_{spac}-*pgpH*	This study
E. coli		
TNH47	pPL2-P_{spac}-*pgpH* in XL1B	This study

5. SUMMARY AND FUTURE RESEARCH

5.1 Summary

Bacteria have developed sophisticated systems to adapt and thrive under various stresses. These systems are essential for their survival, growth, and reproduction in different environments. Cyclic adenosine monophosphate (c-di-AMP) is a prokaryotic signaling molecule that plays a critical role in these processes. In the past ten years, significant advancements in c-di-AMP research have greatly enhanced our understanding of how this second messenger is involved in various signaling pathways. These include regulating osmotic pressure, central metabolism, DNA damage response, biofilm formation, sporulation, host immune responses, and adaptation to environmental changes in bacteria. Despite these advances, numerous aspects of c-di-AMP still require further investigation.

One noteworthy area for study is the ability of c-di-AMP to regulate bacterial antibiotic resistance, particularly against β-lactams, a cell wall-targeting antibiotic. Either low or high intracellular c-di-AMP levels will significantly reduce its activity to β-lactam antibiotics. Although many experiments have been conducted to identify the molecular mechanism of how c-di-AMP regulates β-lactam resistance, many hypotheses, such as the turgor model, have been proposed. The exact regulatory pathways remain unclear. Understanding the molecular foundations of these pathways can reveal pathways that are potential targets for new therapeutic interventions. Here in our study, I applied two approaches. One is to study the function of a c-di-AMP binding protein PstA in β-lactam resistance (Chapter 2 and 3). And another systematic way is to Characterize cell wall metabolism in the DPDE strain to determine how c-di-AMP regulates cell wall homeostasis under the β-lactams stress (Chapter 4).

PstA is a structurally conserved c-di-AMP-binding protein that is broadly present among Firmicutes bacteria. Furthermore, PstA binds c-di-AMP at high affinity and specificity, indicating an important role in the c-di-AMP signaling network. However, the molecular function of PstA remains elusive. Our findings reveal contrasting roles of PstA

in β-lactam resistance depending on c-di-AMP-binding status. In a normal or c-di-AMP-depleted environment, the apo form of PstA increases susceptibility to *L. monocytogenes*. However, when c-di-AMP accumulates due to the deletion of both c-di-AMP phosphodiesterases, PstA binds with c-di-AMP, enhancing bacterial resistance. Interestingly, PstA's role in β-lactam resistance is minimal during hypoxic growth. Additionally, PstA function during aerobic growth requires the cytochrome bd oxidase (CydAB), part of the respiratory electron transport chain. This dependency on CydAB might be linked to its roles in maintaining membrane potential or managing redox stress. Future efforts can exploit these conditions to identify PstA interaction partners under β-lactam stress.

In addition, we isolated and characterized suppressor mutants that can overcome the β-lactam stress on the plate even with the accumulation of c-di-AMP through a screening using ΔPDE EMS library. We identified that mutations in MreB, a cytoskeletal protein that shapes cells by directing cell wall synthesis, reversed the sensitivity of ΔPDE mutants to cefuroxime and their virulence. Further research showed that inhibiting MreB restored ΔPDE strains resistance to β-lactams and peptidoglycan (PG) synthesis. Additionally, we observed that the accumulation of c-di-AMP significantly increased autolysin activity, likely independent of MreB function, pointing to another role for c-di-AMP in maintaining bacterial cell wall integrity. These findings provide a foundation for further exploring the multifaceted role of c-di-AMP in regulating both the synthesis and breakdown of the bacterial wall, offering insights into how imbalances in c-di-AMP levels affect cell wall integrity and virulence.

Our studies revealed that the manipulation of cyclic di-adenosine monophosphate (c-di-AMP) on bacterial β-lactam resistance is multidimensional and requires the precise coordination of various proteins within the bacteria (**Fig. 4.1**). The regulation of c-di-AMP impacts the function of PstA, suggesting its involvement in aerobic respiration under β-lactam stress. Additionally, c-di-AMP appears to directly influence the homeostasis of the bacterial cell wall through MreB, and thereby modulating β-lactam resistance. This indicates a novel role for c-di-AMP beyond its known functions in osmotic homeostasis and central metabolism. Further studies (see below) will involve testing detailed molecular

mechanisms of c-di-AMP regulating PstA and MreB and how they regulate bacteria β-lactam resistance.

5.2 Future research

In Chapters 2 and 3, we demonstrated that apo-PstA plays a role in inducing bacterial β-lactam resistance, particularly under aerobic conditions. Given the structural similarity of PstA to canonical PII proteins, it is suggested that PstA functions in a manner analogous to these proteins, likely interacting with and regulating effector proteins, thereby playing a crucial role in cellular processes. Consequently, identifying PstA's binding partners is essential for understanding its function. However, our attempts to isolate specific proteins during pull-down assays in Chapter 3 were unsuccessful, suggesting that the interactions between PstA and its partners may be transient and occur under stress conditions. To improve our understanding, future pull-down assays for PstA should be performed in the presence of β-lactam antibiotics. Additionally, since many tagged PstA proteins are directly bound to beads, making elution difficult, we propose using an immunoprecipitation (IP) approach with a PstA-specific antibody instead of tags for cleaner and more specific results.

In addition, as powerful genetic tools for microbiology, genetic screening techniques are indispensable for identifying key genes and pathways that govern microbial functions and behaviors. In a recent project, I performed ethyl methanesulfonate (EMS) mutagenesis on the *c-dacA* P_{spac}-*pstA* strain. While rifampicin resistance tests[259,260] indicated a mutation frequency of 0.12 mutations per genome, surprisingly, each isolated strain contained over 10 mutations. This suggests that the current EMS exposure duration may be too long, leading to multiple unwanted mutations that could complicate the analysis and interpretation of results. To isolate single mutations for more precise genetic screening, reducing the EMS treatment time could be an effective adjustment. Furthermore, to enhance our understanding of PstA function, alternative genetic screening approaches should be considered. Generating a transposon library or implementing transposon sequencing (Tn-seq) offers robust methodologies for comprehensive and high-throughput identification of gene functions. These techniques could potentially

provide more targeted insights into the specific roles of PstA in microbial physiology and resistance mechanisms, thereby facilitating more directed and effective interventions.

Moreover, PstA exhibited to be critical when glycerol was used as the sole carbon source in the medium. Given that glycerol is non-fermentable, it is reasonable to hypothesize that PstA plays a role in aerobic metabolism, specifically in the metabolism of glycerol. This creates an ideal screening condition to identify the regulatory pathways in *L. monocytogenes*. Although subsequent experiments indicated that this phenotype of PstA may be unrelated to β-lactam susceptibility, this observation could unveil an additional function for c-di-AMP, given that PstA is a binding protein for this signaling molecule. Exploring this new role could provide significant insights into how c-di-AMP influences not only antibiotic resistance but also basic bacterial metabolism and survival under nutrient-limited conditions. This could potentially lead to the discovery of novel targets for antimicrobial interventions, expanding our understanding of microbial adaptation and resilience.

In Chapter 4, we explored the impact of mutations in MreB, a cytoskeletal protein that determines cell shape by guiding cell wall synthesis. We found that mutations in MreB restored sensitivity to cefuroxime in ΔPDE mutants. Further investigations revealed that inhibition of MreB also restored peptidoglycan (PG) synthesis in these mutants. Additionally, we observed that the accumulation of cyclic di-adenosine monophosphate (c-di-AMP) significantly increased autolysin activity. These findings suggest that c-di-AMP influences both the synthesis and hydrolysis of the bacterial cell wall. However, the precise regulatory pathways through which c-di-AMP acts remain elusive. While the processes involved in bacterial cell wall synthesis are well-documented, with many critical proteins involved in cell division and elongation already identified, our understanding of how c-di-AMP modulates these proteins is still in its infancy. Our future research will focus on elucidating this modulation. Regarding bacterial cell wall hydrolysis, knowledge is particularly sparse, especially in gram-positive bacteria. Employing genetic manipulation on those identified bacterial autolysins could be a promising approach to further investigate the role of c-di-AMP in this process.

In our studies, we observed that mutations in the MreB gene not only rescue ΔPDE mutants from β-lactam susceptibility but also significantly restore their infectivity. Notably,

all suppressor mutants formed plaques that were significantly larger than those formed by the ΔPDE mutants, suggesting a link between cell wall integrity and bacterial virulence. This finding implies that the reduced virulence in ΔPDE mutants may primarily stem from impairments in the bacterial cell wall, although the exact mechanisms influencing this relationship remain elusive.

To hypothesis can be proposed from current results: 1) Impact of c-di-AMP on Cell Wall Synthesis: The direct effect of c-di-AMP on bacterial cell wall synthesis may lead to reduced structural robustness against environmental stressors. Although ΔPDE mutants may retain inherent virulence capabilities, their increased sensitivity to the intracellular environment could lead to higher mortality rates. Investigating how modifications in c-di-AMP levels affect cell wall composition and resistance to osmotic and oxidative stresses could provide deeper insights into these dynamics. 2) Role of Increased Bacterial Hydrolysis: Enhanced hydrolysis in ΔPDE mutants could impair the structural integrity of the cell wall, making it less capable of withstanding severe environmental conditions. Furthermore, the accelerated turnover of peptidoglycan might activate the host's immune response more robustly, leading to improved pathogen clearance. Studies involving immune profiling in response to ΔPDE infection could reveal specific immune pathways activated by altered peptidoglycan dynamics.

The future research directions aim to deeply explore the complex interaction between bacterial cellular mechanisms and host responses: 1) Experimental validation: experimental designs could include constructing ΔPDE mutants with controlled c-di-AMP levels to observe changes in cell wall composition and subsequent effects on virulence and susceptibility to host immune responses. 2) Intracellular behavior studies: observing ΔPDE mutants within macrophage cultures to assess their survivability and interaction with host cellular mechanisms will provide valuable insights into the intracellular sensitivities of these mutants. 3) Immune response elicitation: Investigating the specific immune responses triggered by altered peptidoglycan turnover in host models can help determine the immunological aspects of increased bacterial clearance. By expanding our research to include these aspects, we can more comprehensively understand the multifaceted role of c-di-AMP in bacterial pathogenesis and resistance. This, in turn, could

lead to the development of targeted therapies that exploit these vulnerabilities in pathogenic bacteria.

Our overarching goal is to unravel the complex responses of bacteria to β-lactam antibiotics and to investigate the integral role of c-di-AMP in mediating these responses. This exploration is critical, as c-di-AMP is a pivotal signaling molecule that regulates a wide range of bacterial stress responses, including those activated during antibiotic exposure. Understanding how c-di-AMP impacts bacterial cell wall dynamics and antibiotic resistance mechanisms could open new avenues for therapeutic intervention.

5.3 Figure

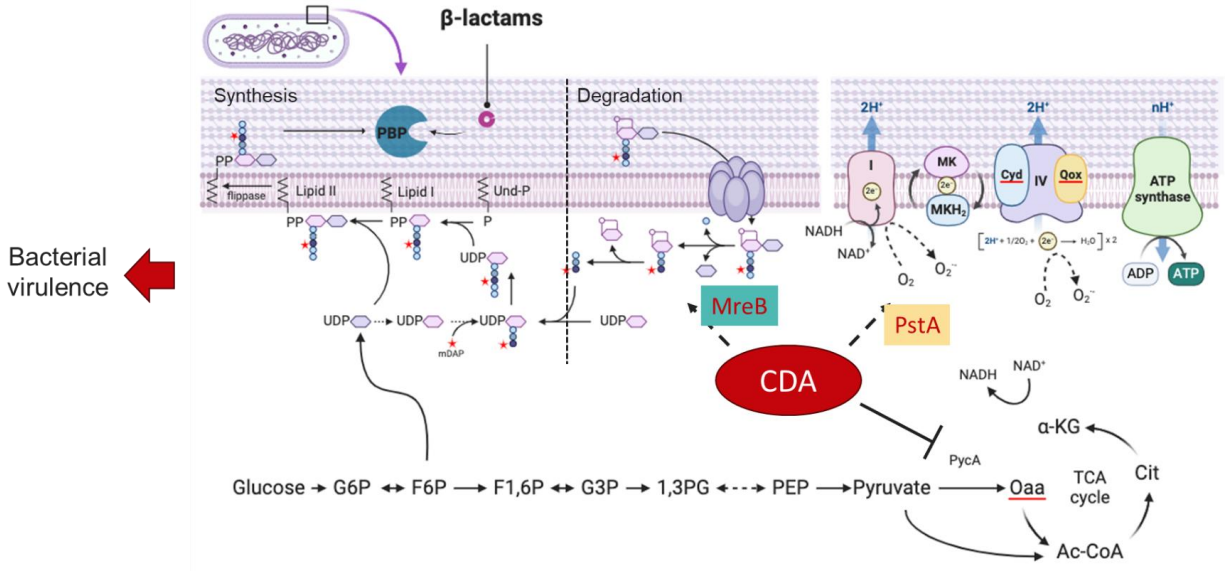

Figure 5.1 Schematic of c-di-AMP regulations on bacterial β-lactam resistance. C-di-AMP mediates different bacterial physiology processes to influence *L. monocytogenes* β-lactam resistance: 1) binding with PycA to regulate bacterial central metabolism. 2) binding with PstA, which is related to aerobic respiration. 3) regulating MreB to adjust bacteria cell wall synthesis and hydrolysis. These regulations may also affect L. monocytogenes virulence.

6. REFERENCES

1. Freitag NE, Port GC, Miner MD. Listeria monocytogenes - from saprophyte to intracellular pathogen. *Nat Rev Microbiol*. Sep 2009;7(9):623-8. doi:10.1038/nrmicro2171
2. Hamon M, Bierne H, Cossart P. Listeria monocytogenes: a multifaceted model. *Nat Rev Microbiol*. Jun 2006;4(6):423-34. doi:10.1038/nrmicro1413
3. Allam M, Tau N, Smouse SL, et al. Whole-Genome Sequences of Listeria monocytogenes Sequence Type 6 Isolates Associated with a Large Foodborne Outbreak in South Africa, 2017 to 2018. *Genome Announc*. Jun 21 2018;6(25)doi:10.1128/genomeA.00538-18
4. Scallan E, Hoekstra RM, Angulo FJ, et al. Foodborne illness acquired in the United States--major pathogens. *Emerg Infect Dis*. Jan 2011;17(1):7-15. doi:10.3201/eid1701.p11101
5. Allerberger F. Listeria: growth, phenotypic differentiation and molecular microbiology. *FEMS Immunol Med Microbiol*. Apr 01 2003;35(3):183-9. doi:10.1016/S0928-8244(02)00447-9
6. Bucur FI, Grigore-Gurgu L, Crauwels P, Riedel CU, Nicolau AI. Resistance of *Listeria monocytogenes* to stress conditions encountered in food and food processing environments. *Front Microbiol*. 2018;9:2700. doi:10.3389/fmicb.2018.02700
7. Wiedmann M, Arvik TJ, Hurley RJ, Boor KJ. General stress transcription factor sigmaB and its role in acid tolerance and virulence of Listeria monocytogenes. *J Bacteriol*. Jul 1998;180(14):3650-6. doi:10.1128/JB.180.14.3650-3656.1998
8. Chaturongakul S, Raengpradub S, Palmer ME, et al. Transcriptomic and phenotypic analyses identify coregulated, overlapping regulons among PrfA, CtsR, HrcA, and the alternative sigma factors sigmaB, sigmaC, sigmaH, and sigmaL in Listeria monocytogenes. *Appl Environ Microbiol*. Jan 2011;77(1):187-200. doi:10.1128/AEM.00952-10
9. Liu Y, Orsi RH, Boor KJ, Wiedmann M, Guariglia-Oropeza V. Home alone: elimination of all but one alternative sigma factor in *Listeria monocytogenes* allows prediction of new roles for sigma(B). *Front Microbiol*. 2017;8:1910. doi:10.3389/fmicb.2017.01910
10. Fraser KR, Sue D, Wiedmann M, Boor K, O'Byrne CP. Role of sigmaB in regulating the compatible solute uptake systems of Listeria monocytogenes: osmotic

induction of opuC is sigmaB dependent. *Appl Environ Microbiol*. Apr 2003;69(4):2015-22. doi:10.1128/AEM.69.4.2015-2022.2003

11. de las Heras A, Cain RJ, Bielecka MK, Vázquez-Boland JA. Regulation of Listeria virulence: PrfA master and commander. *Curr Opin Microbiol*. Apr 2011;14(2):118-27. doi:10.1016/j.mib.2011.01.005

12. Scortti M, Monzó HJ, Lacharme-Lora L, Lewis DA, Vázquez-Boland JA. The PrfA virulence regulon. *Microbes Infect*. Aug 2007;9(10):1196-207. doi:10.1016/j.micinf.2007.05.007

13. Phelps CC, Vadia S, Arnett E, et al. Relative Roles of Listeriolysin O, InlA, and InlB in Listeria monocytogenes Uptake by Host Cells. *Infect Immun*. Oct 2018;86(10)doi:10.1128/IAI.00555-18

14. Birmingham CL, Canadien V, Kaniuk NA, Steinberg BE, Higgins DE, Brumell JH. Listeriolysin O allows Listeria monocytogenes replication in macrophage vacuoles. *Nature*. Jan 17 2008;451(7176):350-4. doi:10.1038/nature06479

15. Portnoy DA, Auerbuch V, Glomski IJ. The cell biology of Listeria monocytogenes infection: the intersection of bacterial pathogenesis and cell-mediated immunity. *J Cell Biol*. Aug 05 2002;158(3):409-14. doi:10.1083/jcb.200205009

16. Hyden P, Pietzka A, Lennkh A, et al. Whole genome sequence-based serogrouping of Listeria monocytogenes isolates. *J Biotechnol*. Oct 10 2016;235:181-6. doi:10.1016/j.jbiotec.2016.06.005

17. Chakraborty T, Hain T, Domann E. Genome organization and the evolution of the virulence gene locus in Listeria species. *Int J Med Microbiol*. May 2000;290(2):167-74. doi:10.1016/S1438-4221(00)80086-7

18. Camilli A, Tilney LG, Portnoy DA. Dual roles of plcA in Listeria monocytogenes pathogenesis. *Mol Microbiol*. Apr 1993;8(1):143-57. doi:10.1111/j.1365-2958.1993.tb01211.x

19. Smith K, Youngman P. Use of a new integrational vector to investigate compartment-specific expression of the Bacillus subtilis spoIIM gene. *Biochimie*. 1992;74(7-8):705-11. doi:10.1016/0300-9084(92)90143-3

20. Lungu B, O'Bryan CA, Muthaiyan A, et al. Listeria monocytogenes: antibiotic resistance in food production. *Foodborne Pathog Dis*. May 2011;8(5):569-78. doi:10.1089/fpd.2010.0718

21. Wei C, Zhou P, Ye Q, Huang X, Li C, Wu A. Clinical characteristics of patients with listeriosis. *Zhong Nan Da Xue Xue Bao Yi Xue Ban*. Mar 28 2021;46(3):257-262. doi:10.11817/j.issn.1672-7347.2021.200399

22. Dos Reis JO, Vieira BS, Cunha Neto A, Castro VS, Figueiredo EES. Antimicrobial Resistance of *Listeria monocytogenes* from Animal Foods to First- and Second-Line Drugs in the Treatment of Listeriosis from 2008 to 2021: A Systematic Review

and Meta-Analysis. *Can J Infect Dis Med Microbiol*. 2022;2022:1351983. doi:10.1155/2022/1351983

23. Chow JTH, Gall AR, Johnson AK, Huynh TN. Characterization of Listeria monocytogenes isolates from lactating dairy cows in a Wisconsin farm: Antibiotic resistance, mammalian cell infection, and effects on the fecal microbiota. *J Dairy Sci*. Apr 2021;104(4):4561-4574. doi:10.3168/jds.2020-18885

24. Schneider T, Sahl HG. An oldie but a goodie - cell wall biosynthesis as antibiotic target pathway. *Int J Med Microbiol*. Feb 2010;300(2-3):161-9. doi:10.1016/j.ijmm.2009.10.005

25. Goldman WE, Klapper DG, Baseman JB. Detection, isolation, and analysis of a released Bordetella pertussis product toxic to cultured tracheal cells. *Infect Immun*. May 1982;36(2):782-94. doi:10.1128/iai.36.2.782-794.1982

26. Jutras BL, Lochhead RB, Kloos ZA, et al. peptidoglycan is a persistent antigen in patients with Lyme arthritis. *Proc Natl Acad Sci U S A*. Jul 02 2019;116(27):13498-13507. doi:10.1073/pnas.1904170116

27. Sorbara MT, Philpott DJ. Peptidoglycan: a critical activator of the mammalian immune system during infection and homeostasis. *Immunol Rev*. Sep 2011;243(1):40-60. doi:10.1111/j.1600-065X.2011.01047.x

28. Dörr T, Moynihan PJ, Mayer C. Editorial: Bacterial Cell Wall Structure and Dynamics. *Front Microbiol*. 2019;10:2051. doi:10.3389/fmicb.2019.02051

29. Höltje JV. Growth of the stress-bearing and shape-maintaining murein sacculus of Escherichia coli. *Microbiol Mol Biol Rev*. Mar 1998;62(1):181-203. doi:10.1128/MMBR.62.1.181-203.1998

30. Pasquina-Lemonche L, Burns J, Turner RD, et al. The architecture of the Gram-positive bacterial cell wall. *Nature*. Jun 2020;582(7811):294-297. doi:10.1038/s41586-020-2236-6

31. Brown S, Santa Maria JP, Walker S. Wall teichoic acids of gram-positive bacteria. *Annu Rev Microbiol*. 2013;67:313-36. doi:10.1146/annurev-micro-092412-155620

32. Vollmer W, Blanot D, de Pedro MA. Peptidoglycan structure and architecture. *FEMS Microbiol Rev*. Mar 2008;32(2):149-67. doi:10.1111/j.1574-6976.2007.00094.x

33. Gan L, Chen S, Jensen GJ. Molecular organization of Gram-negative peptidoglycan. *Proc Natl Acad Sci U S A*. Dec 02 2008;105(48):18953-7. doi:10.1073/pnas.0808035105

34. Rohs PDA, Bernhardt TG. Growth and Division of the Peptidoglycan Matrix. *Annu Rev Microbiol*. Oct 08 2021;75:315-336. doi:10.1146/annurev-micro-020518-120056

35. Barreteau H, Kovac A, Boniface A, Sova M, Gobec S, Blanot D. Cytoplasmic steps of peptidoglycan biosynthesis. *FEMS Microbiol Rev*. Mar 2008;32(2):168-207. doi:10.1111/j.1574-6976.2008.00104.x

36. Bouhss A, Trunkfield AE, Bugg TD, Mengin-Lecreulx D. The biosynthesis of peptidoglycan lipid-linked intermediates. *FEMS Microbiol Rev*. Mar 2008;32(2):208-33. doi:10.1111/j.1574-6976.2007.00089.x

37. Elhenawy W, Davis RM, Fero J, Salama NR, Felman MF, Ruiz N. The O-Antigen Flippase Wzk Can Substitute for MurJ in Peptidoglycan Synthesis in Helicobacter pylori and Escherichia coli. *PLoS One*. 2016;11(8):e0161587. doi:10.1371/journal.pone.0161587

38. Kuk ACY, Hao A, Guan Z, Lee SY. Visualizing conformation transitions of the Lipid II flippase MurJ. *Nat Commun*. Apr 15 2019;10(1):1736. doi:10.1038/s41467-019-09658-0

39. Mohammadi T, van Dam V, Sijbrandi R, et al. Identification of FtsW as a transporter of lipid-linked cell wall precursors across the membrane. *EMBO J*. Apr 20 2011;30(8):1425-32. doi:10.1038/emboj.2011.61

40. Sjodt M, Rohs PDA, Gilman MSA, et al. Structural coordination of polymerization and crosslinking by a SEDS-bPBP peptidoglycan synthase complex. *Nat Microbiol*. Jun 2020;5(6):813-820. doi:10.1038/s41564-020-0687-z

41. Sauvage E, Kerff F, Terrak M, Ayala JA, Charlier P. The penicillin-binding proteins: structure and role in peptidoglycan biosynthesis. *FEMS Microbiol Rev*. Mar 2008;32(2):234-58. doi:10.1111/j.1574-6976.2008.00105.x

42. Macheboeuf P, Di Guilmi AM, Job V, Vernet T, Dideberg O, Dessen A. Active site restructuring regulates ligand recognition in class A penicillin-binding proteins. *Proc Natl Acad Sci U S A*. Jan 18 2005;102(3):577-82. doi:10.1073/pnas.0407186102

43. Morè N, Martorana AM, Biboy J, et al. Peptidoglycan Remodeling Enables Escherichia coli To Survive Severe Outer Membrane Assembly Defect. *mBio*. Feb 05 2019;10(1)doi:10.1128/mBio.02729-18

44. van Teeffelen S, Wang S, Furchtgott L, et al. The bacterial actin MreB rotates, and rotation depends on cell-wall assembly. *Proc Natl Acad Sci U S A*. Sep 20 2011;108(38):15822-7. doi:10.1073/pnas.1108999108

45. Wong F, Garner EC, Amir A. Mechanics and dynamics of translocating MreB filaments on curved membranes. *Elife*. Feb 18 2019;8doi:10.7554/eLife.40472

46. Sjodt M, Brock K, Dobihal G, et al. Structure of the peptidoglycan polymerase RodA resolved by evolutionary coupling analysis. *Nature*. Apr 05 2018;556(7699):118-121. doi:10.1038/nature25985

47. van den Ent F, Johnson CM, Persons L, de Boer P, Löwe J. Bacterial actin MreB assembles in complex with cell shape protein RodZ. *EMBO J*. Mar 17 2010;29(6):1081-90. doi:10.1038/emboj.2010.9

48. Rohs PDA, Buss J, Sim SI, et al. A central role for PBP2 in the activation of peptidoglycan polymerization by the bacterial cell elongation machinery. *PLoS Genet*. Oct 2018;14(10):e1007726. doi:10.1371/journal.pgen.1007726

49. Özbaykal G, Wollrab E, Simon F, et al. The transpeptidase PBP2 governs initial localization and activity of the major cell-wall synthesis machinery in. *Elife*. Feb 20 2020;9doi:10.7554/eLife.50629

50. Leaver M, Errington J. Roles for MreC and MreD proteins in helical growth of the cylindrical cell wall in Bacillus subtilis. *Mol Microbiol*. Sep 2005;57(5):1196-209. doi:10.1111/j.1365-2958.2005.04736.x

51. McQuillen R, Xiao J. Insights into the Structure, Function, and Dynamics of the Bacterial Cytokinetic FtsZ-Ring. *Annu Rev Biophys*. May 06 2020;49:309-341. doi:10.1146/annurev-biophys-121219-081703

52. Bi EF, Lutkenhaus J. FtsZ ring structure associated with division in Escherichia coli. *Nature*. Nov 14 1991;354(6349):161-4. doi:10.1038/354161a0

53. Yang X, Lyu Z, Miguel A, McQuillen R, Huang KC, Xiao J. GTPase activity-coupled treadmilling of the bacterial tubulin FtsZ organizes septal cell wall synthesis. *Science*. Feb 17 2017;355(6326):744-747. doi:10.1126/science.aak9995

54. Xiao J, Goley ED. Redefining the roles of the FtsZ-ring in bacterial cytokinesis. *Curr Opin Microbiol*. Dec 2016;34:90-96. doi:10.1016/j.mib.2016.08.008

55. Rodrigues CD, Harry EJ. The Min system and nucleoid occlusion are not required for identifying the division site in Bacillus subtilis but ensure its efficient utilization. *PLoS Genet*. 2012;8(3):e1002561. doi:10.1371/journal.pgen.1002561

56. Loose M, Mitchison TJ. The bacterial cell division proteins FtsA and FtsZ self-organize into dynamic cytoskeletal patterns. *Nat Cell Biol*. Jan 2014;16(1):38-46. doi:10.1038/ncb2885

57. Marmont LS, Bernhardt TG. A conserved subcomplex within the bacterial cytokinetic ring activates cell wall synthesis by the FtsW-FtsI synthase. *Proc Natl Acad Sci U S A*. Sep 22 2020;117(38):23879-23885. doi:10.1073/pnas.2004598117

58. Do T, Page JE, Walker S. Uncovering the activities, biological roles, and regulation of bacterial cell wall hydrolases and tailoring enzymes. *J Biol Chem*. Mar 06 2020;295(10):3347-3361. doi:10.1074/jbc.REV119.010155

59. Park JT, Uehara T. How bacteria consume their own exoskeletons (turnover and recycling of cell wall peptidoglycan). *Microbiol Mol Biol Rev*. Jun 2008;72(2):211-27, table of contents. doi:10.1128/MMBR.00027-07

60. Reith J, Mayer C. Peptidoglycan turnover and recycling in Gram-positive bacteria. *Appl Microbiol Biotechnol*. Oct 2011;92(1):1-11. doi:10.1007/s00253-011-3486-x

61. Mayer C, Kluj RM, Mühleck M, et al. Bacteria's different ways to recycle their own cell wall. *Int J Med Microbiol*. Nov 2019;309(7):151326. doi:10.1016/j.ijmm.2019.06.006

62. Johnson JW, Fisher JF, Mobashery S. Bacterial cell-wall recycling. *Ann N Y Acad Sci*. Jan 2013;1277(1):54-75. doi:10.1111/j.1749-6632.2012.06813.x

63. van Heijenoort J. Peptidoglycan hydrolases of Escherichia coli. *Microbiol Mol Biol Rev*. Dec 2011;75(4):636-63. doi:10.1128/MMBR.00022-11

64. Jacobs C, Huang LJ, Bartowsky E, Normark S, Park JT. Bacterial cell wall recycling provides cytosolic muropeptides as effectors for beta-lactamase induction. *EMBO J*. Oct 03 1994;13(19):4684-94. doi:10.1002/j.1460-2075.1994.tb06792.x

65. Delaune A, Poupel O, Mallet A, Coic YM, Msadek T, Dubrac S. Peptidoglycan crosslinking relaxation plays an important role in Staphylococcus aureus WalKR-dependent cell viability. *PLoS One*. Feb 28 2011;6(2):e17054. doi:10.1371/journal.pone.0017054

66. Mauck J, Chan L, Glaser L. Turnover of the cell wall of Gram-positive bacteria. *J Biol Chem*. Mar 25 1971;246(6):1820-7.

67. Litzinger S, Duckworth A, Nitzsche K, Risinger C, Wittmann V, Mayer C. Muropeptide rescue in Bacillus subtilis involves sequential hydrolysis by beta-N-acetylglucosaminidase and N-acetylmuramyl-L-alanine amidase. *J Bacteriol*. Jun 2010;192(12):3132-43. doi:10.1128/JB.01256-09

68. Borisova M, Gaupp R, Duckworth A, et al. Peptidoglycan Recycling in Gram-Positive Bacteria Is Crucial for Survival in Stationary Phase. *mBio*. Oct 11 2016;7(5)doi:10.1128/mBio.00923-16

69. Vicente MF, Pérez-Díaz JC, Baquero F, Angel de Pedro M, Berenguer J. Penicillin-binding protein 3 of Listeria monocytogenes as the primary lethal target for beta-lactams. *Antimicrob Agents Chemother*. Apr 1990;34(4):539-42. doi:10.1128/AAC.34.4.539

70. Glaser P, Frangeul L, Buchrieser C, et al. Comparative genomics of Listeria species. *Science*. Oct 26 2001;294(5543):849-52. doi:10.1126/science.1063447

71. Guinane CM, Cotter PD, Ross RP, Hill C. Contribution of penicillin-binding protein homologs to antibiotic resistance, cell morphology, and virulence of Listeria monocytogenes EGDe. *Antimicrob Agents Chemother*. Aug 2006;50(8):2824-8. doi:10.1128/AAC.00167-06

72. Bierne H, Cossart P. Listeria monocytogenes surface proteins: from genome predictions to function. *Microbiol Mol Biol Rev*. Jun 2007;71(2):377-97. doi:10.1128/MMBR.00039-06

73. Korsak D, Markiewicz Z, Gutkind GO, Ayala JA. Identification of the full set of Listeria monocytogenes penicillin-binding proteins and characterization of PBPD2 (Lmo2812). *BMC Microbiol*. Sep 15 2010;10:239. doi:10.1186/1471-2180-10-239

74. Van de Velde S, Carryn S, Van Bambeke F, Hill C, Tulkens PM, Sleator RD. Penicillin-binding proteins (PBP) and Lmo0441 (a PBP-like protein) play a role in Beta-lactam sensitivity of Listeria monocytogenes. *Gut Pathog*. Dec 15 2009;1:23. doi:10.1186/1757-4749-1-23

75. Klumpp J, Staubli T, Schmitter S, Hupfeld M, Fouts DE, Loessner MJ. Genome Sequences of Three Frequently Used Listeria monocytogenes and Listeria ivanovii Strains. *Genome Announc*. May 01 2014;2(2)doi:10.1128/genomeA.00404-14

76. Holch A, Webb K, Lukjancenko O, Ussery D, Rosenthal BM, Gram L. Genome sequencing identifies two nearly unchanged strains of persistent Listeria monocytogenes isolated at two different fish processing plants sampled 6 years apart. *Appl Environ Microbiol*. May 2013;79(9):2944-51. doi:10.1128/AEM.03715-12

77. Faith NG, Kathariou S, Neudeck BL, Luchansky JB, Czuprynski CJ. A P60 mutant of Listeria monocytogenes is impaired in its ability to cause infection in intragastrically inoculated mice. *Microb Pathog*. 2007;42(5-6):237-41. doi:10.1016/j.micpath.2007.01.004

78. Schubert K, Bichlmaier AM, Mager E, Wolff K, Ruhland G, Fiedler F. P45, an extracellular 45 kDa protein of Listeria monocytogenes with similarity to protein p60 and exhibiting peptidoglycan lytic activity. *Arch Microbiol*. Jan 2000;173(1):21-8. doi:10.1007/s002030050003

79. Milohanic E, Jonquières R, Glaser P, et al. Sequence and binding activity of the autolysin-adhesin Ami from epidemic Listeria monocytogenes 4b. *Infect Immun*. Aug 2004;72(8):4401-9. doi:10.1128/IAI.72.8.4401-4409.2004

80. Bublitz M, Polle L, Holland C, Heinz DW, Nimtz M, Schubert WD. Structural basis for autoinhibition and activation of Auto, a virulence-associated peptidoglycan hydrolase of Listeria monocytogenes. *Mol Microbiol*. Mar 2009;71(6):1509-22. doi:10.1111/j.1365-2958.2009.06619.x

81. Machata S, Hain T, Rohde M, Chakraborty T. Simultaneous deficiency of both MurA and p60 proteins generates a rough phenotype in Listeria monocytogenes. *J Bacteriol*. Dec 2005;187(24):8385-94. doi:10.1128/JB.187.24.8385-8394.2005

82. Popowska M, Markiewicz Z. Characterization of Listeria monocytogenes protein Lmo0327 with murein hydrolase activity. *Arch Microbiol*. Jul 2006;186(1):69-86. doi:10.1007/s00203-006-0122-8

83. Wang L, Walrond L, Cyr TD, Lin M. A novel surface autolysin of Listeria monocytogenes serotype 4b, IspC, contains a 23-residue N-terminal signal

peptide being processed in E. coli. *Biochem Biophys Res Commun*. Mar 09 2007;354(2):403-8. doi:10.1016/j.bbrc.2006.12.218

84. Carroll SA, Hain T, Technow U, et al. Identification and characterization of a peptidoglycan hydrolase, MurA, of Listeria monocytogenes, a muramidase needed for cell separation. *J Bacteriol*. Dec 2003;185(23):6801-8. doi:10.1128/JB.185.23.6801-6808.2003

85. Cabanes D, Dussurget O, Dehoux P, Cossart P. Auto, a surface associated autolysin of Listeria monocytogenes required for entry into eukaryotic cells and virulence. *Mol Microbiol*. Mar 2004;51(6):1601-14. doi:10.1111/j.1365-2958.2003.03945.x

86. Milohanic E, Jonquières R, Cossart P, Berche P, Gaillard JL. The autolysin Ami contributes to the adhesion of Listeria monocytogenes to eukaryotic cells via its cell wall anchor. *Mol Microbiol*. Mar 2001;39(5):1212-24. doi:10.1111/j.1365-2958.2001.02208.x

87. Wang L, Lin M. A novel cell wall-anchored peptidoglycan hydrolase (autolysin), IspC, essential for Listeria monocytogenes virulence: genetic and proteomic analysis. *Microbiology (Reading)*. Jul 2008;154(Pt 7):1900-1913. doi:10.1099/mic.0.2007/015172-0

88. Macheboeuf P, Contreras-Martel C, Job V, Dideberg O, Dessen A. Penicillin binding proteins: key players in bacterial cell cycle and drug resistance processes. *FEMS Microbiol Rev*. Sep 2006;30(5):673-91. doi:10.1111/j.1574-6976.2006.00024.x

89. Kampmeier RH, Sweeney A, Quinn RW, Lefkowitz LB, Dupont WD. A survey of 251 patients with acute syphilis treated in the collaborative penicillin study of 1943-1950. *Sex Transm Dis*. 1981;8(4):266-79. doi:10.1097/00007435-198110000-00006

90. Miller EL. The penicillins: a review and update. *J Midwifery Womens Health*. 2002;47(6):426-34. doi:10.1016/s1526-9523(02)00330-6

91. Rolinson GN, Geddes AM. The 50th anniversary of the discovery of 6-aminopenicillanic acid (6-APA). *Int J Antimicrob Agents*. Jan 2007;29(1):3-8. doi:10.1016/j.ijantimicag.2006.09.003

92. Neu HC. The new beta-lactamase-stable cephalosporins. *Ann Intern Med*. Sep 1982;97(3):408-19. doi:10.7326/0003-4819-97-3-408

93. Page MG, Kellenberger L. Stemming the tide? Advances in antibiotic discovery and development in the face of emerging resistance and financial constraint. *Curr Opin Pharmacol*. Oct 2012;12(5):519-21. doi:10.1016/j.coph.2012.07.018

94. Birnbaum J, Kahan FM, Kropp H, MacDonald JS. Carbapenems, a new class of beta-lactam antibiotics. Discovery and development of imipenem/cilastatin. *Am J Med*. Jun 07 1985;78(6A):3-21. doi:10.1016/0002-9343(85)90097-x

95. Maveyraud L, Pratt RF, Samama JP. Crystal structure of an acylation transition-state analog of the TEM-1 beta-lactamase. Mechanistic implications for class A beta-lactamases. *Biochemistry*. Feb 24 1998;37(8):2622-8. doi:10.1021/bi972501b

96. Papp-Wallace KM, Endimiani A, Taracila MA, Bonomo RA. Carbapenems: past, present, and future. *Antimicrob Agents Chemother*. Nov 2011;55(11):4943-60. doi:10.1128/AAC.00296-11

97. Bonfiglio G, Russo G, Nicoletti G. Recent developments in carbapenems. *Expert Opin Investig Drugs*. Apr 2002;11(4):529-44. doi:10.1517/13543784.11.4.529

98. Queenan AM, Shang W, Flamm R, Bush K. Hydrolysis and inhibition profiles of beta-lactamases from molecular classes A to D with doripenem, imipenem, and meropenem. *Antimicrob Agents Chemother*. Jan 2010;54(1):565-9. doi:10.1128/AAC.01004-09

99. Fu HG, Hu XX, Li CR, et al. Design, synthesis and biological evaluation of monobactams as antibacterial agents against gram-negative bacteria. *Eur J Med Chem*. Mar 03 2016;110:151-63. doi:10.1016/j.ejmech.2016.01.024

100. Ellis-Grosse EJ, Babinchak T, Dartois N, et al. The efficacy and safety of tigecycline in the treatment of skin and skin-structure infections: results of 2 double-blind phase 3 comparison studies with vancomycin-aztreonam. *Clin Infect Dis*. Sep 01 2005;41 Suppl 5:S341-53. doi:10.1086/431675

101. King DT, Worrall LJ, Gruninger R, Strynadka NC. New Delhi metallo-β-lactamase: structural insights into β-lactam recognition and inhibition. *J Am Chem Soc*. Jul 18 2012;134(28):11362-5. doi:10.1021/ja303579d

102. Zapun A, Contreras-Martel C, Vernet T. Penicillin-binding proteins and beta-lactam resistance. *FEMS Microbiol Rev*. Mar 2008;32(2):361-85. doi:10.1111/j.1574-6976.2007.00095.x

103. Tomasz A. The mechanism of the irreversible antimicrobial effects of penicillins: how the beta-lactam antibiotics kill and lyse bacteria. *Annu Rev Microbiol*. 1979;33:113-37. doi:10.1146/annurev.mi.33.100179.000553

104. Uehara T, Dinh T, Bernhardt TG. LytM-domain factors are required for daughter cell separation and rapid ampicillin-induced lysis in Escherichia coli. *J Bacteriol*. Aug 2009;191(16):5094-107. doi:10.1128/JB.00505-09

105. Tipper DJ, Strominger JL. Mechanism of action of penicillins: a proposal based on their structural similarity to acyl-D-alanyl-D-alanine. *Proc Natl Acad Sci U S A*. Oct 1965;54(4):1133-41. doi:10.1073/pnas.54.4.1133

106. Wivagg CN, Bhattacharyya RP, Hung DT. Mechanisms of β-lactam killing and resistance in the context of Mycobacterium tuberculosis. *J Antibiot (Tokyo)*. Sep 2014;67(9):645-54. doi:10.1038/ja.2014.94

107. Goebel WF, Avery OT. A STUDY OF PNEUMOCOCCUS AUTOLYSIS. *J Exp Med*. Jan 31 1929;49(2):267-86. doi:10.1084/jem.49.2.267

108. Tomasz A, Albino A, Zanati E. Multiple antibiotic resistance in a bacterium with suppressed autolytic system. *Nature*. Jul 11 1970;227(5254):138-40. doi:10.1038/227138a0

109. Kitano K, Tomasz A. Escherichia coli mutants tolerant to beta-lactam antibiotics. *J Bacteriol*. Dec 1979;140(3):955-63. doi:10.1128/jb.140.3.955-963.1979

110. Rogers HJ, Thurman PF, Burdett ID. The bactericidal action of beta-lactam antibiotics on an autolysin-deficient strain of Bacillus subtilis. *J Gen Microbiol*. Feb 1983;129(2):465-78. doi:10.1099/00221287-129-2-465

111. Tomasz A. The role of autolysins in cell death. *Ann N Y Acad Sci*. May 10 1974;235(0):439-47. doi:10.1111/j.1749-6632.1974.tb43282.x

112. Salamaga B, Kong L, Pasquina-Lemonche L, et al. Demonstration of the role of cell wall homeostasis in *Staphylococcus aureus* growth and the action of bactericidal antibiotics. *Proc Natl Acad Sci U S A*. Nov 02 2021;118(44)doi:10.1073/pnas.2106022118

113. Chung HS, Yao Z, Goehring NW, Kishony R, Beckwith J, Kahne D. Rapid beta-lactam-induced lysis requires successful assembly of the cell division machinery. *Proc Natl Acad Sci U S A*. Dec 22 2009;106(51):21872-7. doi:10.1073/pnas.0911674106

114. Goodell EW, Lopez R, Tomasz A. Suppression of lytic effect of beta lactams on Escherichia coli and other bacteria. *Proc Natl Acad Sci U S A*. Sep 1976;73(9):3293-7. doi:10.1073/pnas.73.9.3293

115. Rice KC, Bayles KW. Molecular control of bacterial death and lysis. *Microbiol Mol Biol Rev*. Mar 2008;72(1):85-109, table of contents. doi:10.1128/MMBR.00030-07

116. Cho H, Uehara T, Bernhardt TG. Beta-lactam antibiotics induce a lethal malfunctioning of the bacterial cell wall synthesis machinery. *Cell*. Dec 04 2014;159(6):1300-11. doi:10.1016/j.cell.2014.11.017

117. Kohanski MA, Dwyer DJ, Hayete B, Lawrence CA, Collins JJ. A common mechanism of cellular death induced by bactericidal antibiotics. *Cell*. Sep 07 2007;130(5):797-810. doi:10.1016/j.cell.2007.06.049

118. Duan X, Huang X, Wang X, et al. l-Serine potentiates fluoroquinolone activity against Escherichia coli by enhancing endogenous reactive oxygen species production. *J Antimicrob Chemother*. Aug 2016;71(8):2192-9. doi:10.1093/jac/dkw114

119. Thomas VC, Kinkead LC, Janssen A, et al. A dysfunctional tricarboxylic acid cycle enhances fitness of Staphylococcus epidermidis during β-lactam stress. *mBio*. Aug 20 2013;4(4)doi:10.1128/mBio.00437-13

120. Frávega J, Álvarez R, Díaz F, et al. Salmonella Typhimurium exhibits fluoroquinolone resistance mediated by the accumulation of the antioxidant molecule H2S in a CysK-dependent manner. *J Antimicrob Chemother*. 12 2016;71(12):3409-3415. doi:10.1093/jac/dkw311

121. Ling J, Cho C, Guo LT, Aerni HR, Rinehart J, Soll D. Protein aggregation caused by aminoglycoside action is prevented by a hydrogen peroxide scavenger. *Mol Cell*. Dec 14 2012;48(5):713-22. doi:10.1016/j.molcel.2012.10.001

122. Feld L, Knudsen GM, Gram L. Bactericidal antibiotics do not appear to cause oxidative stress in Listeria monocytogenes. *Appl Environ Microbiol*. Jun 2012;78(12):4353-7. doi:10.1128/AEM.00324-12

123. Keren I, Wu Y, Inocencio J, Mulcahy LR, Lewis K. Killing by bactericidal antibiotics does not depend on reactive oxygen species. *Science*. Mar 8 2013;339(6124):1213-6. doi:10.1126/science.1232688

124. Covaleda-Cortés G, Mechaly A, Brissac T, et al. The c-di-AMP-binding protein CbpB modulates the level of ppGpp alarmone in Streptococcus agalactiae. *FEBS J*. Jun 2023;290(11):2968-2992. doi:10.1111/febs.16724

125. Torres R, Alonso JC. RecA, DisA, and RadA/Sms Interplay Prevents Replication Stress by Regulating Fork Remodeling. *Front Microbiol*. 2021;12:766897. doi:10.3389/fmicb.2021.766897

126. Gundlach J, Mehne FM, Herzberg C, et al. An Essential Poison: Synthesis and Degradation of Cyclic Di-AMP in Bacillus subtilis. *J Bacteriol*. Oct 2015;197(20):3265-74. doi:10.1128/JB.00564-15

127. Mehne FM, Gunka K, Eilers H, Herzberg C, Kaever V, Stülke J. Cyclic di-AMP homeostasis in bacillus subtilis: both lack and high level accumulation of the nucleotide are detrimental for cell growth. *J Biol Chem*. Jan 18 2013;288(3):2004-17. doi:10.1074/jbc.M112.395491

128. Commichau FM, Heidemann JL, Ficner R, Stülke J. Making and Breaking of an Essential Poison: the Cyclases and Phosphodiesterases That Produce and Degrade the Essential Second Messenger Cyclic di-AMP in Bacteria. *J Bacteriol*. Jan 01 2019;201(1)doi:10.1128/JB.00462-18

129. Witte G, Hartung S, Büttner K, Hopfner KP. Structural biochemistry of a bacterial checkpoint protein reveals diadenylate cyclase activity regulated by DNA recombination intermediates. *Mol Cell*. Apr 25 2008;30(2):167-78. doi:10.1016/j.molcel.2008.02.020

130. Mehne FM, Schröder-Tittmann K, Eijlander RT, et al. Control of the diadenylate cyclase CdaS in Bacillus subtilis: an autoinhibitory domain limits cyclic di-AMP production. *J Biol Chem*. Jul 25 2014;289(30):21098-107. doi:10.1074/jbc.M114.562066

131. Zheng C, Ma Y, Wang X, Xie Y, Ali MK, He J. Functional analysis of the sporulation-specific diadenylate cyclase CdaS in Bacillus thuringiensis. *Front Microbiol*. 2015;6:908. doi:10.3389/fmicb.2015.00908

132. Blötz C, Treffon K, Kaever V, Schwede F, Hammer E, Stülke J. Identification of the Components Involved in Cyclic Di-AMP Signaling in. *Front Microbiol*. 2017;8:1328. doi:10.3389/fmicb.2017.01328

133. El-Gebali S, Mistry J, Bateman A, et al. The Pfam protein families database in 2019. *Nucleic Acids Res*. Jan 08 2019;47(D1):D427-D432. doi:10.1093/nar/gky995

134. Ren A, Patel DJ. c-di-AMP binds the ydaO riboswitch in two pseudo-symmetry-related pockets. *Nat Chem Biol*. Sep 2014;10(9):780-6. doi:10.1038/nchembio.1606

135. Bai Y, Yang J, Eisele LE, et al. Two DHH subfamily 1 proteins in Streptococcus pneumoniae possess cyclic di-AMP phosphodiesterase activity and affect bacterial growth and virulence. *J Bacteriol*. Nov 2013;195(22):5123-32. doi:10.1128/JB.00769-13

136. Huynh TN, Luo S, Pensinger D, Sauer JD, Tong L, Woodward JJ. An HD-domain phosphodiesterase mediates cooperative hydrolysis of c-di-AMP to affect bacterial growth and virulence. *Proc Natl Acad Sci U S A*. Feb 17 2015;112(7):E747-56. doi:10.1073/pnas.1416485112

137. Rao F, See RY, Zhang D, Toh DC, Ji Q, Liang ZX. YybT is a signaling protein that contains a cyclic dinucleotide phosphodiesterase domain and a GGDEF domain with ATPase activity. *J Biol Chem*. Jan 01 2010;285(1):473-82. doi:10.1074/jbc.M109.040238

138. Huynh TN, Woodward JJ. Too much of a good thing: regulated depletion of c-di-AMP in the bacterial cytoplasm. *Curr Opin Microbiol*. Apr 2016;30:22-29. doi:10.1016/j.mib.2015.12.007

139. Rao F, Ji Q, Soehano I, Liang ZX. Unusual heme-binding PAS domain from YybT family proteins. *J Bacteriol*. Apr 2011;193(7):1543-51. doi:10.1128/JB.01364-10

140. Woodward JJ, Iavarone AT, Portnoy DA. c-di-AMP secreted by intracellular Listeria monocytogenes activates a host type I interferon response. *Science*. Jun 25 2010;328(5986):1703-5. doi:10.1126/science.1189801

141. Yamamoto T, Hara H, Tsuchiya K, et al. Listeria monocytogenes strain-specific impairment of the TetR regulator underlies the drastic increase in cyclic di-AMP secretion and beta interferon-inducing ability. *Infect Immun*. Jul 2012;80(7):2323-32. doi:10.1128/IAI.06162-11

142. Crimmins GT, Herskovits AA, Rehder K, et al. Listeria monocytogenes multidrug resistance transporters activate a cytosolic surveillance pathway of innate immunity. *Proc Natl Acad Sci U S A*. Jul 22 2008;105(29):10191-6. doi:10.1073/pnas.0804170105

143. Kaplan Zeevi M, Shafir NS, Shaham S, et al. Listeria monocytogenes multidrug resistance transporters and cyclic di-AMP, which contribute to type I interferon induction, play a role in cell wall stress. *J Bacteriol*. Dec 2013;195(23):5250-61. doi:10.1128/JB.00794-13

144. Gries CM, Bruger EL, Moormeier DE, Scherr TD, Waters CM, Kielian T. Cyclic di-AMP Released from Staphylococcus aureus Biofilm Induces a Macrophage Type I Interferon Response. *Infect Immun*. Dec 2016;84(12):3564-3574. doi:10.1128/IAI.00447-16

145. Andrade WA, Firon A, Schmidt T, et al. Group B Streptococcus Degrades Cyclic-di-AMP to Modulate STING-Dependent Type I Interferon Production. *Cell Host Microbe*. Jul 13 2016;20(1):49-59. doi:10.1016/j.chom.2016.06.003

146. Corrigan RM, Campeotto I, Jeganathan T, Roelofs KG, Lee VT, Gründling A. Systematic identification of conserved bacterial c-di-AMP receptor proteins. *Proc Natl Acad Sci U S A*. May 28 2013;110(22):9084-9. doi:10.1073/pnas.1300595110

147. Moscoso JA, Schramke H, Zhang Y, et al. Binding of Cyclic Di-AMP to the Staphylococcus aureus Sensor Kinase KdpD Occurs via the Universal Stress Protein Domain and Downregulates the Expression of the Kdp Potassium Transporter. *J Bacteriol*. Jan 01 2016;198(1):98-110. doi:10.1128/JB.00480-15

148. Choi PH, Sureka K, Woodward JJ, Tong L. Molecular basis for the recognition of cyclic-di-AMP by PstA, a PII-like signal transduction protein. *Microbiologyopen*. Jun 2015;4(3):361-74. doi:10.1002/mbo3.243

149. Sauer JD, Sotelo-Troha K, von Moltke J, et al. The N-ethyl-N-nitrosourea-induced Goldenticket mouse mutant reveals an essential function of Sting in the in vivo interferon response to Listeria monocytogenes and cyclic dinucleotides. *Infect Immun*. Feb 2011;79(2):688-94. doi:10.1128/IAI.00999-10

150. Devaux L, Kaminski PA, Trieu-Cuot P, Firon A. Cyclic di-AMP in host-pathogen interactions. *Curr Opin Microbiol*. Feb 2018;41:21-28. doi:10.1016/j.mib.2017.11.007

151. McFarland AP, Luo S, Ahmed-Qadri F, et al. Sensing of Bacterial Cyclic Dinucleotides by the Oxidoreductase RECON Promotes NF-κB Activation and Shapes a Proinflammatory Antibacterial State. *Immunity*. Mar 21 2017;46(3):433-445. doi:10.1016/j.immuni.2017.02.014

152. Xia P, Wang S, Xiong Z, et al. The ER membrane adaptor ERAdP senses the bacterial second messenger c-di-AMP and initiates anti-bacterial immunity. *Nat Immunol*. Feb 2018;19(2):141-150. doi:10.1038/s41590-017-0014-x

153. Orr MW, Lee VT. Differential Radial Capillary Action of Ligand Assay (DRaCALA) for High-Throughput Detection of Protein-Metabolite Interactions in Bacteria. *Methods Mol Biol*. 2017;1535:25-41. doi:10.1007/978-1-4939-6673-8_3

154. Sureka K, Choi PH, Precit M, et al. The cyclic dinucleotide c-di-AMP is an allosteric regulator of metabolic enzyme function. *Cell*. Sep 11 2014;158(6):1389-1401. doi:10.1016/j.cell.2014.07.046

155. Kampf J, Gundlach J, Herzberg C, Treffon K, Stülke J. Identification of c-di-AMP-Binding Proteins Using Magnetic Beads. *Methods Mol Biol*. 2017;1657:347-359. doi:10.1007/978-1-4939-7240-1_27

156. Parvatiyar K, Zhang Z, Teles RM, et al. The helicase DDX41 recognizes the bacterial secondary messengers cyclic di-GMP and cyclic di-AMP to activate a type I interferon immune response. *Nat Immunol*. Dec 2012;13(12):1155-61. doi:10.1038/ni.2460

157. Zhang L, Li W, He ZG. DarR, a TetR-like transcriptional factor, is a cyclic di-AMP-responsive repressor in Mycobacterium smegmatis. *J Biol Chem*. Feb 01 2013;288(5):3085-96. doi:10.1074/jbc.M112.428110

158. Müller M, Hopfner KP, Witte G. c-di-AMP recognition by Staphylococcus aureus PstA. *FEBS Lett*. Jan 02 2015;589(1):45-51. doi:10.1016/j.febslet.2014.11.022

159. Gundlach J, Dickmanns A, Schröder-Tittmann K, et al. Identification, characterization, and structure analysis of the cyclic di-AMP-binding PII-like signal transduction protein DarA. *J Biol Chem*. Jan 30 2015;290(5):3069-80. doi:10.1074/jbc.M114.619619

160. Chin KH, Liang JM, Yang JG, et al. Structural Insights into the Distinct Binding Mode of Cyclic Di-AMP with SaCpaA_RCK. *Biochemistry*. Aug 11 2015;54(31):4936-51. doi:10.1021/acs.biochem.5b00633

161. Bai Y, Yang J, Zarrella TM, Zhang Y, Metzger DW, Bai G. Cyclic di-AMP impairs potassium uptake mediated by a cyclic di-AMP binding protein in Streptococcus pneumoniae. *J Bacteriol*. Feb 2014;196(3):614-23. doi:10.1128/JB.01041-13

162. McCown PJ, Corbino KA, Stav S, Sherlock ME, Breaker RR. Riboswitch diversity and distribution. *RNA*. Jul 2017;23(7):995-1011. doi:10.1261/rna.061234.117

163. Barrick JE, Corbino KA, Winkler WC, et al. New RNA motifs suggest an expanded scope for riboswitches in bacterial genetic control. *Proc Natl Acad Sci U S A*. Apr 27 2004;101(17):6421-6. doi:10.1073/pnas.0308014101

164. Block KF, Hammond MC, Breaker RR. Evidence for widespread gene control function by the ydaO riboswitch candidate. *J Bacteriol*. Aug 2010;192(15):3983-9. doi:10.1128/JB.00450-10

165. Nelson JW, Sudarsan N, Furukawa K, Weinberg Z, Wang JX, Breaker RR. Riboswitches in eubacteria sense the second messenger c-di-AMP. *Nat Chem Biol*. Dec 2013;9(12):834-9. doi:10.1038/nchembio.1363

166. Kalvari I, Argasinska J, Quinones-Olvera N, et al. Rfam 13.0: shifting to a genome-centric resource for non-coding RNA families. *Nucleic Acids Res*. Jan 04 2018;46(D1):D335-D342. doi:10.1093/nar/gkx1038

167. Galperin MY, Makarova KS, Wolf YI, Koonin EV. Expanded microbial genome coverage and improved protein family annotation in the COG database. *Nucleic Acids Res*. Jan 2015;43(Database issue):D261-9. doi:10.1093/nar/gku1223

168. Bremer E, Krämer R. Responses of Microorganisms to Osmotic Stress. *Annu Rev Microbiol*. Sep 08 2019;73:313-334. doi:10.1146/annurev-micro-020518-115504

169. Commichau FM, Gibhardt J, Halbedel S, Gundlach J, Stülke J. A Delicate Connection: c-di-AMP Affects Cell Integrity by Controlling Osmolyte Transport. *Trends Microbiol*. Mar 2018;26(3):175-185. doi:10.1016/j.tim.2017.09.003

170. Pham HT, Nhiep NTH, Vu TNM, et al. Enhanced uptake of potassium or glycine betaine or export of cyclic-di-AMP restores osmoresistance in a high cyclic-di-AMP Lactococcus lactis mutant. *PLoS Genet*. Aug 2018;14(8):e1007574. doi:10.1371/journal.pgen.1007574

171. Corratgé-Faillie C, Jabnoune M, Zimmermann S, Véry AA, Fizames C, Sentenac H. Potassium and sodium transport in non-animal cells: the Trk/Ktr/HKT transporter family. *Cell Mol Life Sci*. Aug 2010;67(15):2511-32. doi:10.1007/s00018-010-0317-7

172. Kim H, Youn SJ, Kim SO, Ko J, Lee JO, Choi BS. Structural Studies of Potassium Transport Protein KtrA Regulator of Conductance of K+ (RCK) C Domain in Complex with Cyclic Diadenosine Monophosphate (c-di-AMP). *J Biol Chem*. Jun 26 2015;290(26):16393-402. doi:10.1074/jbc.M115.641340

173. Holtmann G, Bakker EP, Uozumi N, Bremer E. KtrAB and KtrCD: two K+ uptake systems in Bacillus subtilis and their role in adaptation to hypertonicity. *J Bacteriol*. Feb 2003;185(4):1289-98. doi:10.1128/JB.185.4.1289-1298.2003

174. Rocha R, Teixeira-Duarte CM, Jorge JMP, Morais-Cabral JH. Characterization of the molecular properties of KtrC, a second RCK domain that regulates a Ktr channel in Bacillus subtilis. *J Struct Biol*. Mar 01 2019;205(3):34-43. doi:10.1016/j.jsb.2019.02.002

175. Blötz C, Treffon K, Kaever V, Schwede F, Hammer E, Stülke J. Identification of the components involved in cyclic di-AMP signaling in

Mycoplasma pneumoniae. Front Microbiol. 2017;8:1328. doi:10.3389/fmicb.2017.01328

176. Véry AA, Sentenac H. Molecular mechanisms and regulation of K+ transport in higher plants. *Annu Rev Plant Biol*. 2003;54:575-603. doi:10.1146/annurev.arplant.54.031902.134831

177. Quintana IM, Gibhardt J, Turdiev A, et al. The KupA and KupB proteins of *Lactococcus lactis* IL1403 are novel c-di-AMP receptor proteins responsible for potassium uptake. *J Bacteriol*. May 15 2019;201(10)doi:10.1128/JB.00028-19

178. Tascón I, Sousa JS, Corey RA, et al. Structural basis of proton-coupled potassium transport in the KUP family. *Nat Commun*. Jan 31 2020;11(1):626. doi:10.1038/s41467-020-14441-7

179. Gibhardt J, Hoffmann G, Turdiev A, Wang M, Lee VT, Commichau FM. c-di-AMP assists osmoadaptation by regulating the *Listeria monocytogenes* potassium transporters KimA and KtrCD. *J Biol Chem*. Nov 01 2019;294(44):16020-16033. doi:10.1074/jbc.RA119.010046

180. Altendorf K, Voelkner P, Puppe W. The sensor kinase KdpD and the response regulator KdpE control expression of the kdpFABC operon in Escherichia coli. *Res Microbiol*. 1994;145(5-6):374-81. doi:10.1016/0923-2508(94)90084-1

181. Wang X, Cai X, Ma H, et al. A c-di-AMP riboswitch controlling kdpFABC operon transcription regulates the potassium transporter system in Bacillus thuringiensis. *Commun Biol*. 2019;2:151. doi:10.1038/s42003-019-0414-6

182. Gundlach J, Krüger L, Herzberg C, et al. Sustained sensing in potassium homeostasis: Cyclic di-AMP controls potassium uptake by KimA at the levels of expression and activity. *J Biol Chem*. Jun 14 2019;294(24):9605-9614. doi:10.1074/jbc.RA119.008774

183. Fujisawa M, Ito M, Krulwich TA. Three two-component transporters with channel-like properties have monovalent cation/proton antiport activity. *Proc Natl Acad Sci U S A*. Aug 14 2007;104(33):13289-94. doi:10.1073/pnas.0703709104

184. Gundlach J, Herzberg C, Kaever V, et al. Control of potassium homeostasis is an essential function of the second messenger cyclic di-AMP in Bacillus subtilis. *Sci Signal*. Apr 18 2017;10(475)doi:10.1126/scisignal.aal3011

185. Zarrella TM, Metzger DW, Bai G. Stress Suppressor Screening Leads to Detection of Regulation of Cyclic di-AMP Homeostasis by a Trk Family Effector Protein in Streptococcus pneumoniae. *J Bacteriol*. Jun 15 2018;200(12)doi:10.1128/JB.00045-18

186. Whatmore AM, Reed RH. Determination of turgor pressure in Bacillus subtilis: a possible role for K+ in turgor regulation. *J Gen Microbiol*. Dec 1990;136(12):2521-6. doi:10.1099/00221287-136-12-2521

187. Smith WM, Pham TH, Lei L, et al. Heat resistance and salt hypersensitivity in Lactococcus lactis due to spontaneous mutation of llmg_1816 (gdpP) induced by high-temperature growth. *Appl Environ Microbiol*. Nov 2012;78(21):7753-9. doi:10.1128/AEM.02316-12

188. Zhu Y, Pham TH, Nhiep TH, et al. Cyclic-di-AMP synthesis by the diadenylate cyclase CdaA is modulated by the peptidoglycan biosynthesis enzyme GlmM in

Lactococcus lactis. *Mol Microbiol*. Mar 2016;99(6):1015-27. doi:10.1111/mmi.13281

189. Massa SM, Sharma AD, Siletti C, et al. c-di-AMP Accumulation Impairs Muropeptide Synthesis in Listeria monocytogenes. *J Bacteriol*. 11 19 2020;202(24)doi:10.1128/JB.00307-20

190. Romeo Y, Obis D, Bouvier J, et al. Osmoregulation in Lactococcus lactis: BusR, a transcriptional repressor of the glycine betaine uptake system BusA. *Mol Microbiol*. Feb 2003;47(4):1135-47. doi:10.1046/j.1365-2958.2003.03362.x

191. Devaux L, Sleiman D, Mazzuoli MV, et al. Cyclic di-AMP regulation of osmotic homeostasis is essential in Group B Streptococcus. *PLoS Genet*. Apr 2018;14(4):e1007342. doi:10.1371/journal.pgen.1007342

192. Whiteley AT, Garelis NE, Peterson BN, et al. c-di-AMP modulates Listeria monocytogenes central metabolism to regulate growth, antibiotic resistance and osmoregulation. *Mol Microbiol*. Apr 2017;104(2):212-233. doi:10.1111/mmi.13622

193. Whiteley AT, Pollock AJ, Portnoy DA. The PAMP c-di-AMP Is Essential for Listeria monocytogenes Growth in Rich but Not Minimal Media due to a Toxic Increase in (p)ppGpp. [corrected]. *Cell Host Microbe*. Jun 10 2015;17(6):788-98. doi:10.1016/j.chom.2015.05.006

194. Schuster CF, Bellows LE, Tosi T, et al. The second messenger c-di-AMP inhibits the osmolyte uptake system OpuC in Staphylococcus aureus. *Sci Signal*. 08 16 2016;9(441):ra81. doi:10.1126/scisignal.aaf7279

195. Kappes RM, Kempf B, Kneip S, et al. Two evolutionarily closely related ABC transporters mediate the uptake of choline for synthesis of the osmoprotectant glycine betaine in Bacillus subtilis. *Mol Microbiol*. Apr 1999;32(1):203-16. doi:10.1046/j.1365-2958.1999.01354.x

196. Schär J, Stoll R, Schauer K, et al. Pyruvate carboxylase plays a crucial role in carbon metabolism of extra- and intracellularly replicating Listeria monocytogenes. *J Bacteriol*. Apr 2010;192(7):1774-84. doi:10.1128/JB.01132-09

197. Pechter KB, Meyer FM, Serio AW, Stülke J, Sonenshein AL. Two roles for aconitase in the regulation of tricarboxylic acid branch gene expression in Bacillus subtilis. *J Bacteriol*. Apr 2013;195(7):1525-37. doi:10.1128/JB.01690-12

198. Choi PH, Vu TMN, Pham HT, Woodward JJ, Turner MS, Tong L. Structural and functional studies of pyruvate carboxylase regulation by cyclic di-AMP in lactic acid bacteria. *Proc Natl Acad Sci U S A*. Aug 29 2017;114(35):E7226-E7235. doi:10.1073/pnas.1704756114

199. Zeden MS, Schuster CF, Bowman L, Zhong Q, Williams HD, Gründling A. Cyclic di-adenosine monophosphate (c-di-AMP) is required for osmotic regulation in *Staphylococcus aureus* but dispensable for viability in anaerobic conditions. *J Biol Chem*. Mar 02 2018;293(9):3180-3200. doi:10.1074/jbc.M117.818716

200. Steinchen W, Zegarra V, Bange G. (p)ppGpp: Magic Modulators of Bacterial Physiology and Metabolism. *Front Microbiol*. 2020;11:2072. doi:10.3389/fmicb.2020.02072

201. Rallu F, Gruss A, Ehrlich SD, Maguin E. Acid- and multistress-resistant mutants of Lactococcus lactis : identification of intracellular stress signals. *Mol Microbiol*. Feb 2000;35(3):517-28. doi:10.1046/j.1365-2958.2000.01711.x

202. Irnov I, Wang Z, Jannetty ND, Bustamante JA, Rhee KY, Jacobs-Wagner C. Crosstalk between the tricarboxylic acid cycle and peptidoglycan synthesis in Caulobacter crescentus through the homeostatic control of α-ketoglutarate. *PLoS Genet*. Aug 2017;13(8):e1006978. doi:10.1371/journal.pgen.1006978

203. Fahmi T, Port GC, Cho KH. c-di-AMP: An Essential Molecule in the Signaling Pathways that Regulate the Viability and Virulence of Gram-Positive Bacteria. *Genes (Basel)*. Aug 07 2017;8(8)doi:10.3390/genes8080197

204. Corrigan RM, Bowman L, Willis AR, Kaever V, Gründling A. Cross-talk between two nucleotide-signaling pathways in Staphylococcus aureus. *J Biol Chem*. Feb 27 2015;290(9):5826-39. doi:10.1074/jbc.M114.598300

205. Geiger T, Wolz C. Intersection of the stringent response and the CodY regulon in low GC Gram-positive bacteria. *Int J Med Microbiol*. Mar 2014;304(2):150-5. doi:10.1016/j.ijmm.2013.11.013

206. Colomer-Winter C, Flores-Mireles AL, Kundra S, Hultgren SJ, Lemos JA. (p)ppGpp and CodY Promote Enterococcus faecalis Virulence in a Murine Model of Catheter-Associated Urinary Tract Infection. *mSphere*. Jul 24 2019;4(4)doi:10.1128/mSphere.00392-19

207. Danilchanka O, Mekalanos JJ. Cyclic dinucleotides and the innate immune response. *Cell*. Aug 29 2013;154(5):962-970. doi:10.1016/j.cell.2013.08.014

208. Zhou W, Whiteley AT, Kranzusch PJ. Analysis of human cGAS activity and structure. *Methods Enzymol*. 2019;625:13-40. doi:10.1016/bs.mie.2019.04.012

209. Yi G, Brendel VP, Shu C, Li P, Palanathan S, Cheng Kao C. Single nucleotide polymorphisms of human STING can affect innate immune response to cyclic dinucleotides. *PLoS One*. 2013;8(10):e77846. doi:10.1371/journal.pone.0077846

210. DiDonato JA, Mercurio F, Karin M. NF-κB and the link between inflammation and cancer. *Immunol Rev*. Mar 2012;246(1):379-400. doi:10.1111/j.1600-065X.2012.01099.x

211. Corrigan RM, Abbott JC, Burhenne H, Kaever V, Gründling A. c-di-AMP is a new second messenger in Staphylococcus aureus with a role in controlling cell size and envelope stress. *PLoS Pathog*. Sep 2011;7(9):e1002217. doi:10.1371/journal.ppat.1002217

212. St-Onge RJ, Haiser HJ, Yousef MR, et al. Nucleotide second messenger-mediated regulation of a muralytic enzyme in Streptomyces. *Mol Microbiol*. May 2015;96(4):779-95. doi:10.1111/mmi.12971

213. Biswas R, Voggu L, Simon UK, Hentschel P, Thumm G, Götz F. Activity of the major staphylococcal autolysin Atl. *FEMS Microbiol Lett*. Jun 2006;259(2):260-8. doi:10.1111/j.1574-6968.2006.00281.x

214. Ramadurai L, Lockwood KJ, Lockwood J, Nadakavukaren MJ, Jayaswal RK. Characterization of a chromosomally encoded glycylglycine endopeptidase of Staphylococcus aureus. *Microbiology (Reading)*. Apr 1999;145 (Pt 4):801-808. doi:10.1099/13500872-145-4-801

215. Luo Y, Helmann JD. Analysis of the role of Bacillus subtilis σ(M) in β-lactam resistance reveals an essential role for c-di-AMP in peptidoglycan homeostasis. *Mol Microbiol*. Feb 2012;83(3):623-39. doi:10.1111/j.1365-2958.2011.07953.x

216. Rismondo J, Gibhardt J, Rosenberg J, Kaever V, Halbedel S, Commichau FM. Phenotypes Associated with the Essential Diadenylate Cyclase CdaA and Its Potential Regulator CdaR in the Human Pathogen Listeria monocytogenes. *J Bacteriol*. Feb 01 2016;198(3):416-26. doi:10.1128/JB.00845-15

217. Dey B, Dey RJ, Cheung LS, et al. A bacterial cyclic dinucleotide activates the cytosolic surveillance pathway and mediates innate resistance to tuberculosis. *Nat Med*. Apr 2015;21(4):401-6. doi:10.1038/nm.3813

218. Egan AJF, Errington J, Vollmer W. Regulation of peptidoglycan synthesis and remodelling. *Nat Rev Microbiol*. Aug 2020;18(8):446-460. doi:10.1038/s41579-020-0366-3

219. Blötz C, Treffon K, Kaever V, Schwede F, Hammer E, Stülke J. Identification of the components involved in cyclic di-AMP signaling in *Mycoplasma pneumoniae. Front Microbiol*. 2017;8:1328. doi:10.3389/fmicb.2017.01328

220. Latoscha A, Drexler DJ, Al-Bassam MM, et al. c-di-AMP hydrolysis by the phosphodiesterase AtaC promotes differentiation of multicellular bacteria. *Proc Natl Acad Sci U S A*. Mar 31 2020;117(13):7392-7400. doi:10.1073/pnas.1917080117

221. Huynh TN, Choi PH, Sureka K, et al. Cyclic di-AMP targets the cystathionine beta-synthase domain of the osmolyte transporter OpuC. *Mol Microbiol*. 10 2016;102(2):233-243. doi:10.1111/mmi.13456

222. Campeotto I, Zhang Y, Mladenov MG, Freemont PS, Gründling A. Complex structure and biochemical characterization of the Staphylococcus aureus cyclic diadenylate monophosphate (c-di-AMP)-binding protein PstA, the founding member of a new signal transduction protein family. *J Biol Chem*. Jan 30 2015;290(5):2888-901. doi:10.1074/jbc.M114.621789

223. Rosenberg J, Dickmanns A, Neumann P, et al. Structural and biochemical analysis of the essential diadenylate cyclase CdaA from Listeria monocytogenes. *J Biol Chem*. Mar 06 2015;290(10):6596-606. doi:10.1074/jbc.M114.630418

224. Rubin BE, Huynh TN, Welkie DG, et al. High-throughput interaction screens illuminate the role of c-di-AMP in cyanobacterial nighttime survival. *PLoS Genet*. Apr 2018;14(4):e1007301. doi:10.1371/journal.pgen.1007301

225. Görke B, Stülke J. Carbon catabolite repression in bacteria: many ways to make the most out of nutrients. *Nat Rev Microbiol*. Aug 2008;6(8):613-24. doi:10.1038/nrmicro1932

226. Witte CE, Whiteley AT, Burke TP, Sauer JD, Portnoy DA, Woodward JJ. Cyclic di-AMP is critical for Listeria monocytogenes growth, cell wall homeostasis, and establishment of infection. *mBio*. May 28 2013;4(3):e00282-13. doi:10.1128/mBio.00282-13

227. Miller C, Kong J, Tran TT, Arias CA, Saxer G, Shamoo Y. Adaptation of Enterococcus faecalis to daptomycin reveals an ordered progression to resistance. *Antimicrob Agents Chemother*. Nov 2013;57(11):5373-83. doi:10.1128/AAC.01473-13

228. Wang X, Davlieva M, Reyes J, Panesso D, Arias CA, Shamoo Y. A Novel Phosphodiesterase of the GdpP Family Modulates Cyclic di-AMP Levels in Response to Cell Membrane Stress in Daptomycin-Resistant Enterococci. *Antimicrob Agents Chemother*. Mar 2017;61(3)doi:10.1128/AAC.01422-16

229. Dengler V, McCallum N, Kiefer P, et al. Mutation in the C-di-AMP cyclase dacA affects fitness and resistance of methicillin resistant Staphylococcus aureus. *PLoS One*. 2013;8(8):e73512. doi:10.1371/journal.pone.0073512

230. Banerjee R, Gretes M, Harlem C, Basuino L, Chambers HF. A mecA-negative strain of methicillin-resistant Staphylococcus aureus with high-level β-lactam resistance contains mutations in three genes. *Antimicrob Agents Chemother*. Nov 2010;54(11):4900-2. doi:10.1128/AAC.00594-10

231. Griffiths JM, O'Neill AJ. Loss of function of the gdpP protein leads to joint β-lactam/glycopeptide tolerance in Staphylococcus aureus. *Antimicrob Agents Chemother*. Jan 2012;56(1):579-81. doi:10.1128/AAC.05148-11

232. Cheng X, Zheng X, Zhou X, et al. Regulation of oxidative response and extracellular polysaccharide synthesis by a diadenylate cyclase in Streptococcus mutans. *Environ Microbiol*. Mar 2016;18(3):904-22. doi:10.1111/1462-2920.13123

233. Cho KH, Kang SO. Streptococcus pyogenes c-di-AMP phosphodiesterase, GdpP, influences SpeB processing and virulence. *PLoS One*. 2013;8(7):e69425. doi:10.1371/journal.pone.0069425

234. Wichgers Schreur PJ, van Weeghel C, Rebel JM, Smits MA, van Putten JP, Smith HE. Lysozyme resistance in Streptococcus suis is highly variable and multifactorial. *PLoS One*. 2012;7(4):e36281. doi:10.1371/journal.pone.0036281

235. Stülke J, Krüger L. Cyclic di-AMP Signaling in Bacteria. *Annu Rev Microbiol*. Sep 08 2020;74:159-179. doi:10.1146/annurev-micro-020518-115943

236. Corrigan RM, Gründling A. Cyclic di-AMP: another second messenger enters the fray. *Nat Rev Microbiol*. Aug 2013;11(8):513-24. doi:10.1038/nrmicro3069

237. Commichau FM, Dickmanns A, Gundlach J, Ficner R, Stülke J. A jack of all trades: the multiple roles of the unique essential second messenger cyclic di-AMP. *Mol Microbiol*. Jul 2015;97(2):189-204. doi:10.1111/mmi.13026

238. He J, Yin W, Galperin MY, Chou SH. Cyclic di-AMP, a second messenger of primary importance: tertiary structures and binding mechanisms. *Nucleic Acids Res*. Apr 06 2020;48(6):2807-2829. doi:10.1093/nar/gkaa112

239. Smith HB, Li TL, Liao MK, Chen GY, Guo Z, Sauer JD. Listeria monocytogenes MenI Encodes a DHNA-CoA Thioesterase Necessary for Menaquinone Biosynthesis, Cytosolic Survival, and Virulence. *Infect Immun*. 04 16 2021;89(5)doi:10.1128/IAI.00792-20

240. Lobritz MA, Belenky P, Porter CB, et al. Antibiotic efficacy is linked to bacterial cellular respiration. *Proc Natl Acad Sci U S A*. Jul 07 2015;112(27):8173-80. doi:10.1073/pnas.1509743112

241. Corbett D, Goldrick M, Fernandes VE, et al. *Listeria monocytogenes* Has Both Cytochrome bd-Type and Cytochrome aa3-Type Terminal Oxidases, Which Allow Growth at Different Oxygen Levels, and Both Are Important in Infection. *Infect Immun*. Nov 2017;85(11)doi:10.1128/IAI.00354-17

242. Light SH, Su L, Rivera-Lugo R, et al. A flavin-based extracellular electron transfer mechanism in diverse Gram-positive bacteria. *Nature*. 10 2018;562(7725):140-144. doi:10.1038/s41586-018-0498-z

243. Chen GY, McDougal CE, D'Antonio MA, Portman JL, Sauer JD. A Genetic Screen Reveals that Synthesis of 1,4-Dihydroxy-2-Naphthoate (DHNA), but Not Full-Length Menaquinone, Is Required for. *mBio*. Mar 21 2017;8(2)doi:10.1128/mBio.00119-17

244. Kaila VRI, Wikström M. Architecture of bacterial respiratory chains. *Nat Rev Microbiol*. May 2021;19(5):319-330. doi:10.1038/s41579-020-00486-4

245. Dwyer DJ, Belenky PA, Yang JH, et al. Antibiotics induce redox-related physiological alterations as part of their lethality. *Proc Natl Acad Sci U S A*. May 20 2014;111(20):E2100-9. doi:10.1073/pnas.1401876111

246. Keller MR, Dörr T. Bacterial metabolism and susceptibility to cell wall-active antibiotics. *Adv Microb Physiol*. 2023;83:181-219. doi:10.1016/bs.ampbs.2023.04.002

247. Forchhammer K, Lüddecke J. Sensory properties of the PII signalling protein family. *FEBS J*. Feb 2016;283(3):425-37. doi:10.1111/febs.13584

248. Peterson BN, Young MKM, Luo S, et al. (p)ppGpp and c-di-AMP Homeostasis Is Controlled by CbpB in Listeria monocytogenes. *mBio*. 08 25 2020;11(4)doi:10.1128/mBio.01625-20

249. Krüger L, Herzberg C, Wicke D, et al. A meet-up of two second messengers: the c-di-AMP receptor DarB controls (p)ppGpp synthesis in Bacillus subtilis. *Nat Commun*. Feb 22 2021;12(1):1210. doi:10.1038/s41467-021-21306-0

250. Forchhammer K, Selim KA, Huergo LF. New views on PII signaling: from nitrogen sensing to global metabolic control. *Trends Microbiol*. Aug 2022;30(8):722-735. doi:10.1016/j.tim.2021.12.014

251. Borisov VB, Siletsky SA, Paiardini A, et al. Bacterial Oxidases of the Cytochrome *bd* Family: Redox Enzymes of Unique Structure, Function, and Utility As Drug Targets. *Antioxid Redox Signal*. Jun 01 2021;34(16):1280-1318. doi:10.1089/ars.2020.8039

252. Belenky P, Ye JD, Porter CB, et al. Bactericidal Antibiotics Induce Toxic Metabolic Perturbations that Lead to Cellular Damage. *Cell Rep*. Nov 03 2015;13(5):968-80. doi:10.1016/j.celrep.2015.09.059

253. Hammer ND. Quantifying Staphylococcus aureus Membrane Potential Using Flow Cytometry. *Methods Mol Biol*. 2021;2341:95-101. doi:10.1007/978-1-0716-1550-8_12

254. Pensinger DA, Gutierrez KV, Smith HB, et al. Listeria monocytogenes GlmR Is an Accessory Uridyltransferase Essential for Cytosolic Survival and Virulence. *mBio*. Apr 25 2023;14(2):e0007323. doi:10.1128/mbio.00073-23

255. Clasquin MF, Melamud E, Rabinowitz JD. LC-MS data processing with MAVEN: a metabolomic analysis and visualization engine. *Curr Protoc Bioinformatics*. Mar 2012;Chapter 14:Unit14.11. doi:10.1002/0471250953.bi1411s37

256. Forchhammer K. P(II) signal transducers: novel functional and structural insights. *Trends Microbiol*. Feb 2008;16(2):65-72. doi:10.1016/j.tim.2007.11.004

257. Tu Z, Stevenson DM, McCaslin D, Amador-Noguez D, Huynh TN. The role of *Listeria monocytogenes* PstA in β-lactam resistance requires the cytochrome *bd* oxidase activity. *J Bacteriol*. Jul 12 2024:e0013024. doi:10.1128/jb.00130-24

258. Pizarro-Cerdá J, Cossart P. *Listeria monocytogenes*: cell biology of invasion and intracellular growth. *Microbiol Spectr*. Nov 2018;6(6)doi:10.1128/microbiolspec.GPP3-0013-2018

259. Morse R, O'Hanlon K, Virji M, Collins MD. Isolation of rifampin-resistant mutants of Listeria monocytogenes and their characterization by rpoB gene sequencing, temperature sensitivity for growth, and interaction with an epithelial cell line. *J Clin Microbiol*. Sep 1999;37(9):2913-9. doi:10.1128/JCM.37.9.2913-2919.1999

260. Kari L, Goheen MM, Randall LB, et al. Generation of targeted Chlamydia trachomatis null mutants. *Proc Natl Acad Sci U S A*. Apr 26 2011;108(17):7189-93. doi:10.1073/pnas.1102229108

261. Sambrook J, Russell DW. Directional cloning into plasmid vectors. *CSH Protoc*. Jun 01 2006;2006(1)doi:10.1101/pdb.prot3919

262. Young KD. The selective value of bacterial shape. *Microbiol Mol Biol Rev*. Sep 2006;70(3):660-703. doi:10.1128/MMBR.00001-06

263. Cabeen MT, Jacobs-Wagner C. Skin and bones: the bacterial cytoskeleton, cell wall, and cell morphogenesis. *J Cell Biol*. Nov 05 2007;179(3):381-7. doi:10.1083/jcb.200708001

264. van den Ent F, Izoré T, Bharat TA, Johnson CM, Löwe J. Bacterial actin MreB forms antiparallel double filaments. *Elife*. May 02 2014;3:e02634. doi:10.7554/eLife.02634

265. Carballido-López R, Formstone A, Li Y, Ehrlich SD, Noirot P, Errington J. Actin homolog MreBH governs cell morphogenesis by localization of the cell wall hydrolase LytE. *Dev Cell*. Sep 2006;11(3):399-409. doi:10.1016/j.devcel.2006.07.017

266. Carballido-López R, Errington J. The bacterial cytoskeleton: in vivo dynamics of the actin-like protein Mbl of Bacillus subtilis. *Dev Cell*. Jan 2003;4(1):19-28. doi:10.1016/s1534-5807(02)00403-3

267. Defeu Soufo HJ, Graumann PL. Dynamic movement of actin-like proteins within bacterial cells. *EMBO Rep*. Aug 2004;5(8):789-94. doi:10.1038/sj.embor.7400209

268. Jones LJ, Carballido-López R, Errington J. Control of cell shape in bacteria: helical, actin-like filaments in Bacillus subtilis. *Cell*. Mar 23 2001;104(6):913-22. doi:10.1016/s0092-8674(01)00287-2

269. Takahashi D, Fujiwara I, Sasajima Y, Narita A, Imada K, Miyata M. ATP-dependent polymerization dynamics of bacterial actin proteins involved in *Spiroplasma* swimming. *Open Biol*. Oct 2022;12(10):220083. doi:10.1098/rsob.220083

270. Commichau FM, Stülke J. Coping with an Essential Poison: a Genetic Suppressor Analysis Corroborates a Key Function of c-di-AMP in Controlling Potassium Ion

Homeostasis in Gram-Positive Bacteria. *J Bacteriol*. Jun 15 2018;200(12)doi:10.1128/JB.00166-18

271. Dobihal GS, Brunet YR, Flores-Kim J, Rudner DZ. Homeostatic control of cell wall hydrolysis by the WalRK two-component signaling pathway in. *Elife*. Dec 06 2019;8doi:10.7554/eLife.52088

272. Sauer JD, Herskovits AA, O'Riordan MXD. Metabolism of the Gram-Positive Bacterial Pathogen *Listeria monocytogenes*. *Microbiol Spectr*. Jul 2019;7(4)doi:10.1128/microbiolspec.GPP3-0066-2019

273. Ursell TS, Nguyen J, Monds RD, et al. Rod-like bacterial shape is maintained by feedback between cell curvature and cytoskeletal localization. *Proc Natl Acad Sci U S A*. Mar 18 2014;111(11):E1025-34. doi:10.1073/pnas.1317174111

274. Dion MF, Kapoor M, Sun Y, et al. Bacillus subtilis cell diameter is determined by the opposing actions of two distinct cell wall synthetic systems. *Nat Microbiol*. Aug 2019;4(8):1294-1305. doi:10.1038/s41564-019-0439-0

275. Takahashi D, Fujiwara I, Sasajima Y, Narita A, Imada K, Miyata M. ATP-dependent polymerization dynamics of bacterial actin proteins involved in. *Open Biol*. Oct 2022;12(10):220083. doi:10.1098/rsob.220083

276. Bean GJ, Flickinger ST, Westler WM, et al. A22 disrupts the bacterial actin cytoskeleton by directly binding and inducing a low-affinity state in MreB. *Biochemistry*. Jun 09 2009;48(22):4852-7. doi:10.1021/bi900014d

277. Dajkovic A, Tesson B, Chauhan S, et al. Hydrolysis of peptidoglycan is modulated by amidation of meso-diaminopimelic acid and Mg. *Mol Microbiol*. Jun 2017;104(6):972-988. doi:10.1111/mmi.13673

278. Cornett JB, Shockman GD. Cellular lysis of Streptococcus faecalis induced with triton X-100. *J Bacteriol*. Jul 1978;135(1):153-60. doi:10.1128/jb.135.1.153-160.1978

279. Sun AN, Camilli A, Portnoy DA. Isolation of Listeria monocytogenes small-plaque mutants defective for intracellular growth and cell-to-cell spread. *Infect Immun*. Nov 1990;58(11):3770-8. doi:10.1128/iai.58.11.3770-3778.1990

280. Tosi T, Hoshiga F, Millership C, et al. Inhibition of the Staphylococcus aureus c-di-AMP cyclase DacA by direct interaction with the phosphoglucosamine mutase GlmM. *PLoS Pathog*. Jan 2019;15(1):e1007537. doi:10.1371/journal.ppat.1007537

281. Miura C, Komatsu K, Maejima K, et al. Functional characterization of the principal sigma factor RpoD of phytoplasmas via an in vitro transcription assay. *Sci Rep*. Jul 07 2015;5:11893. doi:10.1038/srep11893

282. Reniere ML, Whiteley AT, Portnoy DA. An In Vivo Selection Identifies Listeria monocytogenes Genes Required to Sense the Intracellular Environment and

Activate Virulence Factor Expression. *PLoS Pathog*. Jul 2016;12(7):e1005741. doi:10.1371/journal.ppat.1005741

283. Maki H, Miura K, Yamano Y. Katanosin B and plusbacin A(3), inhibitors of peptidoglycan synthesis in methicillin-resistant Staphylococcus aureus. *Antimicrob Agents Chemother*. Jun 2001;45(6):1823-7. doi:10.1128/AAC.45.6.1823-1827.2001